Paleomagnetic dating of late Pleistocene vegetation and climate recorded in sediment from Sutherland Pond, Black Rock Forest, Orange County, New York

Kiersten Jennings
Barnard College
Department of Environmental Science
30 April 1998

ABSTRACT

A paleomagnetic secular variation curve resulting from measurement of depositional remanent magnetism in basal sediment from a 10.6 m core of Sutherland Pond in Black Rock Forest represents the time period immediately following deglaciation in southeastern New York. The secular variation recorded in the lacustrine sediment varied from -35.2° to 40.0° declination and from 18.6° to 49.9° inclination. The resulting curve was correlated with the paleomagnetic secular variation recorded in Lake Ontario sediment, placing an age of about 17,500 years BP at the base of the Sutherland Pond core. This age is in accord with other estimates for the termination of glaciation in the region (Connally and Sirkin, 1986; Cotter et al, 1986). Determining the onset and duration of inorganic sediment deposition that followed deglaciation and preceded a resurgence of organic sediment deposition in Sutherland Pond has applications for paleoenvironmental investigators in the Hudson Highlands. The results of this study suggest that a period of 2,700 years elapsed between deglaciation and the full resurgence of temperate vegetation during the Holocene epoch in southeastern New York. This information contributes to the climate history and ultimately to the better understanding of climate dynamics in the region at the end of the Pleistocene.

TABLE OF CONTENTS

LIST OF FIGURES

LIST OF TABLES

INTRODUCTION

During the last ice age, the Laurentide ice sheet covered the northeastern United States as far south as eastern Pennsylvania, northern New Jersey and southern New York. When climate warmed significantly, the retreat of this glacier left scattered lakes in its path where meltwater collected in depressions formed by the ice sheet. The ages of these lakes are valuable in understanding the migration of the ice margin, but are largely unstudied (Muller and Calkin, 1993). Pollen studies have been performed on cores of glacial lakes which are central to understanding climate change since deglaciation, but a key bit of information which has been missing is the age of formation of the lakes.

Paleomagnetism offers one solution to understanding the timing of deglaciation. Correlation of paleomagnetic secular variation performed on glaciolacustrine sediments can be used to estimate the absolute age of a lake, thus dating glacial retreat in certain regions. Such studies have been performed in the Great Lakes (Carmichael at al, 1990) and Finger Lakes (Brennan et al, 1984; Brennan 1988) regions of northeastern New York, as well as glacial Lake Hitchcock in the Connecticut Valley and the Mohawk Valley (Ridge et al, 1990).

This study is focused on paleomagnetic dating of sediment from Sutherland Pond in Black Rock Forest. The resulting estimate of the timing of pond formation and thus glacial retreat in southeastern New York coupled with paleoecological analyses of the region suggest the timing and duration of inorganic deposition following deglaciation and preceding the resurgence of organic deposition and a warmer climate (Muller and Calkin, 1993). This information coupled with paleoecological evidence of vegetation dynamics as indicative of environmental change is valuable in understanding regional climate history at the end of the Pleistocene and contributes to

the knowledge of climate dynamics. The dynamics of ice sheets during glacial climates are one component of this knowledge, as is the speed of the transition from cooler to warmer temperatures at the end of the last ice age.

Black Rock Forest, Sutherland Pond and Glacial History

Black Rock Forest is a 1500 ha natural preserve which lies at the interface of the Hudson Highlands and Hudson River Basin ecosystems, about 80 km north of New York City. The location of the forest allows for biological diversity and a variety of terrestrial and aquatic habitats within the forest (Black Rock Forest, 1997). The Highlands are underlain by Precambrian granites and gneisses which are the basement rocks for the Reading Prong Province that extends from eastern Pennsylvania into western Connecticut.

Black Rock Forest serves as a pristine example of the regional natural ecosystem which developed following the most recent (Wisconsinan) deglaciation in the northeastern United States. The Pleistocene epoch began between two and three million years ago. In an examination of the glacial geology of Black Rock Forest, Denny (1938) determined that Wisconsinan till was deposited on the uplands of Black Rock Forest as the Laurentide ice sheet melted. Sutherland Pond is one of many small water bodies that formed in the Hudson Highlands at the end of the Pleistocene epoch. As such, the glaciolacustrine deposits must postdate the maximum extent of late Wisconsinan ice, which was dated at 21,500 years BP[1] in eastern Pennsylvania (Cotter et al, 1986). Wisconsin terminal moraines are also located in

[1] Unless otherwise noted, all ages in this paper are presented in calendar years, denoted "years BP". Radiocarbon ages, denoted "C-14 years BP", were converted wherever possible using calibration tables (Stuiver and Pearson, 1993; Stuiver et al, 1986).

northern New Jersey and southern New York (Long Island), and are shown on the map in Figure 1.

By dating organic sediments related to the last glacial maximum in New Jersey and Long Island, Connally & Sirkin (1973) suggested a slightly younger age (an average of 20,100 years BP) of glacial retreat than previously thought. Previous attempts placed dates of 22,000 years (Urry, 1948) and 27,000 years (Antevs, 1953) on the retreat of the Wisconsin glacier from its outer limit at New York. At Francis Lake (site 7 in Figure 1), which is about 45 km south of the New York State border in New Jersey, pollen-bearing sediments below the peat layer yielded an age of 21,950 years BP for sedimentation that could only have taken place after the start of glacial retreat in the area (Cotter et al, 1986). In the Hudson Valley closer to Black Rock Forest, near-basal organic matter from five closely spaced cores in Eagle Hill Camp Bog (site 5 in Figure 1) yielded an age of 16,400 years BP (Connally and Sirkin, 1986). Connally and Sirkin (1986) estimated that 2272 years had elapsed between glacial retreat and the beginning of peat accumulation, which suggests glacial retreat in the Hudson Valley north of Black Rock Forest at 18,670 years BP.

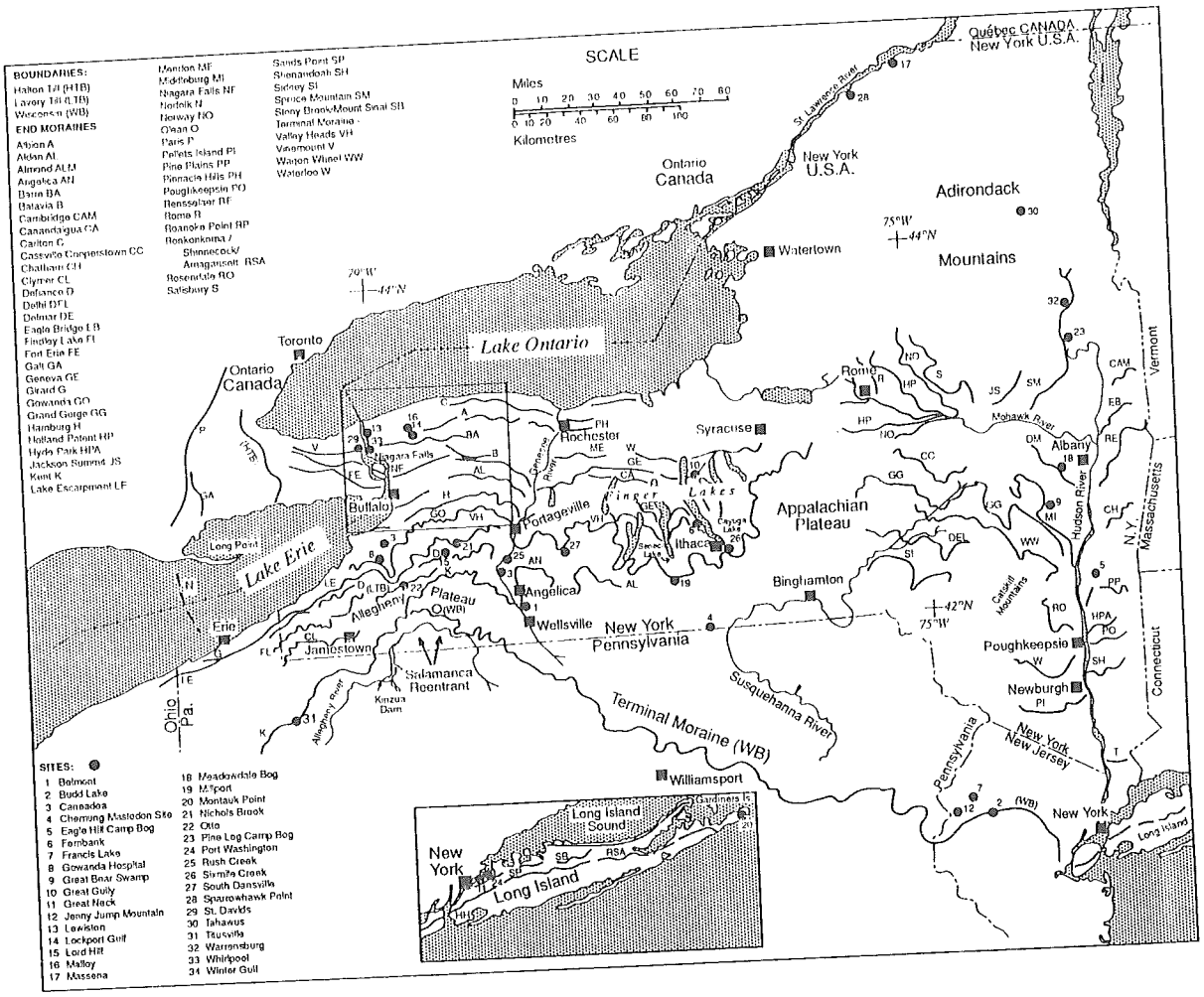

Figure 1: Map showing maximum extent of Wisconsinan ice sheet (terminal moraine) as well as locations of dated sites in New York (Muller and Calkin, 1993)

Sutherland Pond Core BRF-1

The Sutherland Pond sediment core, known as BRF-1, is 10.6 m long and was one of two sampled for a paleoenvironmental study of the Holocene events following glaciation in the Hudson Highlands (Maenza-Gmelch, 1997a). The second core was taken from Spruce Pond located in Harriman State Park 22.5 km to the southwest of Black Rock Forest. Maenza-Gmelch (1997a) points out the importance of the characterization and age determination of vegetation

assemblages for clarifying the timing of deglaciation and the speed of climate change. Analyses of fossil pollen, plant-macrofossil and charcoal content coupled with AMS radiocarbon dates from the Sutherland Pond core demonstrate commencement of organic deposition at a core depth of 8.3 m. At this depth, pollen influx, the first occurrence of macrofossils, and the establishment of a mixed boreal-temperate forest indicate dramatic environmental change such as climate warming about 12,600 C-14 years BP (calibrated to 14,800 calendar years BP) (Maenza-Gmelch, 1997b). Maenza-Gmelch (1997) concluded that prior to 14,800 years BP an open vegetation such as a forest tundra existed at Sutherland Pond. The duration of this assemblage could not be determined due to insufficient presence of datable organic material in the bottom two meters of lacustrine clay and silt in the core, a problem also discussed by Ridge and others (1990) and Muller and Calkin (1993). In their review of age data from numerous studies, Muller and Calkin (1993) conclude that the chronostratigraphic framework of Pleistocene glacial events in New York State is not yet well constructed. Ridge and others (1990) proposed that declination records of long duration would ultimately make interregional correlations of glacial sequences possible. Although AMS radiocarbon dating of organic peat fragments from the bottoms of bog cores is another promising method of establishing the timing of these glacial events, this is not possible with Sutherland Pond sediments because of the inorganic lithology at the base of the core. The paleomagnetic investigation is an attempt to date the lower two meters of inorganic sediment in the core using an alternative method.

Paleomagnetic Record

The Earth generates a magnetic field that is in appearance much like the magnetic field around a simple bar magnet. This field is thought to be generated by a self-sustaining dynamo in the Earth's liquid outer core (Merrill et al., 1996). This field has a north and south magnetic pole, the positions of which correspond roughly to the positions of the geographical north and south poles of the Earth. Magnetic lines of force pass through the Earth and extend from one pole to the other. A compass needle, which is itself a small magnet, aligns itself with these lines of force and thus points toward the magnetic poles (Takeuchi et al, 1967). When a compass needle points north, it is pointing to the magnetic north pole, which does not occur at exactly the same point on the surface of the Earth as the geographic north pole. The angle of deviation of magnetic north to the east or west of the geographic north pole is called *declination* (D). In paleomagnetic studies, this angle D is always measured clockwise (eastwards) from geographic north and consequently takes on any angle between 0° and 360° (McElhinny, 1973). Over long periods of time (generally 100,000 years or more) the average declination averages to approximately zero degrees. Also since a compass needle will point directly to the magnetic poles, it will not rest horizontally if it is balanced at its center of gravity. In the Northern Hemisphere during Normal Polarity, the north seeking end of the needle will dip downward as will the south seeking end in the Southern Hemisphere. This angle of deviation from the horizontal is called the *inclination* (I), or the magnetic dip. Inclination, like declination, varies according to location on the surface of the Earth. The line across the surface of the earth for which the inclination is zero is called the *magnetic equator*, while the magnetic poles are points

on the earth where the angle of inclination is $\pm$ 90° depending on the hemisphere and polarity (McElhinny, 1973). For Normal Polarity, the *north magnetic pole* is situated where I = +90°, and the *south magnetic pole* is situated where I = -90°. The third property which characterizes the Earth's magnetic field at any one point is its intensity, which is measured in gauss. The Earth's magnetic field is relatively weak, varying from about 0.3 gauss near the Equator to about 0.7 gauss in the polar regions (Takeuchi et al, 1967).

The Earth's magnetic field is not constant, but varies continuously. There are small daily variations regularly in the field and occasional larger disturbances called magnetic storms resulting in a several degree difference in declination. These changes are due to electric currents in the upper atmosphere rather than changes in the Earth's interior magnetic mechanism. These small shifts in the declination or inclination of the Earth's magnetic field are called secular variations and historic records of them are limited to magnetic observatory records and to data compiled from magnetic compass readings recorded in the logs of sailing ships. These data can be compiled globally to produce maps of elements of the earth's magnetic field at a given time which the data cover. These maps show that the declination, inclination and intensity of the geomagnetic field have changed with time during the last approximately 400 years (Merrill et al, 1996).

Paleomagnetism is the study of the history of the Earth's magnetic field as recorded in rocks or sediment. It relies on the fact that magnetic grains in rocks act as small compass needles and align themselves with the magnetic field at the time they were formed. Secular variation records spanning thousands to millions of years form the basis of the paleomagnetic investigation of sedimentary deposits from glacial lakes (Liddicoat et al, 1980). An essential concept of rock

magnetism is *remanent magnetism*, which is the magnetization of a substance such as sediment in the absence of an applied magnetic field (McElhinny, 1973). Remanent magnetism is one of two components which describe the magnetization of any material. The other component, *induced magnetization*, is that induced by an applied magnetic field but which disappears after the removal of that field. Paleomagnetism is concerned with remanent magnetism contained in igneous rocks and undisturbed sediments.

Paleomagnetic studies of lake sediments rely on the property of recorded magnetism in the sediments due to the process called *depositional detrital remanent magnetization* (depositional DRM). As the magnetic grains settle out of the water column in the sedimentation process at the bottom of a lake, they will also align with the position of the Earth's magnetic field at the time (McElhinny, 1973). These grains may also acquire depositional DRM by rotating into the direction of the applied field when they are in the water-filled interstitial holes of a wet sediment (Irving, 1964). Glaciolacustrine sediments should retain good records of the geomagnetic field because their high sedimentation rates favor rapid compaction and dewatering of sediment which lock the magnetic particles in their orientations (Ridge et al, 1990). Thus in a sediment core, a continuous record of small (secular) oscillations in the Earth's magnetic field is available. Relative dating is possible when these can be compared with dated secular variation curves (paleodeclination or paleoinclination logs) from previous studies. These logs may be radiocarbon dated if they contain sufficient organic material, or may be dated by the technique of counting annual varves in clay rich sediment.

Paleomagnetic secular variation curves for similar lake studies, as well as the location of some of the cores used for comparison by Pair et al (1994), are represented in Figure 2. This

figure compiles the paleomagnetic declination in lacustrine sediment in the midwestern and northeastern United States for the interval 9,000 to 17,000 C-14 years BP. The east to west swing at 13,000 - 14,000 C-14 years BP is prominent at Kylen Lake, Minnesota and in the Genesee and Mohawk valleys. The rapid declination change of nearly 60° precedes several thousand years of westerly declination that are assigned to the age 9,500 - 11,500 C-14 years BP. Separate secular variation records can be correlated by matching several consecutive amplitude maxima. Similar declination patterns in two sections from separate cores can only provide supporting evidence for time-equivalence (Ridge et al, 1990). These recognizable patterns, especially drawn over large areas, support relative dating used in combination with absolute (radiocarbon) dating techniques.

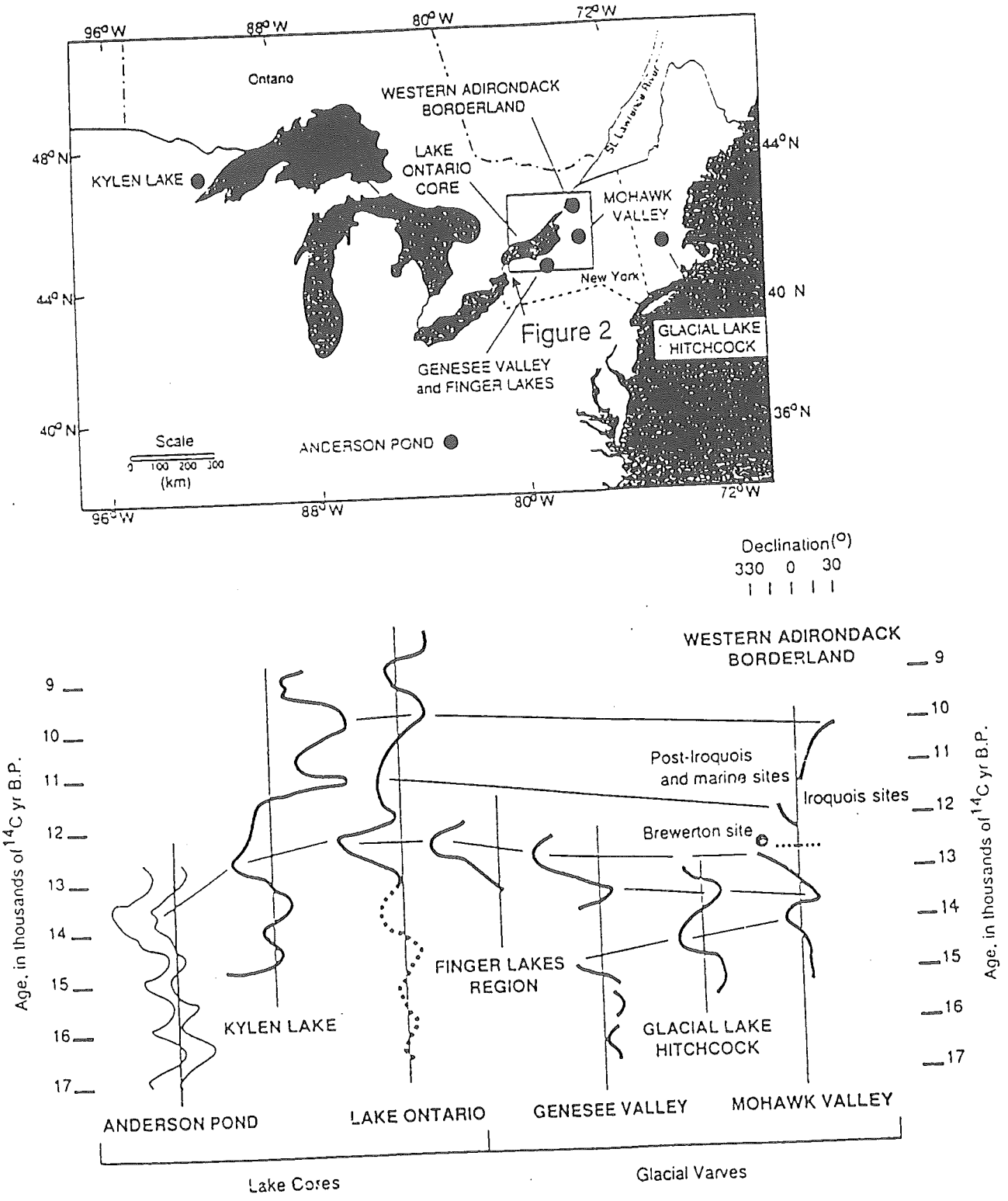

Figure 2: Location map and declination secular variation curves for lake sediment in the midwestern and northeastern United States (Pair et al., 1994)

A paleomagnetic investigation of glaciolacustrine sediment had not yet been conducted in the southeastern New York State region. The correlation of the secular variation record from Sutherland Pond was compared to that of Lake Ontario in northern New York State (Carmichael et al., 1990), Mono Basin, California (Lund et al., 1989), Anderson Pond, Tennessee (Lund and Banerjee, 1985). Through this correlation method the timing of the formation of the pond, the onset of pond sedimentation and therefore glacial retreat in the region of Black Rock Forest, southeastern New York was estimated.

METHODS

Field

Sutherland Pond (41°23'29"N, 74°02'16"W) is located in Black Rock Forest, Orange County, New York. It is 4.05 hectares in surface area and is at 380 meters altitude. The core was taken in August 1991 at a depth of 2.57 m (the maximum depth of the pond), using a square-rod piston sampler of 5-cm diameter (Maenza-Gmelch, 1997). It has since been in cold (4°C) storage at the Biology Department of New York University, where it was sampled soon after recovery for the paleoenvironmental study and then was further sampled in August 1997 for the paleomagnetic study.

Laboratory

Five vertically oriented core segments of about 50 cm each from depths of 700 to 1080 cm were sampled as continuously as possible. The segments had dried significantly and thus were subject to some shrinking (~20%). Sediment compaction need not be treated as postdepositional disturbance unless the compaction is associated with conspicuous deformation (Pair et al, 1994). Intervals which were considered questionable in terms of disturbances such as swirling of sediments due to the twisting of the core barrel during the coring process were either excluded from sampling, or samples were taken from near the middle of the core where disturbance was assumed to be minimal. From visual inspection, the two core segments from 750 cm to 850 cm depth were determined inappropriate for sampling. Each sample was oriented according to an azimuth relative to each core segment. Each core segment had been sliced lengthwise for the previous study, leaving in most cases two halves of the cylindrical segment available for sampling. The orientation for sampling of each core segment was estimated as best as possible from the lengthwise slice, as the segments were roughly aligned when sliced.

The upper three core segments sampled (700 cm - 950 cm) contained clayey sediment which was still moist enough to be cut with a stainless steel razor blade. Although samples were taken from core depths of 702 cm - 744 cm and 852 cm - 931 cm in these segments, only the samples from 852 cm - 931 cm were measured. They were sampled by cutting 2-cm cubes and trimming them to fit in plastic sampling cubes calibrated for use with the instruments in the lab. These plastic sampling cubes were marked with axes so that the sample was oriented in three dimensions, and the core depth of each sample was recorded. The lower two core segments sampled (950 cm - 1052 cm) contained more silty sediment which had dried significantly and

thus were cut with a band saw into cubes of roughly the same size. Althoug samples were taken from core depths of 952 cm - 1052 cm in these segments, samples from 1000 cm - 1052 cm were not demagnetized. The orientation of the cube samples in all three planes along with the core depth were penciled on the surface of each cube.

At the Paleomagnetism Laboratory of the University of California at Santa Cruz (UCSC), the samples were first measured for the intensity and direction of natural remanent magnetism using a 2-G Enterprises Cryogenic Magnetometer. The clayey samples from the upper segments of core sampled were then demagnetized, or magnetically cleaned, using a Sapphire Instruments SI-4 Alternating Field Demagnetizer at increments of 50 oersteds through 400 oe and then at increments of 100 oe through 1000 oe. This instrument creates an alternating field of a specified value (H) which decreases to zero, during the process of which domains with progressively lower coercive force become fixed in random directions. Thus all domains in the sample with coercive forces less than the peak alternating field will have random orientations (McElhinny, 1973). Samples were measured for remanent magnetism after each demagnetization step. The stability of the remanent magnetism was evaluated by recording the persistence of the direction of remanence at higher fields, which was displayed on Zijderveld (1967) diagrams, generated by the computer program during the demagnetization process.

The silt samples from the lower segments of the core were thermally demagnetized using an oven custom built for the lab at UCSC. The samples were heated at intervals of 50° from 100°C to 500°C, then at increasingly smaller intervals to the unblocking temperature, or 625°C, and were measured in the magnetometer between heatings. The step-wise method of thermal cleaning was used, whereby the samples are heated to progressively higher temperatures and

cooled in a field-free space after which they are measured before the subsequent heating. A companion sample from each depth was also treated by alternating-field demagnetization for comparison.

In a separate lab also connected to the Earth Sciences Department at UCSC, hysteresis and isothermal remanence tests were also performed on samples from core depths of 956 cm and 878 cm using a Kappabridge KLY-2 Magnetic Susceptibility Meter and a Princeton Measurements Corp. 'MICROMAG' Alternating Force Magnetometer Model 2900. These high field measurements provide information on the nature and quantity of the magnetic minerals in the samples (Collinson, 1983).

RESULTS

Demagnetization

The Zijderveld diagrams from the paired demagnetization of samples from core depth 983 cm are represented in Figure 3. Sample 983A was demagnetized by the alternating-field method, while sample 983B was demagnetized by the progressive thermal demagnetization method. The distance from each point on the diagram to the origin is relative to the intensity of the magnetization of the sample after the application of a demagnetization field. The changes in the magnetic direction and intensity through alternating-field or thermal demagnetization steps of increasing strength are small, which indicates magnetically stable samples.

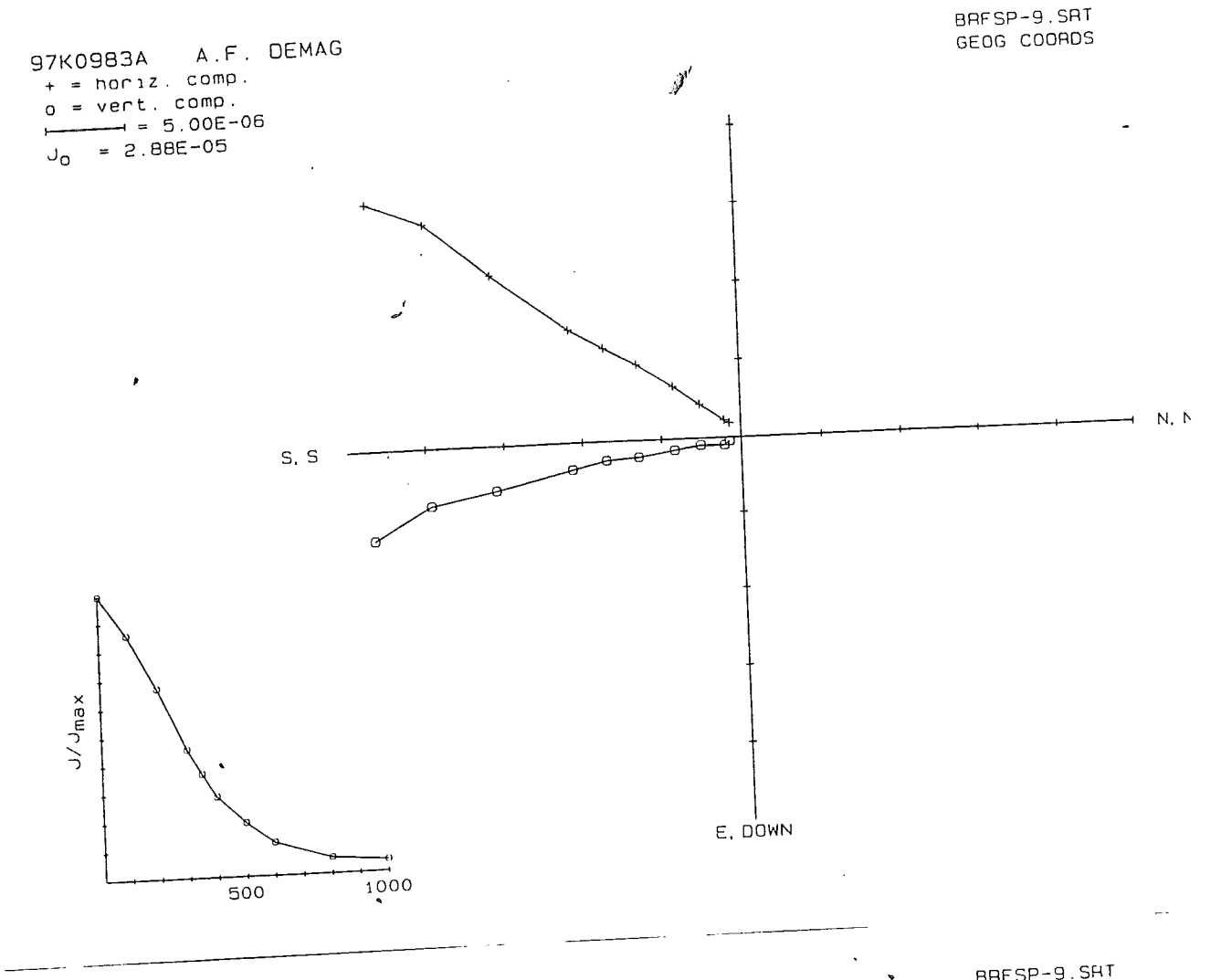

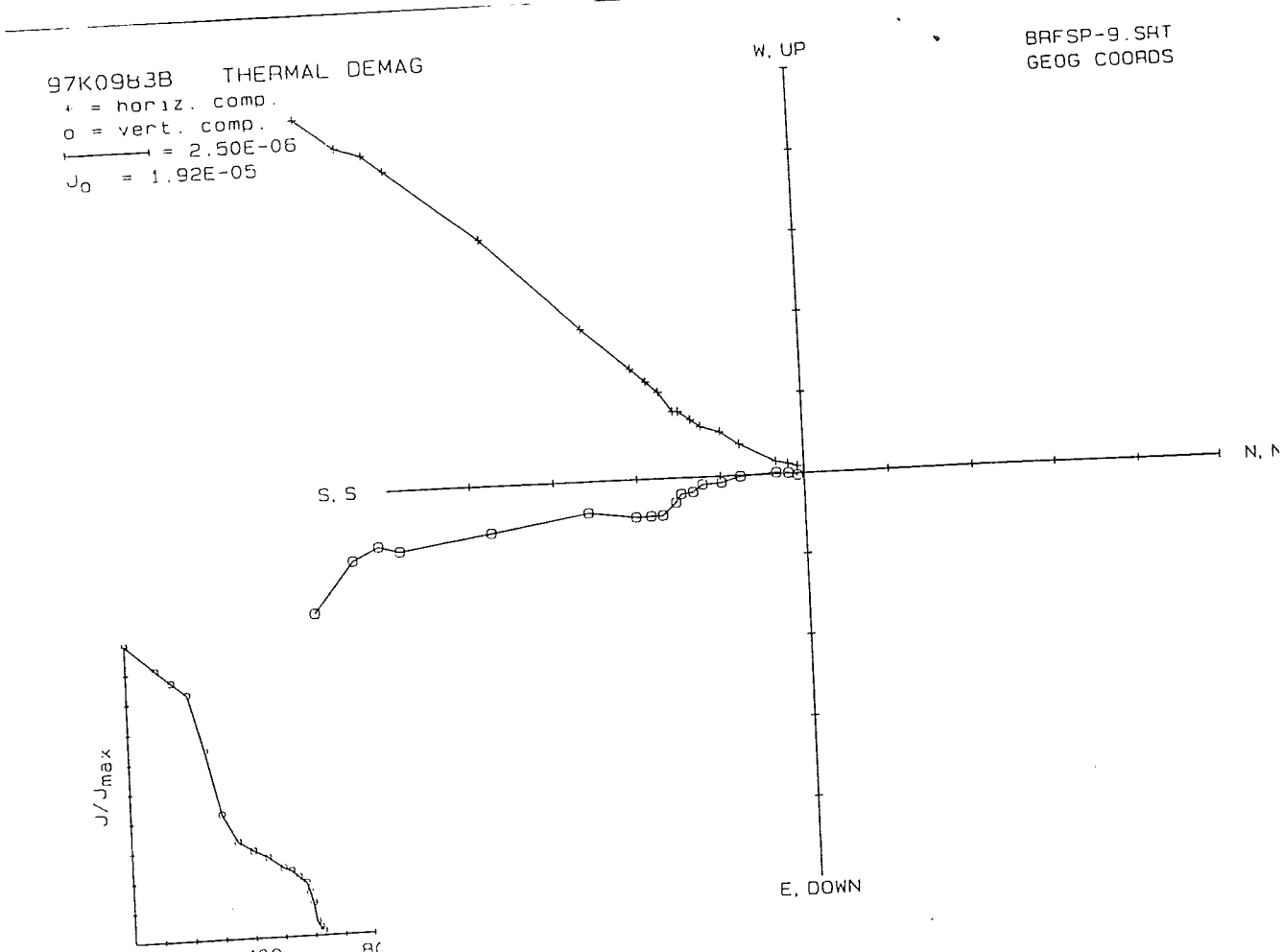

Figure 3: Representative Zijderveld diagrams showing stepwise demagnetization both A-F and thermal) of paired samples from core depth 983 cm. Remanent magnetization remains essentially unchanged by demagnetization process. Azimuth is relative.

The demagnetization data were analyzed using a program which determines the line which would best fit between the points if forced through the origin of the Zijderveld diagrams. This results in the best estimate for the magnetic declination, inclination and intensity at the time of deposition for each sample. Table 1 presents the best fit data from A-F demagnetization at all sample depths. The declination and inclination measurements were used to create the secular variation curves for the Sutherland Pond core BRF-1. The values for paleolatitude (north) and paleolongitude (east) together identify the position of the magnetic north pole at the time of deposition of the sediments in each sample. These can be used for separate analyses not undertaken in this paper which track the movement of the virtual geomagnetic pole (VGP) across the surface of the Earth with changes in the field.

Table 1: Paleomagnetic data from all samples

No.	Depth	Incl	Decl 1	Decl 2	Intensity (emu)	N	PLAT (N)	LONG (E)
52	852	28.1	171	40	7.22E-07	1	46.49	41.58
51	854	19.7	118.6	347.6	9.29E-07	1	56.8	128.71
50	856	42.6	104.6	333.6	7.29E-07	1	59.7	131.6
49	858	42.9	112.3	341.3	8.40E-07	1	67.3	154.9
48	860	36.2	126.1	355.1	1.18E-06	1	68.2	118.47
47	862	29.3	121.9	350.9	1.03E-06	1	63	125.6
46	864	29.8	119.1	348.1	1.24E-06	1	62.49	131.42
45	866	44.6	122.5	351.5	1.38E-06	1	73.2	133.3
44	868	32.3	153.9	22.9	1.92E-06	1	59	59.8
43	870	31.6	146.2	15.2	1.26E-06	1	62.3	73.3
42	872	33.5	132.4	1.4	1.44E-06	1	66.8	102.6
41	874	40.2	138.4	7.4	1.53E-06	1	70.4	85.3
40	876	42.8	124.9	353.9	1.79E-06	1	72.6	124.8
39	878	41.9	121.7	350.7	1.65E-06	1	71	133
38	880	40.5	127.9	356.9	1.67E-06	1	71.4	115
37	882	43.2	140.4	9.4	1.46E-06	1	71.9	77.6
36	886	39.9	141.8	9.4	1.49E-06	1	69.6	80.4
35	888	49.6	148	15.6	2.83E-06	1	73.3	52.4
34	890	50.5	134.1	1.7	1.87E-06	1	79.7	97.9
33	892	53.1	153.5	21.1	1.52E-06	1	71.6	34.4
32	894	43.9	143.5	11.1	1.68E-06	1	71.7	72.4
31	896	38.1	145.1	12.7	1.85E-06	1	67.2	74.1
30	898	38	138.1	5.7	2.24E-06	1	69.3	90.9
29	902	33.3	296.3	5.7	1.30E-06	1	66.2	92.5
28	904	30.5	296.1	5.5	1.68E-06	1	64.5	93.7
27	905	29.9	295.4	4.8	2.15E-06	1	64.2	95.4
26	907	36.4	300.6	10	1.71E-06	1	67.1	81.2
25	912	31.1	207	10	1.96E-06	1	63.8	83.9
24	914	37	236.3	39.3	1.59E-06	1	50.9	36
23	916	33.7	235.6	38.6	1.45E-06	1	49.9	39.3
22	921	36	242.1	38.6	2.03E-06	1	50.9	37.5
21	923	36	222.5	19	2.07E-06	1	63.1	63.4
20	924	32.7	237	34	1.92E-06	1	52.5	44.9
19	931	42.5	238.6	34	2.09E-06	1	57.2	36.2
18	952	15	275.4	34	1.48E-06	1	44.7	54.8
17	954	37	239.1	357.7	1.36E-06	1	69.14	112.58
16	956	47.7	235.2	353.8	1.69E-06	1	76.42	129.77
15	958	38	245.9	4.5	1.55E-06	1	69.58	93.91
14	960	34.4	242.4	1	2.39E-06	1	67.48	103.53
13	962	32.1	242.9	1.5	2.78E-06	1	65.98	102.48
12	968	22.9	257.7	1.5	2.58E-06	1	60.5	103.02
11	970	23.5	253.8	357.5	3.29E-06	1	60.78	111.01
10	972	32.6	256.2	0.5	2.07E-06	1	66.33	104.81
9	975	32.5	247.7	351.4	2.10E-06	1	65.15	125.82
8	979	33.5	241.6	351.4	1.91E-06	1	65.77	126.24
7	981	22.2	243.8	353.6	2.30E-06	1	59.61	118.47
6	983	10	215	324.8	8.14E-06	1	41.96	156.55
5	986	18.6	228.1	337.8	4.06E-06	1	52.66	143.72
4	988	26.6	241.6	351.4	1.56E-06	1	61.65	123.79
3	992	24.5	256.7	351.4	2.29E-06	1	60.47	123.2
2	994	24.5	240.7	335.4	1.86E-06	1	54.28	150.05
1	996	31.6	259.2	353.9	2.06E-06	1	65.14	119.98

Key:
Decl 1- raw declination measurements
Decl 2- adjusted declination measurements (fit to central axis for comparison)
Int- Intensity (emu) of remanent magnetisation of samples demagnetized to 40mT
N- Number of samples at that depth used in best fit analysis
PLAT (N)- Paleolatitude (North) of magnetic north pole
PLONG (E)- Paleolongitude (East) of magnetic north pole

Paleomagnetic Secular Variation Record

Curves representing variation in the orientation (both declination and inclination) of the magnetic grains in the sediment through time were created for Sutherland Pond by plotting the best fit data from each core depth. These curves are presented in Figure 4. The curves are not continuous as the core was segmented and, as previously noted, certain segments of the core were determined unacceptable for sampling. The core segments appear to have rotated resulting in the discontinuity of the declination curve on the right. Thus the secular shift between core segments was assumed to be zero and the outlying curve segments were connected accordingly to produce the corrected declination curve in the middle of the Figure 4. The inclination curve does not require correction as rotation of core segments would not have the same effect on inclination measurements as that on declination measurements.

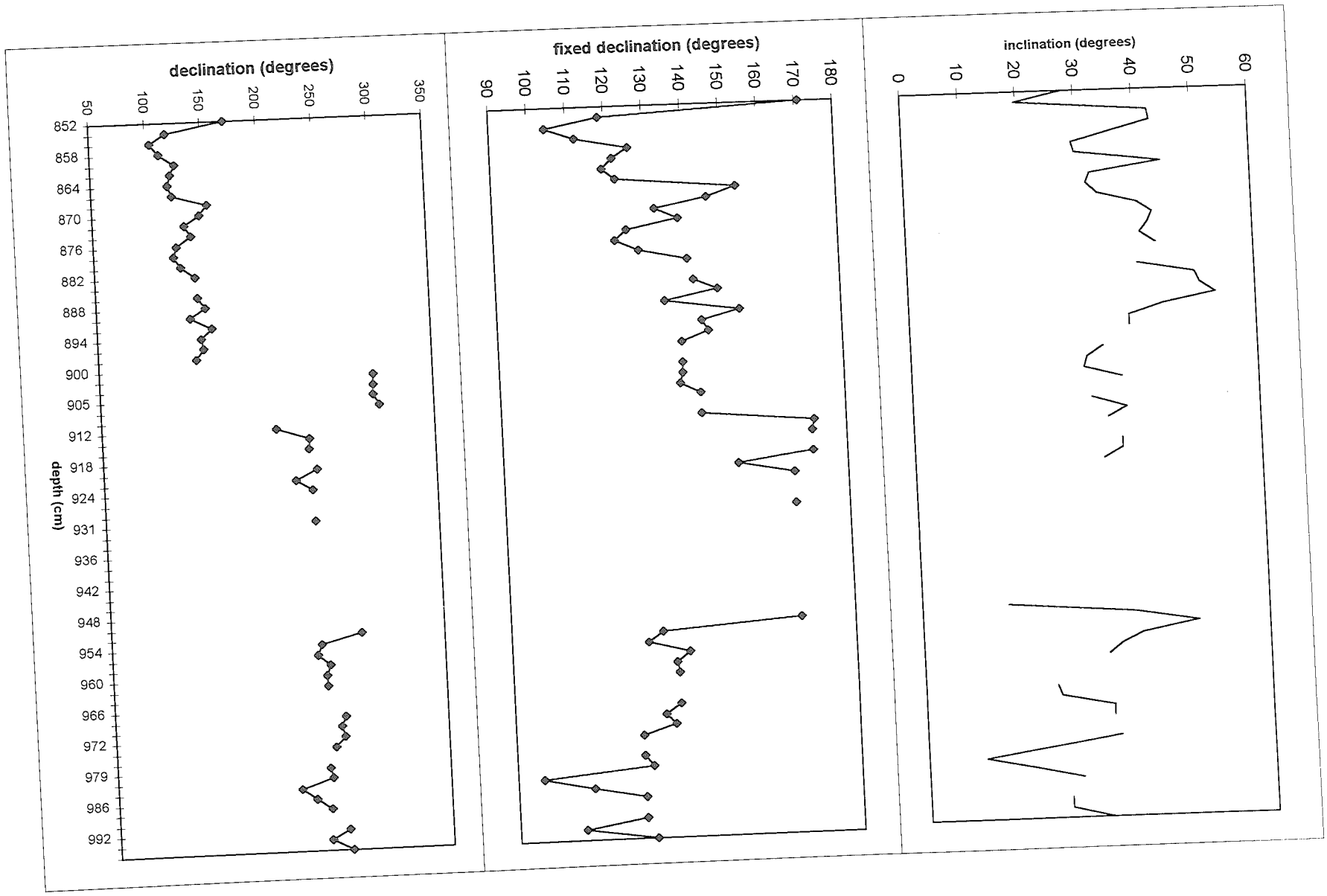

Figure 4: Secular variation curves of both declination and inclination measurements for Sutherland Pond core BRF-1. The declination curve on the right was corrected for possible core segment rotation to produce the middle declination curve.

The paleomagnetic secular variation record from Sutherland Pond was compared to results from a similar study done in Lake Ontario (Carmichael et al, 1990). Curves from both studies are represented in Figure 5 for comparison and relative dating of the Sutherland Pond core. Both the declination and inclination curves from the Sutherland Pond core are compared to those from Lake Ontario sediments. The axis on the left of the figure represents the depths (m) of the Lake Ontario core record, which do not correlate with those of Sutherland Pond, located above the curves in the center of the figure. The depths of two separate records should not necessarily coincide since sedimentation rates differ at the two sites due to location, the separate natures of the two bodies of water, and inputs to the system. The right hand axis designates the age scale of the Lake Ontario core, in calendar years. This age scale was adopted by Carmichael and others (1990) by comparing the Lake Ontario secular variation records for both declination and inclination to a dated core from Elk Lake in Minnesota studied by Sprowl and Banerjee (1985). The Elk Lake sediments were dated in calendar years based on counted varves covering the last approximately 7,000 years. The upper half of the Lake Ontario paleomagnetic curves were matched to those for Elk Lake sediments in order to estimate the age of 7,000 years BP at about 5 m depth. A curve derived by Creer and Tucholka (1982) which compiles dated information from lakes Kylen and St. Croix (Banerjee et al 1979) and Lake Superior (Mothersill, 1979) and Lake Huron (Mothersill, 1981) was also used for comparison. This curve also showed agreement with the Lake Ontario curve and placed an estimated age of 7,000 years BP at 5 m depth. This age scale was then linearly extended to the bottom of the Lake Ontario curve. This age scale is now also used to put an age estimate on the bottom of the Sutherland Pond core, allowable due to the possible correlation between the secular variation records.

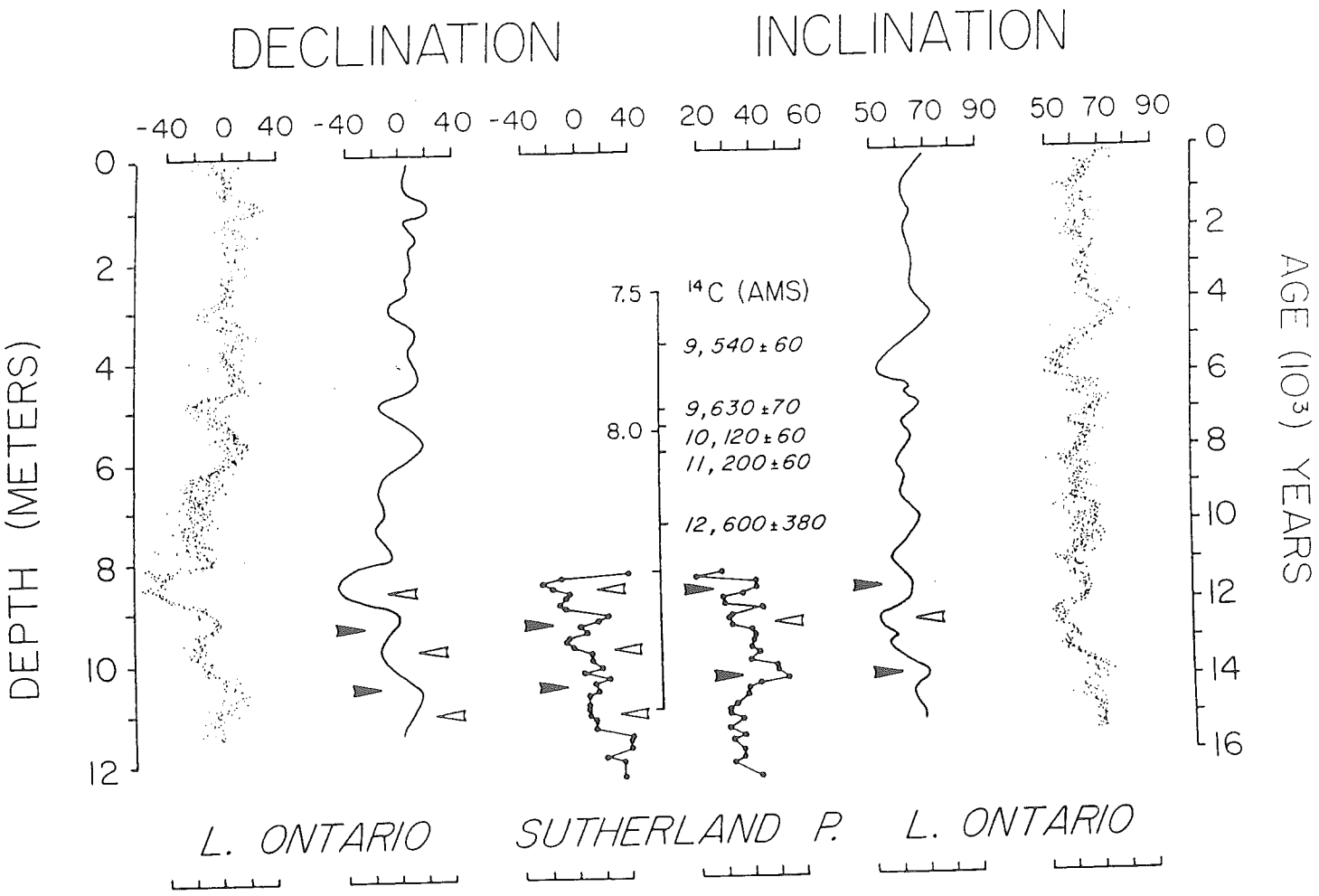

Figure 5: Secular declination and inclination variation curves of both Sutherland Pond core BRF-1 and Lake Ontario (Carmichael et al, 1990) core for comparison

Rock Magnetism

The results of hysteresis and isothermal remanence tests, intended to determine the magnetic mineralogy of two representative silt and clay samples, are represented in Figures 6 and 7. During these tests samples are exposed to applied magnetic fields that domains within the sample will align with but will return to their previous position if the field is weak. As progressively stronger fields are applied, the domain walls will rotate past impurities or vacancies in the material and thus will not return to their previous orientation. The resulting remanent magnetization of the sample, called *isothermal remanence,* is acquired by the application of magnetic fields at a constant temperature. At higher fields the intensity of isothermal remanence increases until it reaches its peak value, the *saturation moment.* When a magnetic field is applied in the opposite direction, the isothermal remanence is overcome and the magnetization of the sample is reduced to zero in a field called the *coercive force* or *coercivity* (H-c). The application of magnetic fields in one direction followed by the reverse direction results in a *hysteresis loop* due to the systematic behavior of the magnetization. This loop defines important characteristics of rock magnetism such as the saturation moment (M-sat), the field required to attain it (H-sat), and the reverse direction field required to reduce the isothermal remanence back to zero, called the *back field coercivity* (H-cr). The area bounded by a hysteresis loop is directly related to the specific composition of the magnetic mineral present and can thus be used to identify the material (Tarling, 1983). Both tests showed saturation moments ranging from 193 to 569 μemu and back field coercivities of 258 Oe and 298 Oe. These parameters indicate that magnetite is the primary carrier of magnetism in the samples.

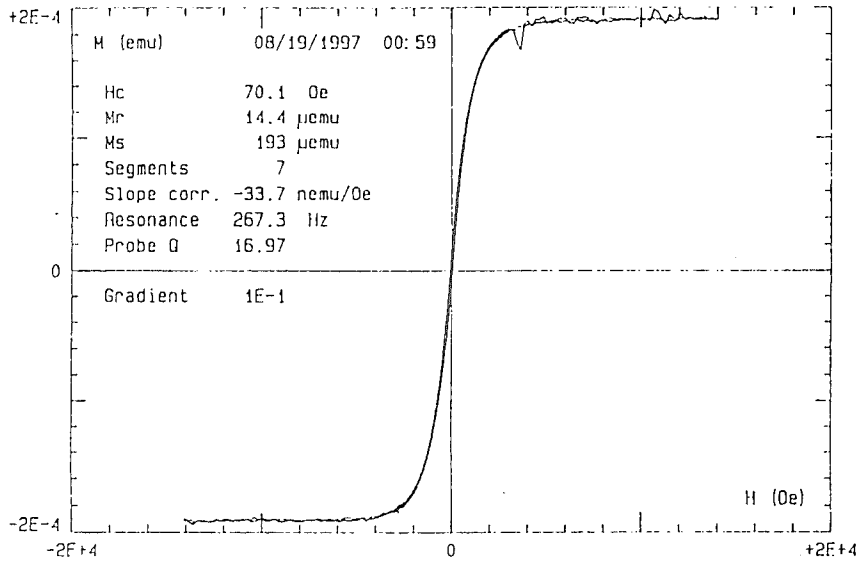

956c
File: 956C.HYS

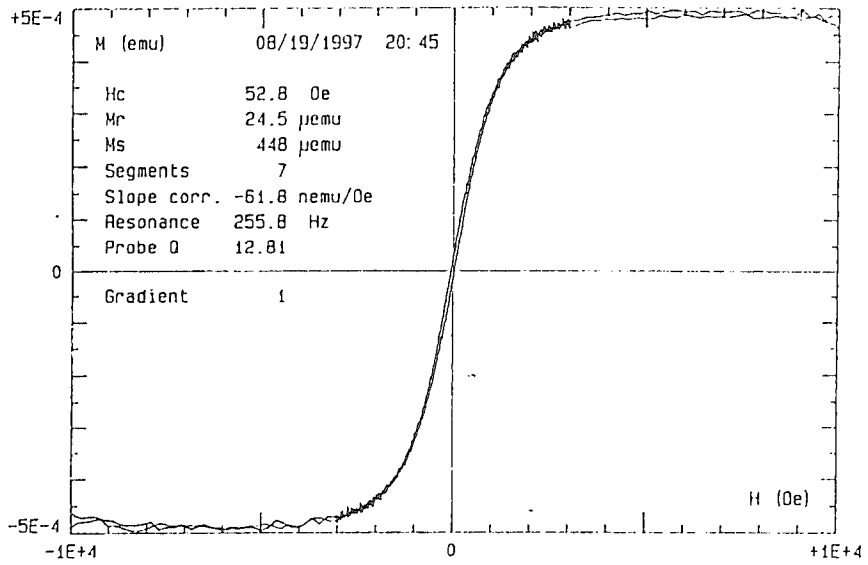

879
File: 879.HYS

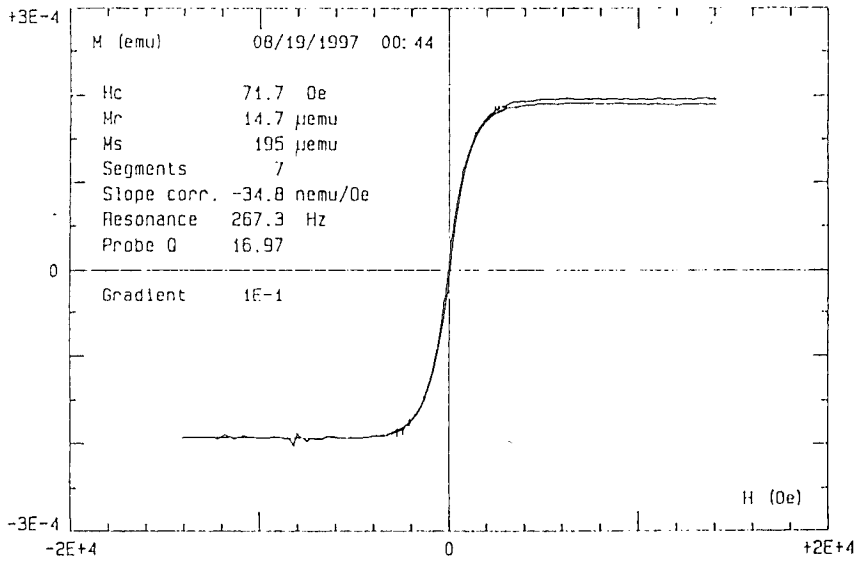

956c
File: 956C.HYS

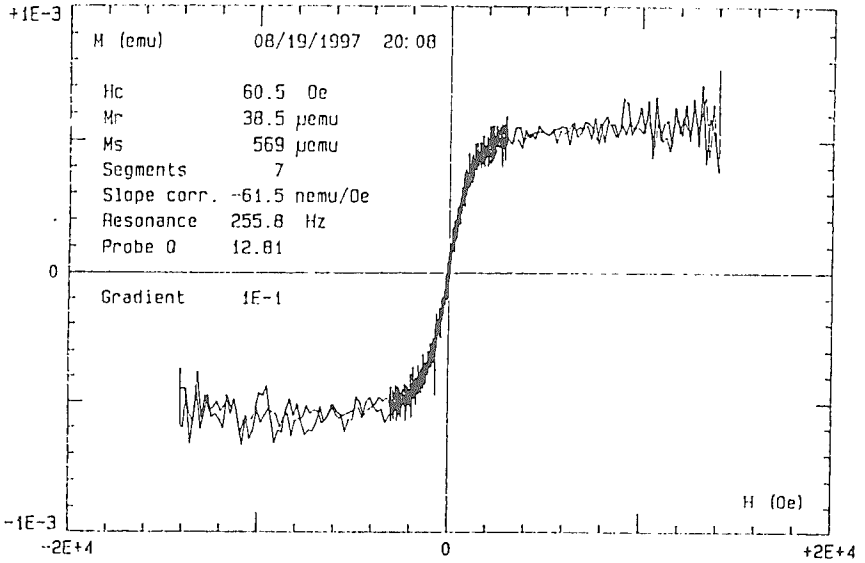

879
File: 879.HYS

Figure 6: Results of hysteresis tests performed on samples from core depths 879cm (clay) and 956cm (silt)

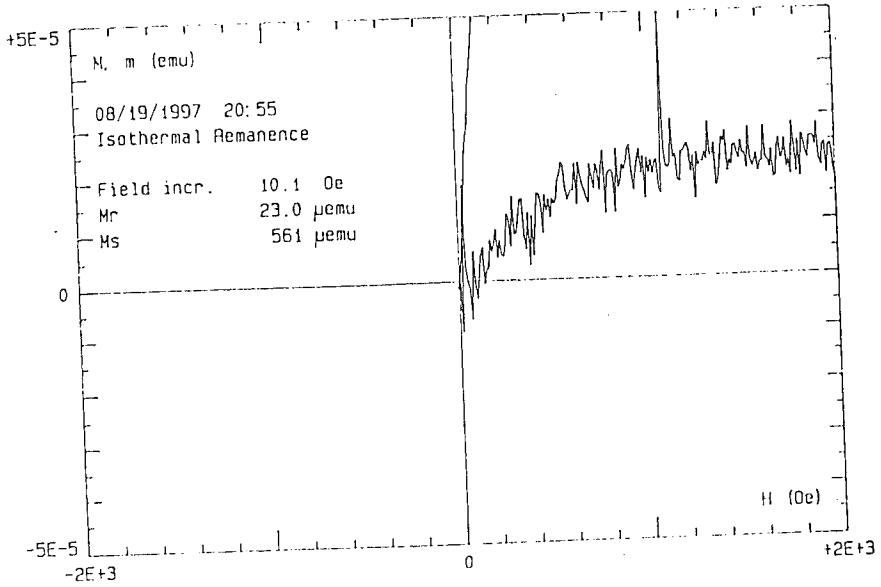

879
File: 879.IRM

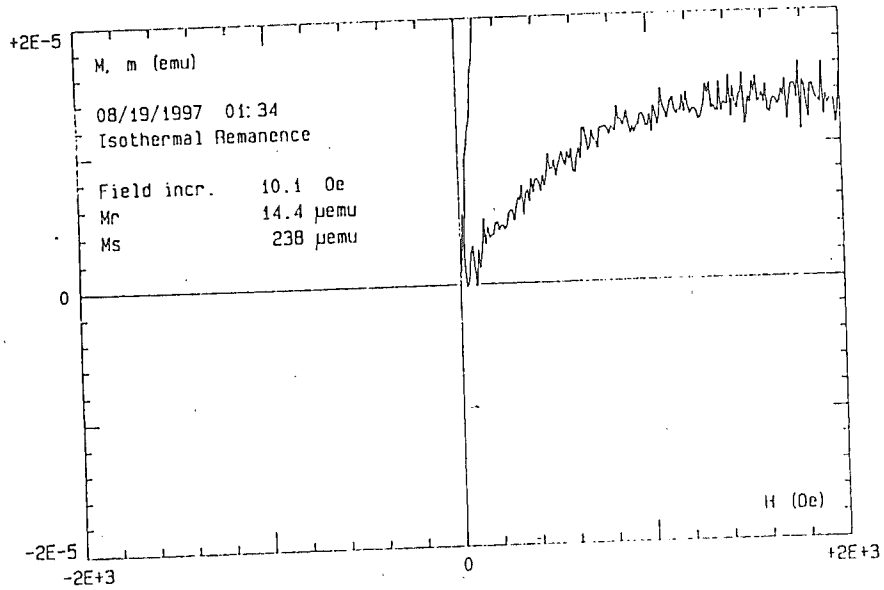

956
File: 956C.IRM

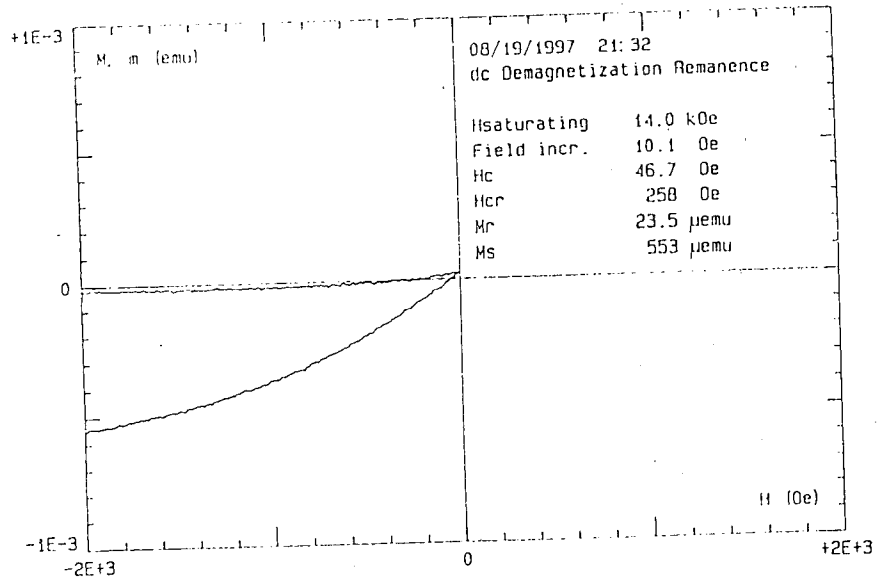

879.dcd

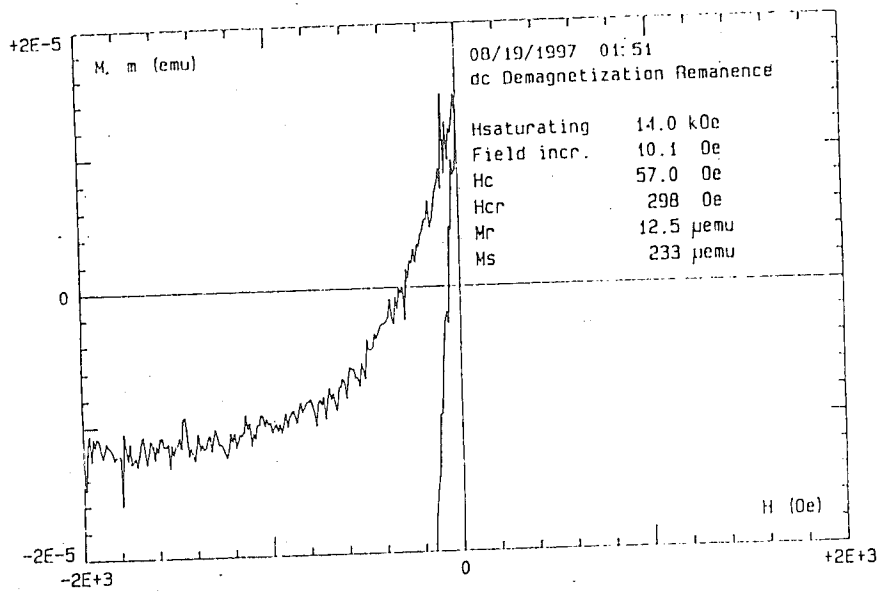

956c
F : 956C.DCD

Figure 7: Results of isothermal remanence tests performed on samples from core depths 879cm (clay) and 956cm (silt)

DISCUSSION

Comparison of Secular Variation Records

The secular variation of the Earth's magnetic field over time is recorded in the sediment when fine-grained magnetic minerals such as magnetite align with the field at the time of deposition. The diagram in Figure 5 shows the correlated portions of the horizontal and vertical components (relative declination and inclination) of the paleomagnetic field in BRF-1 plotted versus depth and matched with those found in Lake Ontario sediment.

The paired declination curves of Sutherland Pond and Lake Ontario in Figure 5 are highly correlated. The arrows on the figure designate suggested amplitude maxima shared by the two records. The youngest of the paired maxima both involve a westward drift in declination of similar amplitude and duration followed by a swing back in the eastward direction to the second point of comparison. The third paired amplitude maximum involves a shallower and slower westward drift in declination. This drift is more exaggerated in the Sutherland Pond record but is still a valid companion to Lake Ontario. The two older matched amplitude maxima are not as strongly correlated as the younger three. Below core depth 9 m, the two records could not be compared, as Sutherland Pond's record is older. An age estimate of 16,000 years BP can be placed at core depth 9.3 m for BRF-1 based on the Lake Ontario age scale. In roughly a meter of sediment measured from the oldest radiocarbon age (calibrated to 14,800 years BP) to the bottom of the usable portion of the declination curve, about 1,900 years of sedimentation are represented. The bottom portion of the Sutherland Pond paleomagnetic record is not pictured in Figure 5, since it is older and thus not able to be matched to the Lake Ontario record.

The inclination record comparison is not as strong as that for declination due to discrepancies in their ranges. Inclinations in the Sutherland Pond record range from roughly 20° to 50°, while in the Lake Ontario record they range from roughly 50° to 70°. This may be attributable to compaction of the Sutherland Pond sediments due to drying out over 6 years of storage (Ridge et al, 1990). The youngest compared maximum consists of an inclination shallowing which appears more gradual in the Lake Ontario sediments than Sutherland Pond's. With the exception of one point, which may just be incidental, the second point of comparison is a shift back towards steeper inclination measurements. A more convincing comparison is evident in the strong shallowing seen in both records designated the third (oldest) matched amplitude maximum. The correlation in the inclination records, while not quite as strong as that of declination, provides further evidence as to the validity of age comparison between the two curves.

The inclination record below 9.5 m, while not useful for correlation with Lake Ontario sediments, is useful in estimating the age to the bottom of the Sutherland Pond core. As can be seen in Figure 4, the bottom portion of the inclination record steepens from about 20° to 40° through roughly a meter of sediment. This inclination steepening is suspected to have taken roughly 1,500 years based on a similar change in inclination noted in radiocarbon dated Mono Lake sediments (Lund et al, 1988). It is possible that this silty basal portion of the core was rapidly deposited following deglaciation, when the dynamic periglacial environment may have caused high sedimentation rates from glacial outwash.

If the silty portion of the core was rapidly deposited over roughly 1,500 years in the periglacial period following the Wisconsinan Ice age, this can be added to the estimated age at

9.3 m based on correlation with Lake Ontario. This results in an age estimate age of roughly 17,500 years BP at the base of the core (10.6 m depth), which is therefore the suggested timing of glacial retreat. That estimate is comparable to the estimated age for the termination of glaciation in the Great Valley west of the Hudson Highlands (Connally et al, 1989; Connally & Sirkin, 1973). This is also in accord with estimates of glacial retreat at 18,670 years BP based on organic dating of cored peat from Eagle Hill Camp Bog in the Hudson Valley about 80 km north of Black Rock Forest (Connally and Sirkin, 1986). Since glaciolacustrine deposits must postdate the maximum extent of the Wisconsinan ice sheet dated, this suggested timing is reasonable as maximum glacial coverage in western Pennsylvania was dated at 21,500 years BP (Cotter et al, 1986).

Sedimentation Rate

Figure 8 plots depth vs. age in calendar years for the dated organic portion of core BRF-1. The lower two meters of the core consist of a meter of laminated clay underlain by a meter of fine-grained silt. The sedimentation rate for sediment rich in organic matter is much faster than silt or clay. A rise in sedimentation rate at 8 meters (the onset of heavy organic deposition) is evident.

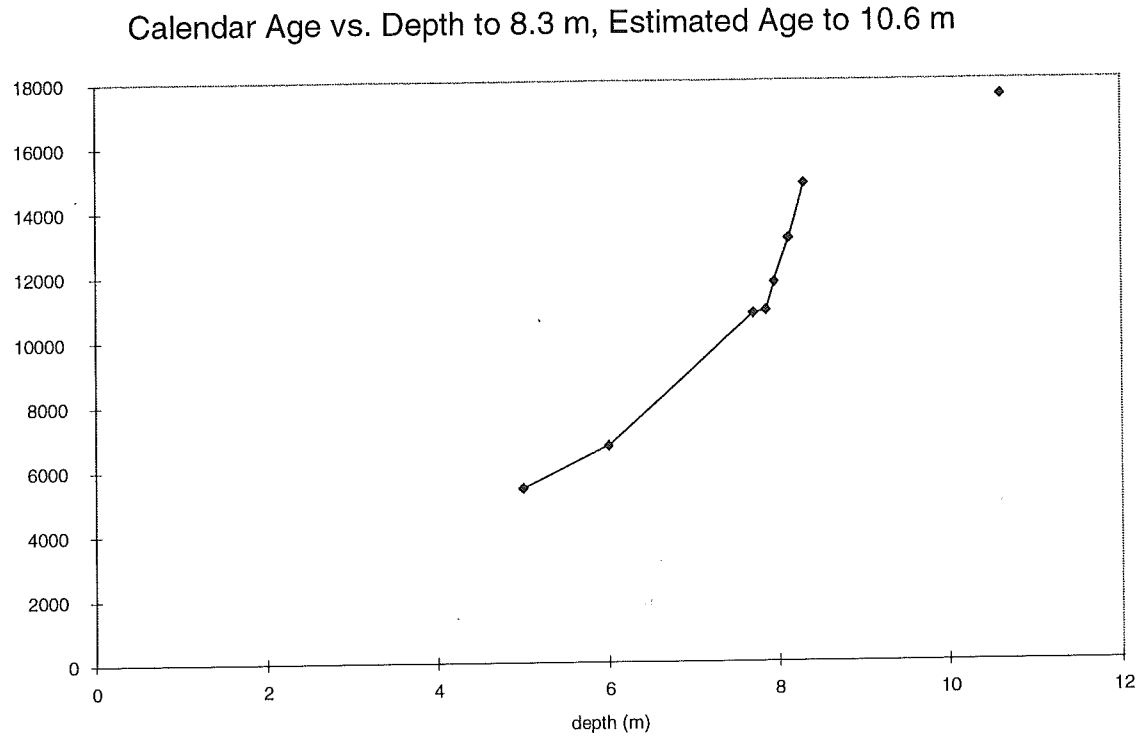

Figure 8: Scatter plot showing depth vs. age (calendar years BP) for Sutherland Pond Core BRF-1 (Maenza-Gmelch, 1997b). The datum point (17,500 years BP) at 10.6 m was estimated by the technique outlined.

The age vs. depth curve in Figure 8 shows a slowed sedimentation rate near the bottom of the core at approximately 8 m depth, where organic content was minimal. Sedimentation rate increases from ~3 cm/1000 years (1 cm/300 years) to ~1m/1000 years with the onset of organic deposition, which is the average sedimentation rate for lakes in this region (Peteet, D.M., 1997, pers. comm.). Sometime after the increased organic flux 14,800 years BP noted by Maenza-Gmelch (1997b), the sedimentation rate increased as well, between 9,000 and 10,000 years BP. This fluctuation in sedimentation rate serves as an example of the unreliability of assumed rates

in downward extrapolation from dated surfaces pointed out by Muller and Calkin (1993). The sedimentation rate in the inorganic region near the bottom of the core may have been even slower, creating the need for an alternative means of estimating the age of onset of lake sedimentation such as paleomagnetic investigation.

The sedimentation rates during deposition of the studied silt and clay portions of the core may be very different. It is possible that the proximity of the glacier during the time of deposition of the silty basal portion of the core could have caused a faster deposition rate by releasing or stirring up sediments. This may have subsided as the glacier retreated further north resulting in a slowed deposition rate in the younger laminated clay portion of the core. In Figure 8 a line of slope m=2.7 can be drawn between the age data points for depths 7.7 m to 8.3 m, representing sedimentation rate shortly after organic deposition resumed. A line of slope m=0.5 can also be drawn connecting the radiocarbon age at 8.3 m to the paleomagnetically estimated age at 10.6 m. This suggests that an inorganic sedimentation rate approximately 5.5 times faster preceded a slowing in sedimentation around the resurgence of vegetation. Sedimentation then appears to gradually increase following the onset of organic deposition 14,800 years BP.

It is likely that the sedimentation rate was not constant throughout the bottom 2 m of the core. A faster inorganic sedimentation rate in the basal region of the core may have been caused by the glacier's proximity and may have occurred in a shorter interval which could not be determined through the scope of this study. It was assumed by this analysis that the portion of the silt layer that was sampled was deposited over a period of about 1,500 years. It is also not possible in the scope of this study to determine the magnitude or constancy of the silt sedimentation following deglaciation. The unreliability of assumed sedimentation rates may still

be responsible for an inaccurate date on glacial retreat found at Sutherland Pond in comparison to adjacent regions, as some linear extrapolation was relied upon to estimate the age at the base of the Sutherland Pond core.

Correlations Across the United States

Composite information from paleomagnetic studies of rock outcrops and lake cores of simultaneous deposition may allow correlations of secular variation to be drawn over large areas. Recently Lund (1996) has shown that distinctive magnetic-field features in Holocene records of paleomagnetic secular variation can be traced across North America for more than 4000 km without change in pattern. Figure 9 compiles secular variation curves from declination and inclination measurements from Sutherland Pond, Lake Ontario (Carmichael et al, 1990), Anderson Pond, Tennessee (Lund and Banerjee, 1985), and Mono Basin, California (Lund et al, 1988). The Sutherland Pond, Lake Ontario and Anderson Pond studies were all performed on lake cores, while the Mono Basin paleomagnetic analysis was performed on fully oriented samples from an outcrop. This is intended to show the possible correlations of secular variation records drawn across the United States using published records and the Sutherland Pond curves. The set of curves on the right-hand side have been drawn on to show these possible correlations and matched amplitude maxima. Figure 10 shows the locations of each of the study sites used for correlation.

In the inclination curves, the pattern of high to low and return to high is evident on the Mono Lake curve and the Anderson Pond curve. These are represented by the H and L markers

on the right hand set of curves in Figure 9. The curves for Lake Ontario and Sutherland Pond, as younger records compared to Anderson Pond and Mono Lake, contain only two of the amplitude maxima (a low followed by a high). Similar patterns of matched amplitude maxima can be seen in the declination curves, as designated by the darts and the lines drawn on the right set of curves. All of the declination curves follow a pattern of high frequency oscillation of amplitude 10° about magnetic north. An east to west swing in average declination when the field is traced from young to old is evident especially in the three center curves, as noted by the best fit lines drawn through the curves. The lake cores (Anderson Pond, Lake Ontario and Sutherland Pond) are each aligned according to a relative north azimuth due to the coring process whereas the Mono Lake outcrop samples were aligned and measured according to absolute north azimuth, which may explain differences in the trends of declination patterns.

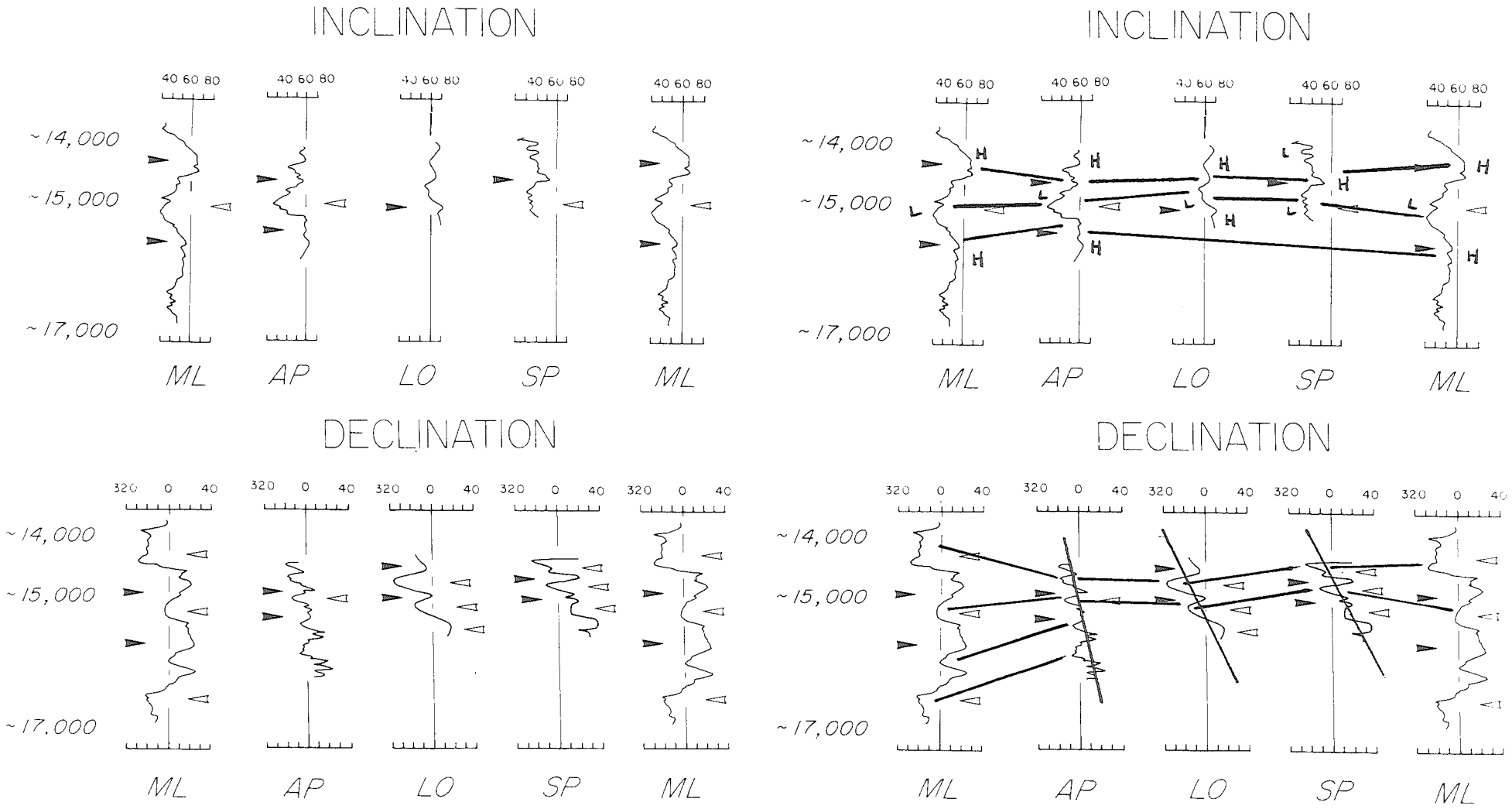

Figure 9: Composite of secular variation curves from published records of Sutherland Pond, Lake Ontario (Carmichael et al, 1990), Anderson Pond, Tennessee (Lund and Banerjee, 1985), and Mono Basin, California (Lund et al, 1988)

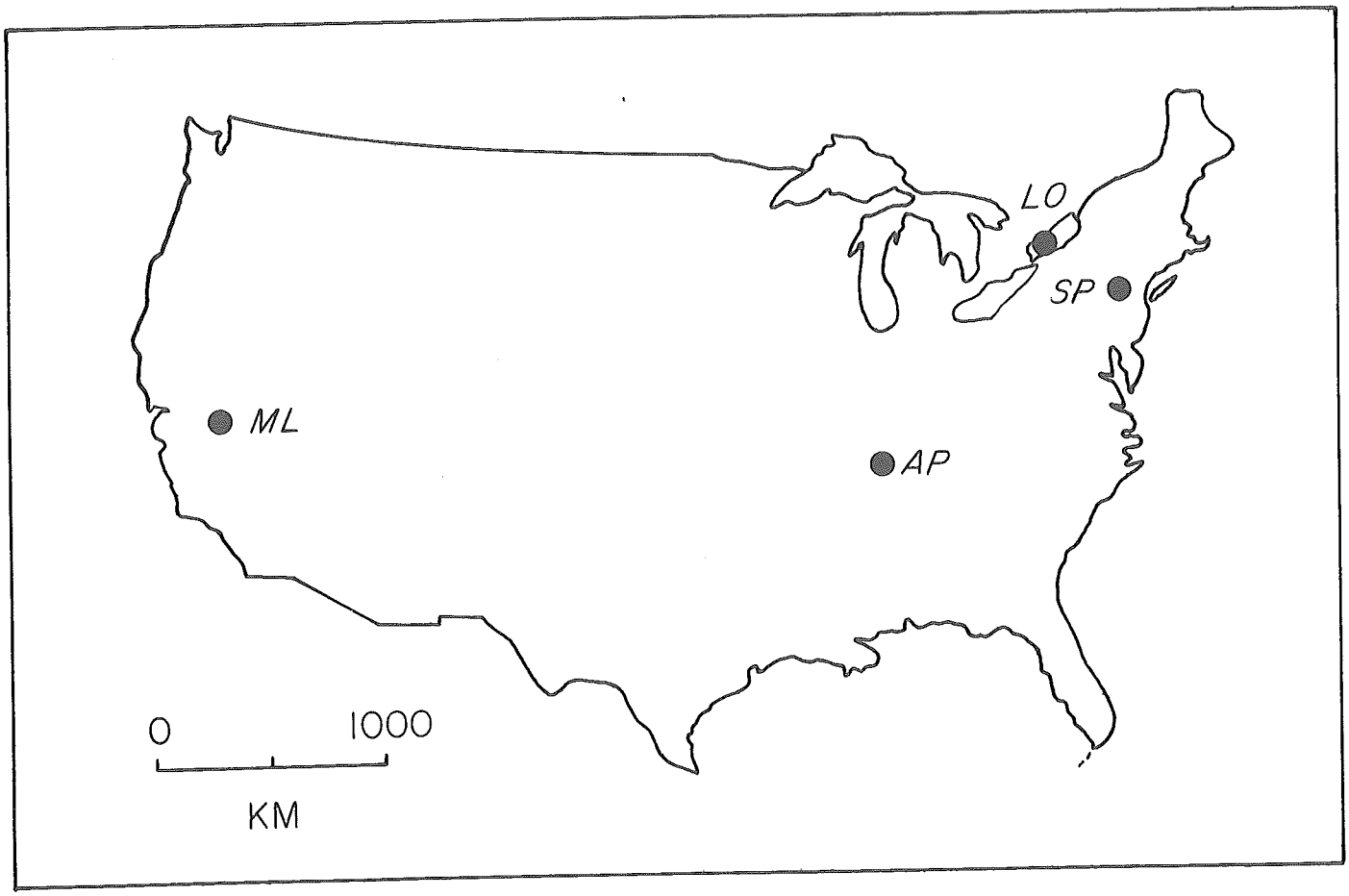

Figure 10: Map of United States showing locations of the four sites studied and represented in the secular variation curves in Figure 9

CONCLUSION

The Holocene epoch is characterized by higher temperatures than the Pleistocene, and thus dramatic vegetational change followed deglaciation. With this climate warming, tree populations migrated northward from glacial refuges south of the ice margin (Maenza-Gmelch, 1997a). Paleoenvironmental information within core BRF-1 points to distinct vegetational assemblies which have existed since deglaciation that indicate episodes of successive climate warming and cooling. A summary of the paleoenvironmental and paleomagnetic information contained in the Sutherland Pond core is presented in Figure 11.

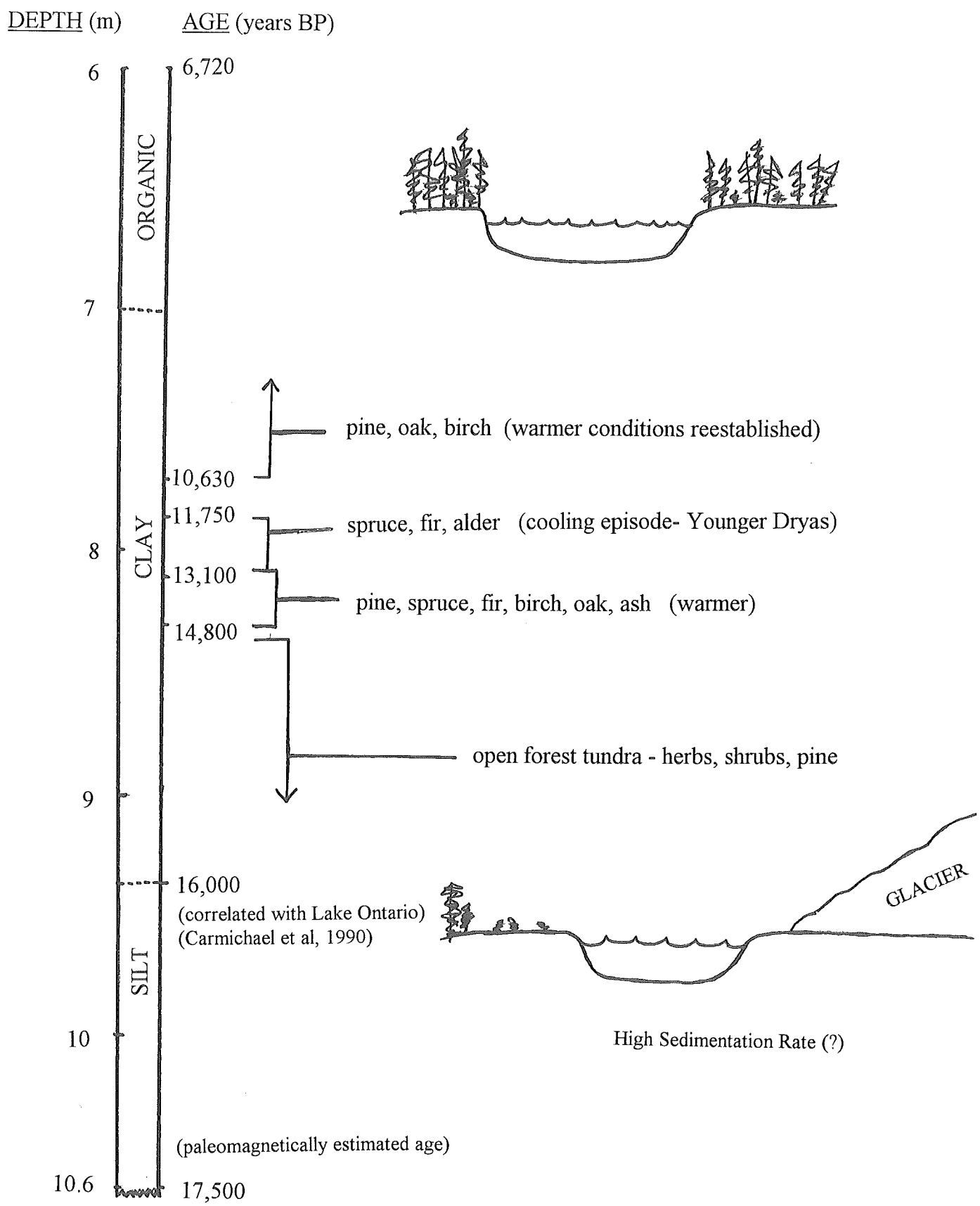

Figure 11: Summary of paleoenvironmental (Maenza-Gmelch, 1997b) and paleomagnetic information contained in BRF-1, Sutherland Pond

The first vegetational assemblage which existed after deglaciation included herbs, shrubs, pine and possibly spruce, which is interpreted to represent an open vegetation such as a forest tundra (Maenza-Gmelch, 1997b). The gradual postglacial warming evident in the increased organic deposition, large increase in pollen influx and the first occurrence of macrofossils noted in Sutherland Pond sediments by Maenza-Gmelch (1997b) was dated at 14,800 years BP. Based on evidence, the arboreal assemblage between 14,800 years BP and 13,100 years BP included pine, spruce, fir, birch, oak and ash trees, indicating warmer temperatures. A cooling episode interpreted as the Younger Dryas is evident between 13,100 years BP and 11,750 years BP due to the dominance of spruce, fir and alder (Maenza-Gmelch, 1997b). This preceded the sharper Holocene warming about 11,000 years BP characterized by pine, oak and birch dominance around Sutherland Pond. It is about this time that the pond sediments began to contain less clay and more rich organic matter, indicating a probable rise in sedimentation rate.

The analysis outlined in this paper suggests a period of roughly 2700 years following deglaciation 17,500 years BP of relative cool climate until sufficient postglacial warming allowed the resurgence of temperate vegetation. The periglacial environment directly following glacial cover in the region may have been too harsh a climate for temperate vegetation due to the proximity of the glacier, possible ice wasting, high winds and low temperatures. Short intervals of cooling may have occurred which could have slowed or halted glacial retreat. While the timing of climate change is regionally unsure, 2700 years may be an underestimate of the speed of change from glacial to postglacial climates. This may be due to the unreliability of the age scale, estimated in varve years by Carmichael and others (1990), used for correlation and dating

purposes in this study, as well as that of assumed sedimentation rates in the basal meter of the core.

RECOMMENDATIONS

Since this study involved downward extrapolation of the age scale, and was based on data from other studies which also relied upon downward extrapolation, the resulting estimate of age of lake formation is perhaps inadequate. This study serves better as an example of a probable technique for dating inorganic glaciolacustrine sediments. A further study of this type should involve a core which is taken and sampled immediately. It is also important that the core segments be well oriented to minimize segment rotation which invalidates declination measurements, as well as sediment drying and compaction which invalidate inclination measurements. A problem encountered in this research was finding adequate dated secular variation records in the northeastern United States with which to compare the results. While numerous records of this type do exist, those located to the north postdate the record from Sutherland Pond. This information will become more valuable once sufficient studies are performed to show regional trends as I have attempted for the United States. Records from points south of the glaciated zone might be more valuable for purposes of dating glacial lakes as they may be older. These older lakes may be able to not only provide an adequate paleomagnetic secular variation curve for comparison, but are more likely to have sufficient datable organic matter which predates glaciation in the north.

Wellner and Dwyer (1996) state that in order to better understand past climate change, and to potentially predict that of the future, high-resolution stratigraphic records are needed of glacial to postglacial periods. A possible further study for this region should involve chronostratigraphic correlation of this glacial to postglacial transition based on sediment lithologies, mineralogy, pollen and magnetic data. This combination of paleoecological and paleomagnetic information should be complimentary and allow for valid age estimation. As can be seen through the results of this study, the perfect solution to this type of analysis would be a radiocarbon dated and paleomagnetically analyzed core from a site nearby which would be a more trustworthy standard with which to relatively date the inorganic sediments. But as noted, both goals usually cannot be obtained due to the lack of datable organic material at the bottom of all glaciolacustrine sediment cores (Muller and Calkin, 1993; Ridge et al, 1990). However if paleomagnetic analyses were combined with sediment studies of inorganic glaciolacustrine sediment as well as radiocarbon dating and paleoecological analyses of organic sediment from bog cores, chronostratigraphic correlations of glacial sequences is possible (Muller and Calkin, 1993).

A similar paleomagnetic investigation of cored sediments from Spruce Pond located in Harriman State Forest 22.5 km southwest of Black Rock Forest would also be valuable in either providing supporting evidence or suggesting flaws in the Sutherland Pond core analysis. These sediments are available for sampling as they were also used for the paleoecological analysis of Holocene climate, vegetation and fire history of the Hudson Highlands performed by Maenza-Gmelch (1997a).

ACKNOWLEDGEMENTS

I thank my advisors J.C. Liddicoat, T.E. Maenza-Gmelch, M. Stute and S.L. Pfirman; R.S. Coe of the U.C.S.C Paleomagnetism Lab for use of the lab and measurement equipment. Rock magnetic analyses were performed by J.M. Glen at U.C.S.C. Paleomagnetism Lab. Research was funded by the Black Rock Forest Consortium.

REFERENCES

Antevs, E. (1953) Geochronology of the Deglacial and Neothermal ages. Journ. Geol. 61: 195-230 *as cited in* Nilsson, T. (1983) The Pleistocene: Geology and Life in the Quaternary Ice Age, Boston: D. Reidel Publishing Company

Banerjee, S.K, S.P. Lund, and S. Levi (1979) Geomagnetic record in Minnesota Lake sediments - absences of the Gothenburg and Eriean excursions. Geology 7: 588-591

Brennan W.J. (1988) Geophysical investigations of glacial drift. In "Late Wisconsinan deglaciation of the Genesee Valley" 15-28. Guidebook of the 51st Annual Meeting of the Friends of the Pleistocene, Geneseo, NY *as cited in* Pair, D.L., E.H. Muller and P.W. Plumley (1994) Correlation of late Pleistocene glaciolacustrine and marine deposits by means of geomagnetic secular variation, with examples from northern New York and southern Ontario, Quaternary Research 42: 277-287

Brennan, W.J., M. Hamilton, R. Kilbury, R.L. Reeves, and L. Covert (1984) Holocene and Late Pleistocene secular variation of the horizontal component of the geomagnetic field in western New York, Earth and Planetary Science Letters 70: 363-372

Carmichael, C.M., J.S. Mothersill and W.A. Morris (1990) Paleomagnetic and pollen chronostratigraphic correlations of the late glacial and postglacial sediments in Lake Ontario, Canadian Journal of Earth Sciences 27: 131-147

Collinson, D.W. (1983) Methods in Rock Magnetism and Palaeomagnetism: Techniques and Instrumentation, New York: Chapman and Hall

Connally, G.G. and L. Sirkin (1973) Wisconsinan history of the Hudson-Champlain lobe. Geological Society of America Mem. 136:47-69

Connally, G.G., L. Sirkin, and D.H. Calwell (1989) Deglacial history and environments of the upper Wallkill Valley, New York State Geological Association, Field Trip Guidebook 61: 205-229, as cited by Maenza-Gmelch, T.E. (1997) Holocene vegetation, climate, and fire history of the Hudson Highlands, southeastern New York, USA, The Holocene 7: 25-37

Cotter, J.F.P., J.C. Ridge, E.B. Evenson, W.D. Sevon, L. Sirkin and R. Stuckenrath (1986) The Wisconsinan history of the Great Valley, Pennsylvania and New Jersey, and the age of the "Terminal Moraine" *in* Cadwell, D.H., ed., The Wisconsinan Stage of the First Geological District, Eastern New York: New York State Museum Bulletin 455:22-49 *as cited in* Ridge, J.C., W.J. Brennan and E.H. Muller (1990) The use of paleomagnetic declination to test correlations of late Wisconsinan glaciolacustrine sediments in central New York, Geological Society of America Bulletin 102: 26-44

Creer, K.M., D.L. Gross, and J.A. Lineback (1976) Origin of regional geomagnetic variations recorded by Wisconsinan and Holocene sediments from Lake Michigan, U.S.A. and Lake Windemere, England. Geological Society of America Bulletin 87: 530-541

Creer, K.M. (1977) Geomagnetic secular variation during the last 25,000 years; an interpretation of data obtained from rapidly deposited sediments, Geophys. Jour. Roy. Astron. Soc. 48: 91-110

Creer, K.M. and P. Tucholka (1982) Construction of type curves of geomagnetic secular variation for dating lake sediments from east central North America, Canadian Journal of Earth Sciences, 19: 1106-1115

Denny, C.S. (1938) Glacial geology of the Black Rock Forest, Black Rock Forest Publication No. 8 *as cited in* Maenza-Gmelch, T.E. (1997) Holocene vegetation, climate, and fire history of the Hudson Highlands, southeastern New York, USA. The Holocene 7: 25-37

Irving, E. and A. Major (1964) Post-depositional detrital remanent magnetism in a synthetic sediment. Sedimentology 3: 135-143

Liddicoat, J.C., N.D. Opdyke and G.I. Smith (1980) Paleomagnetic polarity in a 930 meter core from Searles Valley, CA. Nature 286: 22-25

Lund, S.P. and S.K. Banerjee (1985) Late Quaternary paleomagnetic field secular variation from two Minnesota Lakes. Journal of Geophysical Research 90:803-825

Lund, S.P., J.C. Liddicoat, K.R. Lajoie, T.L. Henyey, and S.W. Robinson (1988) Paleomagnetic evidence for long-term (million year) memory and periodic behavior in the Earth's core dynamo process. Geophysical Research Letters 15: 1101-1104

Lund, S.P. (1996) A comparison of Holocene paleomagnetic secular variation records from North America. Journal of Geophysical Research 101: 8007-8024

Maenza-Gmelch, T.E. (1997a) Holocene vegetation, climate, and fire history of the Hudson Highlands, southeastern New York, USA, The Holocene 7: 25-37

Maenza-Gmelch, T.E. (1997b) Late-glacial - early Holocene vegetation, climate, and fire at Sutherland Pond, Hudson Highlands, southeastern New York, U.S.A. Canadian Journal of Botany 75: 431-439

McElhinny, M.W. (1973) Palaeomagnetism and plate tectonics, Cambridge: University Press

Merrill, R.T., M.W McElhinny and P.L. McFadden (1996) The Magnetic Field of the Earth: Paleomagnetism, the Core and Deep Mantle. San Diego: Academic Press, Inc.

Mothersill, J.S. (1979) The paleomagnetic record of the late Quaternary sediments of Thunder Bay, Canadian Journal of Earth Sciences 16: 1016-1023

Mothersill, J.S. (1981) Late Quaternary paleomagnetic record of the Goderich Basin, Lake Huron. Canadian Journal of Earth Sciences 18: 448-456

Muller, E.H. and P.E. Calkin (1993) Timing of Pleistocene glacial events in New York State, Canadian Journal of Earth Science 30:1829-45

Nilsson, T. (1983) The Pleistocene: Geology and Life in the Quaternary Ice Age, Boston: D. Reidel Publishing Company

Pair, D.L., E.H. Muller and P.W. Plumley (1994) Correlation of late Pleistocene glaciolacustrine and marine deposits by means of geomagnetic secular variation, with examples from northern New York and southern Ontario, Quaternary Research 42:277-287

Ridge, J.C., W.J. Brennan and E.H. Muller (1990) The use of paleomagnetic declination to test correlations of late Wisconsinan glaciolacustrine sediments in central New York, Geological Society of America Bulletin 102:26-44

Sprowl, D.R. and Banerjee, S.K. (1985) High-resolution paleomagnetic record of geomagnetic field fluctuations from the varved sediments of Elk Lake, Minnesota. Geology 13:531-533

Stuiver, M. and Pearson, G.W. (1993) Calibration 1993, Radiocarbon 35n. 1

Stuiver, M., B. Kromer, B. Becker, and C.W. Ferguson (1986) Radiocarbon age calibration back to 13,300 years B.P. and the radiocarbon age matching of the German oak and U.S. bristlecone pine chronologies, Radiocarbon 28:969-979

Takeuchi, H., S. Uyeda and H. Kanamori (1967) Debate About the Earth: Approach to Geophysics through Analysis of Continental Drift, San Francisco: Freeman, Cooper & Co.

Tarling, D.H. (1983) Paleomagnetism: Principles and Applications in Geology, Geophysics and Archaeology, New York: Chapman and Hall

Urry, W.D. (1948) The radium content of varved clay and a possible age of the Hartford, Connecticut deposits. American Journal of Science 246: 689-700 *as cited in* Nilsson, T. (1983) The Pleistocene: Geology and Life in the Quaternary Ice Age. Boston: D. Reidel Publishing Company

Wellner, R.W. and T.R . Dwyer (1996) Late Pleistocene-Holocene lake-level fluctuations and paleoclimates at Canandaigua Lake, New York. Geological Society of America Special Paper 311: 65-76

Zijderveld, J.D.A. (1967) Demagnetization of Rocks: Analysis of results. *In* "Methods in Paleomagnetism" (D.W. Collinson, K.M. Creer and S.K. Runcorn, Eds.), pp. 254-286. Amsterdam: Elsevier Scientific

Black Rock Forest Home Page (http://www.dalton.org/groups/brf/geography/geography.shtml) 10/2/97

APPENDIX A

Article printed in Black Rock Forest Newsletter

Research

Black Rock Forest Turtle Study

Krista McKinsey, Earth and Environmental Science Journalism Program, Columbia University

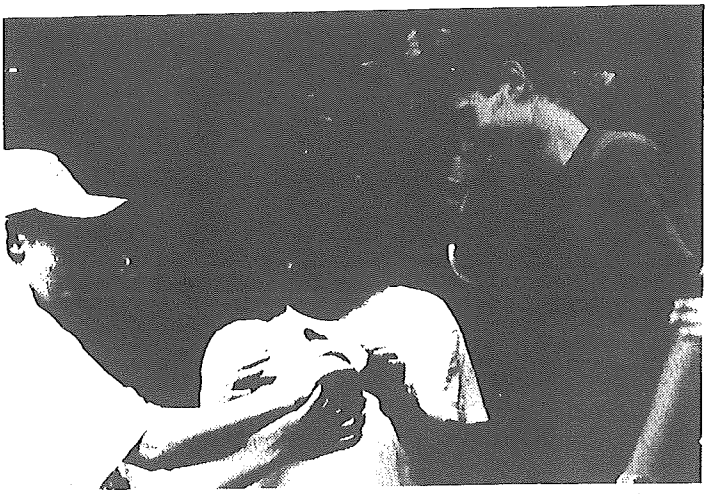

Summer intern Sara Helm shows a marked turtle to students

"Can I hold it?" "What does he eat?" "Have you ever been bitten?" "What are you doing?" If there's anything I learned this summer, it's that inquisitive children (and adults) can rapid-fire questions faster than a feisty snapping turtle can pop it's neck out in a defensive rage. With a small research grant from the Black Rock Forest Consortium, I and two student assistants proudly became known as "the turtle people" for families and field trips passing through the forest between June and August. We were, in fact, a little hard to miss. In thigh-high rubber boots with buckets of equipment in each hand, we moved into our operations base in the Stone House in the heart of the forest. Our goal was to learn about Black Rock's aquatic turtles and their pond environments.

Under the guidance of Dr. Christopher Raxworthy of **Columbia University**'s Center for Environmental Research and Conservation, and with much help from the Black Rock staff, we trapped, tagged, measured, aged, and sexed aquatic turtle populations in five ponds in the forest. We were then able to estimate how many turtles lived in each pond. To compare the different populations, we measured the acidity, oxygen levels, and amount of primary producers in each study pond. By August, we were able not only to navigate between ponds without a map, but also draw some conclusions from the data we had gathered. Sutherland Pond and Aleck Meadow, the most neutral, life rich ponds, are also home to the largest populations of painted turtles (*Chrysemys picta)*, and snapping turtles

(continued on page 7)

Paleomagnetic Dating Of Sutherland Pond Sediment For Paleoclimate And Palynology Investigations in the Hudson Highlands

Kiersten Jennings, Barnard College

Sutherland Pond is one of many small water bodies that formed in the Hudson Highlands when the Laurentide ice sheet melted at the end of the Pleistocene. A paleomagnetic study of sediment cored from the pond was begun last summer to help date the retreat of the ice sheets in the Highlands. The objective is to compare gradual change (secular variation) of the earth's past magnetic field recorded in the sediment with dated secular variation curves from elsewhere in the northeastern United States, especially Lake Ontario, reported by other investigators.

The Sutherland Pond core, known as BRF-1, is 10.5 meters long and was recovered in August 1991 by investigators from **New York University** for a palynology study. Analysis of the pollen, plant microfossils, and charcoal content, coupled with AMS radiation dates, indicate organic deposition commenced in the pond about 12,600 years ago. However, the lack of sufficient organic material in the lower two meters of the core does not permit radiocarbon dating as a means of determining the age of the oldest sediment recovered. Working with J. Liddicoat of **Barnard College** and T. Maenza-Gmelch of **New York University**, our paleomagnetic study is an attempt to date that basal portion of the core. (continued on page 7)

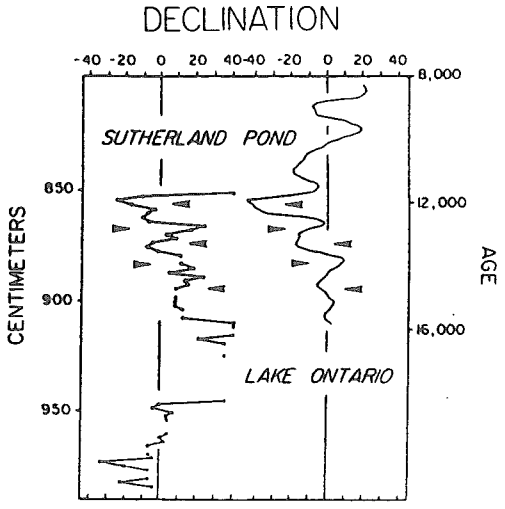

Secular variation in Black Rock Forest core

Paleomagnetic Dating

(continued from page 3)

The secular variation is recorded in the sediment when fine-grained magnetic minerals such as magnetite are aligned with the earth's magnetic field at the time of deposition. The accompanying diagram shows the horizontal component (relative declination) of the paleomagnetic field in BRF-1 matched with the relative declination in Lake Ontario sediment. The comparison places an age of about 16,000 years B.P. (before present) at 9.1 meters.

The lower two meters of the core consist of a meter of laminated clay underlain by a meter of fine-grained silt. If the sedimentation rate of the laminated clay was slower by a factor of four compared to the rate of the silt, the extrapolated age of the sediment at the base of the core is 17,500 years B.P. That agrees well with the estimated age of the termination of glaciation in the Great Valley west of the Hudson Highlands.

Turtle Study

(continued from page 3)

(*Chelydra serpentina*). In contrast, the most acidic, lemon juice-like ponds, Tamarack and Sphagnum, are home to very small populations. The fifth pond, Arthurs, has been drained to a puddle in recent years and, unsurprisingly, also has very small turtle populations. How the different pond habitats affect the turtles' abilities to mate and successfully raise their young is not entirely clear, but there does seem to be a relationship between the condition of the pond and the number of its inhabitants. Each turtle trapped was permanently marked so future researchers will be able to identify individuals and build records of each turtle's history. Now we can answer a few more of the tough questions posed by those Sunday afternoon hikers last summer, but there is still much to be learned.

(Special thanks to John Brady for supplying us with jugs of water, occasional transportation, and company!)

Where are the Data Going?

(continued from page 4)

ing curricula based on the data.

At about the same time we began making much of the data available through our web site (http://www.dalton.org/groups/brf). We cannot at this time determine how many of the hundreds of "hits" on this site have been for the purpose of obtaining environmental data. But during the first full year of operation of the Network we logged sixteen more direct requests for data. Nine were made by researchers, six by educators, and one by an organization looking to develop their own environmental monitoring station.

In 1997, 25 direct requests for data have been received as of November. Ten of the requests were made by researchers, ten were made by educators, and three were made by organizations looking for advice on establishing their own stations. Two of the data requests came from an unexpected source. An insurance agent for the Catskill Cougars (a AAA baseball team) was interested in precipitation records during game hours for home games!

Of all the requests that we have had, ten were made related to classes in the K-12 range and one was made for an undergraduate course. Research requests can be divided into three categories: undergraduate research (5 requests), graduate level research (3 requests), post doctoral/professional researcher (7 requests). Six requests were made by persons interested in curriculum development.

In the Network's two years of existence it has provided more than a big data set. No fewer than 25 school groups have been shown the monitoring stations and radiotelemetry equipment, learning how technology can be used to provide valuable information about environments of the Forest. The data from the stations have helped support grant proposals for researchers to further advance our knowledge of the forest. Our environmental database offers an important platform for the construction of a framework for many academic pursuits in the Black Rock Forest.

Join Us! Become a Friend of Black Rock Forest...

Detach and return this portion with your contribution... thank you!

☐ New member ☐ Renewal

☐ White Oak	$500 or more
☐ Hemlock Tree	$250
☐ Sugar Maple	$100
☐ Individual	$20
☐ Student/over 65	$15
☐ Family	$25

Please make checks payable to the: *Black Rock Forest Consortium*
All contributions are tax deductible as we are a 501 (c) (3) organization

Name _____

Address _____

_____ Phone ( ) _____

☐ My company will match my gift
Company name and address: _____

☐ Please send me information concerning:
( ) gifts of land/real estate ( ) memorial gifts

☐ I would like to volunteer to help with the following: _____

Mail to: *Black Rock Forest • 129 Continental Road, Cornwall, NY 12518*

APPENDIX B

Best fit data from all samples

Record File: B

Study: 97K0852A
RFSP-17

1/3/83 ?

0:?? PM
Location; Long: 284.0 Lat: 41.4
General Attitude; Strike: 0.0 Dip: 0.0
Age: 12K
Local: BRF-1
Description: 852 CM

==========

ID: 97K0852A Strike: 0.0, Dip: 0.0 Long: 284.0, Lat: 41.4
Core Y: 0.0, Z': 0.0

C	DMT	Range	n	P	St	G_Dec	G_Inc	G_Long	G_Lat	S_Dec	S_Inc	S_Long	S_lat
0	N	0- 0	1			173.3	30.3	291.6	-32.0	173.3	30.3	291.6	-32.0
1	H	1-600	1+			171.0	28.1	294.4	-33.0	171.0	28.1	294.4	-33.0

ID: 97K0854A Strike: 0.0, Dip: 0.0 Long: 284.0, Lat: 41.4
Core Y: 0.0, Z': 0.0

C	DMT	Range	n	P	St	G_Dec	G_Inc	G_Long	G_Lat	S_Dec	S_Inc	S_Long	S_lat
0	N	0- 0	1			138.0	27.8	328.2	-21.7	138.0	27.8	328.2	-21.7
1	H	100-500	8+			118.6	19.7	346.8	-13.7	118.6	19.7	346.8	-13.7

ID: 97K0854B Strike: 0.0, Dip: 0.0 Long: 284.0, Lat: 41.4
Core Y: 0.0, Z': 0.0

C	DMT	Range	n	P	St	G_Dec	G_Inc	G_Long	G_Lat	S_Dec	S_Inc	S_Long	S_lat
0	N	0- 0	1			164.4	16.3	303.8	-38.3	164.4	16.3	303.8	-38.3
1	H	1-150	4+			164.3	19.1	303.4	-36.8	164.3	19.1	303.4	-36.8

ID: 97K0856A Strike: 0.0, Dip: 0.0 Long: 284.0,
Lat: 41.4

Core Y: 0.0, Z': 0.0

C	DMT	Range	n	P	St	G_Dec	G_Inc	G_Long	G_Lat	S_Dec	S_Inc	S_Long	S_lat
0	N	0- 0	1			101.8	39.2	349.7	6.2	101.8	39.2	349.7	6.2
1	H	1-250	6+			104.6	42.6	346.1	6.0	104.6	42.6	346.1	6.0

ID: 97K0856B Strike: 0.0, Dip: 0.0 Long: 284.0,
Lat: 41.4

Core Y: 0.0, Z': 0.0

C	DMT	Range	n	P	St	G_Dec	G_Inc	G_Long	G_Lat	S_Dec	S_Inc	S_Long	S_lat
0	N	0- 0	1			124.3	25.9	340.1	-14.8	124.3	25.9	340.1	-14.8
1	H	100-600	9+			118.3	32.5	341.9	-7.9	118.3	32.5	341.9	-7.9

ID: 97K0858A Strike: 0.0, Dip: 0.0 Long: 284.0,
Lat: 41.4

Core Y: 0.0, Z': 0.0

C	DMT	Range	n	P	St	G_Dec	G_Inc	G_Long	G_Lat	S_Dec	S_Inc	S_Long	S_lat
0	N	0- 0	1			110.2	36.8	345.5	-0.6	110.2	36.8	345.5	-0.6
1	H	1-600	1+			112.3	42.9	341.1	1.2	112.3	42.9	341.1	1.2

Study: 97K0860A Record File: B
RFSP-18.PMG
1/3/83 ?
0:?? PM
Location; Long: 284.0 Lat: 41.4
General Attitude; Strike: 0.0 Dip: 0.0
Age: 12K
Local: BRF-1
Description: 860 CM

ID: 97K0860A Strike: 0.0, Dip: 0.0 Long: 284.0, Lat: 41.4
Core Y: 0.0, Z': 0.0

C	DMT	Range	n	P	St	G_Dec	G_Inc	G_Long	G_Lat	S_Dec	S_Inc	S_Long	S_lat
0	N	0- 0	1			115.5	35.8	342.4	-4.6	115.5	35.8	342.4	-4.6
1	H	50-400	8+			126.1	36.2	334.6	-10.8	126.1	36.2	334.6	-10.8

ID: 97K0862A Strike: 0.0, Dip: 0.0 Long: 284.0, Lat: 41.4
Core Y: 0.0, Z': 0.0

C	DMT	Range	n	P	St	G_Dec	G_Inc	G_Long	G_Lat	S_Dec	S_Inc	S_Long	S_lat
0	N	0- 0	1			114.4	27.3	346.9	-7.7	114.4	27.3	346.9	-7.7
1	H	50-400	8+			121.9	29.3	340.6	-11.7	121.9	29.3	340.6	-11.7

ID: 97K0864A Strike: 0.0, Dip: 0.0 Long: 284.0, Lat: 41.4
Core Y: 0.0, Z': 0.0

C	DMT	Range	n	P	St	G_Dec	G_Inc	G_Long	G_Lat	S_Dec	S_Inc	S_Long	S_lat
0	N	0- 0	1			113.4	26.2	348.0	-7.5	113.4	26.2	348.0	-7.5
1	H	50-600	1+			119.1	29.8	342.5	-9.7	119.1	29.8	342.5	-9.7

ID: 97K0866A Strike: 0.0, Dip: 0.0 Long: 284.0, Lat: 41.4

Core Y: 0.0, Z': 0.0

C	DMT	Range	n	P	St	G_Dec	G_Inc	G_Long	G_Lat	S_Dec	S_Inc	S_Long	S_lat
0	N	0- 0	1			105.2	43.3	345.4	6.0	105.2	43.3	345.4	6.0
1	H	150-600	8+			122.5	44.6	333.3	-4.0	122.5	44.6	333.3	-4.0

ID: 97K0868A Strike: 0.0, Dip: 0.0 Long: 284.0, Lat: 41.4

Core Y: 0.0, Z': 0.0

C	DMT	Range	n	P	St	G_Dec	G_Inc	G_Long	G_Lat	S_Dec	S_Inc	S_Long	S_lat
0	N	0- 0	1			148.1	32.4	317.5	-24.0	148.1	32.4	317.5	-24.0
1	H	50-700	1+			153.9	32.3	311.9	-26.3	153.9	32.3	311.9	-26.3

ID: 97K0870A Strike: 0.0, Dip: 0.0 Long: 284.0, Lat: 41.4

Core Y: 0.0, Z': 0.0

C	DMT	Range	n	P	St	G_Dec	G_Inc	G_Long	G_Lat	S_Dec	S_Inc	S_Long	S_lat
0	N	0- 0	1			140.2	36.2	323.3	-18.3	140.2	36.2	323.3	-18.3
1	H	150-700	7+			146.2	31.6	319.5	-23.7	146.2	31.6	319.5	-23.7

Record File: B

Study: 97K0872A
RFSP-19.PMG

1/3/83 ?

0:?? PM
Location; Long: 284.0 Lat: 41.4
General Attitude; Strike: 0.0 Dip: 0.0
Age: 12K
Local: BRF-1
Description: 872 CM

==========

ID: 97K0872A Strike: 0.0, Dip: 0.0 Long: 284.0, Lat: 41.4
Core Y: 0.0, Z': 0.0

C	DMT	Range	n	P	St	G_Dec	G_Inc	G_Long	G_Lat	S_Dec	S_Inc	S_Long	S_lat
0	N	0- 0	1			121.3	20.1	344.6	-15.3	121.3	20.1	344.6	-15.3
1	H	50-500	9+			132.4	33.5	330.8	-15.8	132.4	33.5	330.8	-15.8

ID: 97K0872B Strike: 0.0, Dip: 0.0 Long: 284.0, Lat: 41.4
Core Y: 0.0, Z': 0.0

C	DMT	Range	n	P	St	G_Dec	G_Inc	G_Long	G_Lat	S_Dec	S_Inc	S_Long	S_lat
0	N	0- 0	1			162.0	32.7	303.6	-28.5	162.0	32.7	303.6	-28.5
1	H	50-500	9+			150.9	39.8	312.6	-20.5	150.9	39.8	312.6	-20.5

ID: 97K0874A Strike: 0.0, Dip: 0.0 Long: 284.0, Lat: 41.4
Core Y: 0.0, Z': 0.0

C	DMT	Range	n	P	St	G_Dec	G_Inc	G_Long	G_Lat	S_Dec	S_Inc	S_Long	S_lat
0	N	0- 0	1			144.4	30.8	321.4	-23.3	144.4	30.8	321.4	-23.3
1	H	50-600	1+			138.4	40.2	323.3	-15.0	138.4	40.2	323.3	-15.0

ID: 97K0876A Strike: 0.0, Dip: 0.0 Long: 284.0, Lat: 41.4

Core Y: 0.0, Z': 0.0

C	DMT	Range	n	P	St	G_Dec	G_Inc	G_Long	G_Lat	S_Dec	S_Inc	S_Long	S_lat
0	N	0- 0	1			119.2	33.3	340.9	-8.1	119.2	33.3	340.9	-8.1
1	H	50-600	1			124.9	42.8	332.5	-6.4	124.9	42.8	332.5	-6.4

ID: 97K0876B Strike: 0.0, Dip: 0.0 Long: 284.0, Lat: 41.4

Core Y: 0.0, Z': 0.0

C	DMT	Range	n	P	St	G_Dec	G_Inc	G_Long	G_Lat	S_Dec	S_Inc	S_Long	S_lat
0	N	0- 0	1			137.2	35.6	326.0	-17.2	137.2	35.6	326.0	-17.2
1	H	50-500	9+			145.7	39.5	317.4	-18.7	145.7	39.5	317.4	-18.7

ID: 97K0878A Strike: 0.0, Dip: 0.0 Long: 284.0, Lat: 41.4

Core Y: 0.0, Z': 0.0

C	DMT	Range	n	P	St	G_Dec	G_Inc	G_Long	G_Lat	S_Dec	S_Inc	S_Long	S_lat
0	N	0- 0	1			118.0	35.4	340.8	-6.3	118.0	35.4	340.8	-6.3
1	H	1-350	8+			121.7	41.9	335.2	-5.1	121.7	41.9	335.2	-5.1

Study: 97K0880A
RFSP-20.PMG

Record File: B

1/3/83 ?

0:?? PM
Location; Long: 284.0 Lat: 41.4
General Attitude; Strike: 0.0 Dip: 0.0
Age: 12K
Local: BRF-1
Description: 880 CM

==========

ID: 97K0880A Strike: 0.0, Dip: 0.0 Long: 284.0, Lat: 41.4
Core Y: 0.0, Z': 0.0

C	DMT	Range	n	P	St	G_Dec	G_Inc	G_Long	G_Lat	S_Dec	S_Inc	S_Long	S_lat
0	N	0- 0	1			120.5	36.7	338.5	-7.2	120.5	36.7	338.5	-7.2
1	H	50-500	9+			127.9	40.5	331.4	-9.4	127.9	40.5	331.4	-9.4

ID: 97K0882A Strike: 0.0, Dip: 0.0 Long: 284.0, Lat: 41.4
Core Y: 0.0, Z': 0.0

C	DMT	Range	n	P	St	G_Dec	G_Inc	G_Long	G_Lat	S_Dec	S_Inc	S_Long	S_lat
0	N	0- 0	1			141.3	38.6	321.5	-17.4	141.3	38.6	321.5	-17.4
1	H	1-250	6+			140.4	43.2	320.5	-14.0	140.4	43.2	320.5	-14.0

ID: 97K0886A Strike: 0.0, Dip: 0.0 Long: 284.0, Lat: 41.4
Core Y: 0.0, Z': 0.0

C	DMT	Range	n	P	St	G_Dec	G_Inc	G_Long	G_Lat	S_Dec	S_Inc	S_Long	S_lat
0	N	0- 0	1			137.9	33.4	326.3	-18.8	137.9	33.4	326.3	-18.8
1	H	50-300	6+			141.8	39.9	320.6	-16.8	141.8	39.9	320.6	-16.8

ID: 97K0888B Strike: 0.0, Dip: 0.0 Long: 284.0, Lat: 41.4

Core Y: 0.0, Z': 0.0

C	DMT	Range	n	P	St	G_Dec	G_Inc	G_Long	G_Lat	S_Dec	S_Inc	S_Long	S_lat
0	N	0- 0	1			143.0	46.6	317.1	-12.7	143.0	46.6	317.1	-12.7
1	H	50-300	6+			148.0	49.6	311.9	-12.3	148.0	49.6	311.9	-12.3

Record File: B

Study: 97K0890A
RFSP-21.PMG

1/3/83 ?

0:?? PM
Location; Long: 284.0 Lat: 41.4
General Attitude; Strike: 0.0 Dip: 0.0
Age: 12K
Local: BRF-1
Description: 890 CM

==========

ID: 97K0890A Strike: 0.0, Dip: 0.0 Long: 284.0, Lat: 41.4
Core Y: 0.0, Z': 0.0

C	DMT	Range	n	P	St	G_Dec	G_Inc	G_Long	G_Lat	S_Dec	S_Inc	S_Long	S_lat
0	N	0- 0	1			130.2	44.3	327.9	-8.3	130.2	44.3	327.9	-8.3
1	H	100-300	5+			134.1	50.5	322.1	-5.9	134.1	50.5	322.1	-5.9

ID: 97K0892A Strike: 0.0, Dip: 0.0 Long: 284.0, Lat: 41.4
Core Y: 0.0, Z': 0.0

C	DMT	Range	n	P	St	G_Dec	G_Inc	G_Long	G_Lat	S_Dec	S_Inc	S_Long	S_lat
0	N	0- 0	1			154.0	48.0	307.4	-15.6	154.0	48.0	307.4	-15.6
1	H	1-400	9+			153.5	53.1	306.2	-11.1	153.5	53.1	306.2	-11.1

ID: 97K0894A Strike: 0.0, Dip: 0.0 Long: 284.0, Lat: 41.4
Core Y: 0.0, Z': 0.0

C	DMT	Range	n	P	St	G_Dec	G_Inc	G_Long	G_Lat	S_Dec	S_Inc	S_Long	S_lat
0	N	0- 0	1			142.4	36.7	321.2	-19.0	142.4	36.7	321.2	-19.0
1	H	1-400	9+			143.5	43.9	317.7	-14.9	143.5	43.9	317.7	-14.9

ID: 97K0896A Strike: 0.0, Dip: 0.0 Long: 284.0, Lat: 41.4

Core Y: 0.0, Z': 0.0

C	DMT	Range	n	P	St	G_Dec	G_Inc	G_Long	G_Lat	S_Dec	S_Inc	S_Long	S_lat
0	N	0- 0	1			140.2	34.6	323.9	-19.2	140.2	34.6	323.9	-19.2
1	H	1-999	1+			145.1	38.1	318.4	-19.4	145.1	38.1	318.4	-19.4

ID: 97K0898A Strike: 0.0, Dip: 0.0 Long: 284.0, Lat: 41.4

Core Y: 0.0, Z': 0.0

C	DMT	Range	n	P	St	G_Dec	G_Inc	G_Long	G_Lat	S_Dec	S_Inc	S_Long	S_lat
0	N	0- 0	1			140.7	35.6	323.1	-18.9	140.7	35.6	323.1	-18.9
1	H	1-500	1+			138.1	38.0	324.4	-16.2	138.1	38.0	324.4	-16.2

Record File: B

Study: 97K0902A
RFSP-12.PMG

1/3/83 ?

0:?? PM

Location; Long: 284.0 Lat: 41.4
General Attitude; Strike: 0.0 Dip: 0.0
Age: 12K
Local: BRF-1
Description: 902 CM

ID: 97K0902A Strike: 0.0, Dip: 0.0 Long: 284.0, Lat: 41.4

Core Y: 0.0, Z': 0.0

C	DMT	Range	n	P	St	G_Dec	G_Inc	G_Long	G_Lat	S_Dec	S_Inc	S_Long	S_lat
0	N	0- 0	1			292.7	33.2	193.4	28.7	292.7	33.2	193.4	28.7
1	H	1-800	1+			296.3	33.3	191.0	31.5	296.3	33.3	191.0	31.5

ID: 97K0904A Strike: 0.0, Dip: 0.0 Long: 284.0, Lat: 41.4

Core Y: 0.0, Z': 0.0

C	DMT	Range	n	P	St	G_Dec	G_Inc	G_Long	G_Lat	S_Dec	S_Inc	S_Long	S_lat
0	N	0- 0	1			291.5	30.7	192.8	26.9	291.5	30.7	192.8	26.9
1	H	50-400	8+			296.1	30.5	189.5	30.2	296.1	30.5	189.5	30.2

ID: 97K0905A Strike: 0.0, Dip: 0.0 Long: 284.0, Lat: 41.4

Core Y: 0.0, Z': 0.0

C	DMT	Range	n	P	St	G_Dec	G_Inc	G_Long	G_Lat	S_Dec	S_Inc	S_Long	S_lat
0	N	0- 0	1			290.5	30.7	193.5	26.1	290.5	30.7	193.5	26.1
1	H	50-800	9+			295.4	29.9	189.7	29.5	295.4	29.9	189.7	29.5

ID: 97K0907A Strike: 0.0, Dip: 0.0 Long: 284.0,
Lat: 41.4 Core Y: 0.0, Z': 0.0

C	DMT	Range	n	P	St	G_Dec	G_Inc	G_Long	G_Lat	S_Dec	S_Inc	S_Long	S_lat
0	N	0- 0	1			294.7	36.0	193.8	31.4	294.7	36.0	193.8	31.4
1	H	50-500	9+			300.6	36.4	190.0	35.9	300.6	36.4	190.0	35.9

ID: 97K0912A Strike: 0.0, Dip: 0.0 Long: 284.0,
Lat: 41.4 Core Y: 0.0, Z': 0.0

C	DMT	Range	n	P	St	G_Dec	G_Inc	G_Long	G_Lat	S_Dec	S_Inc	S_Long	S_lat
0	N	0- 0	1			199.9	40.2	264.1	-23.1	199.9	40.2	264.1	-23.1
1	H	100-600	8+			207.0	31.1	254.9	-26.7	207.0	31.1	254.9	-26.7

ID: 97K0914A Strike: 0.0, Dip: 0.0 Long: 284.0,
Lat: 41.4 Core Y: 0.0, Z': 0.0

C	DMT	Range	n	P	St	G_Dec	G_Inc	G_Long	G_Lat	S_Dec	S_Inc	S_Long	S_lat
0	N	0- 0	1			227.2	42.3	241.1	-11.0	227.2	42.3	241.1	-11.0
1	H	50-500	9+			236.3	37.0	232.0	-9.0	236.3	37.0	232.0	-9.0

ID: Strike: 0.0, Dip: 0.0 Long: 284.0,
Lat: 41.4 Core Y: 0.0, Z': 0.0

C	DMT	Range	n	P	St	G_Dec	G_Inc	G_Long	G_Lat	S_Dec	S_Inc	S_Long	S_lat

Record File: B

Study: 97K0916A
RFSP-13.PMG

1/3/83 ?

0:?? PM
Location; Long: 284.0 Lat: 41.4
General Attitude; Strike: 0.0 Dip: 0.0
Age: 12K
Local: BRF-1
Description: 916 CM

==========

ID: 97K0916A Strike: 0.0, Dip: 0.0 Long: 284.0,
Lat: 41.4
Core Y: 0.0, Z': 0.0

C P	DMT	Range	n	St	G_Dec	G_Inc	G_Long	G_Lat	S_Dec	S_Inc	S_Long	S_lat
0	N	0- 0	1		225.5	39.7	241.4	-13.4	225.5	39.7	241.4	-13.4
1	H	50-400	7+		235.6	33.7	231.1	-11.1	235.6	33.7	231.1	-11.1

ID: 97K0921A Strike: 0.0, Dip: 0.0 Long: 284.0,
Lat: 41.4
Core Y: 0.0, Z': 0.0

C P	DMT	Range	n	St	G_Dec	G_Inc	G_Long	G_Lat	S_Dec	S_Inc	S_Long	S_lat
0	N	0- 0	1		233.4	42.0	236.4	-7.8	233.4	42.0	236.4	-7.8
1	H	50-400	8+		242.1	36.0	227.4	-6.0	242.1	36.0	227.4	-6.0

ID: 97K0923A Strike: 0.0, Dip: 0.0 Long: 284.0,
Lat: 41.4
Core Y: 0.0, Z': 0.0

C P	DMT	Range	n	St	G_Dec	G_Inc	G_Long	G_Lat	S_Dec	S_Inc	S_Long	S_lat
0	N	0- 0	1		215.5	38.8	249.3	-18.7	215.5	38.8	249.3	-18.7
1	H	50-600	8+		222.5	36.0	242.4	-17.1	222.5	36.0	242.4	-17.1

ID: 97K0924A Strike: 0.0, Dip: 0.0 Long: 284.0, Lat: 41.4

Core Y: 0.0, Z': 0.0

C	DMT	Range	n	P	St	G_Dec	G_Inc	G_Long	G_Lat	S_Dec	S_Inc	S_Long	S_lat
0	N	0- 0	1			230.7	39.2	237.1	-11.0	230.7	39.2	237.1	-11.0
1	H	50-400	8+			237.0	32.7	229.6	-10.8	237.0	32.7	229.6	-10.8

ID: 97K0931A Strike: 0.0, Dip: 0.0 Long: 284.0, Lat: 41.4

Core Y: 0.0, Z': 0.0

C	DMT	Range	n	P	St	G_Dec	G_Inc	G_Long	G_Lat	S_Dec	S_Inc	S_Long	S_lat
0	N	0- 0	1			232.0	45.1	238.8	-6.7	232.0	45.1	238.8	-6.7
1	H	50-500	8+			238.6	42.5	232.9	-4.6	238.6	42.5	232.9	-4.6

ID: Strike: 0.0, Dip: 0.0 Long: 284.0, Lat: 41.4

Core Y: 0.0, Z': 0.0

C	DMT	Range	n	P	St	G_Dec	G_Inc	G_Long	G_Lat	S_Dec	S_Inc	S_Long	S_lat

Study: 97K0956A
rfsp-3.pmg

Record File: b

1/3/83 ?

0:?? PM
Location; Long: 284.0 Lat: 41.4
General Attitude; Strike: 0.0 Dip: 0.0
Age: 12K
Local: BRF-1
Description: 956 CM

==========

ID: 97K0956A Strike: 0.0, Dip: 0.0 Long: 284.0, Lat: 41.4
Core Y: 0.0, Z': 0.0

C	DMT	Range	n	P	St	G_Dec	G_Inc	G_Long	G_Lat	S_Dec	S_Inc	S_Long	S_lat
0	N	0- 0	1			230.1	52.5	244.0	-2.4	230.1	52.5	244.0	-2.4
1	H	100-500	7+			235.2	47.7	237.9	-3.3	235.2	47.7	237.9	-3.3

ID: 97K0956B Strike: 0.0, Dip: 0.0 Long: 284.0, Lat: 41.4
Core Y: 0.0, Z': 0.0

C	DMT	Range	n	P	St	G_Dec	G_Inc	G_Long	G_Lat	S_Dec	S_Inc	S_Long	S_lat
0	N	0- 0	1			276.6	48.1	213.0	23.4	276.6	48.1	213.0	23.4
1	T	100-400	7+			285.9	37.7	200.4	25.5	285.9	37.7	200.4	25.5

Study: 97K0958A Record File: B
RFSP-4.PMG

1/3/83 ?

0:?? PM

Location; Long: 284.0 Lat: 41.4
General Attitude; Strike: 0.0 Dip: 0.0
Age: 12K
Local: BRF-1
Description: 958 CM

==========

ID: 97K0958A Strike: 0.0, Dip: 0.0 Long: 284.0, Lat: 41.4

Core Y: 0.0, Z': 0.0

C	DMT	Range	n	P	St	G_Dec	G_Inc	G_Long	G_Lat	S_Dec	S_Inc	S_Long	S_lat
0	N	0- 0	1			238.8	45.8	234.4	-2.5	238.8	45.8	234.4	-2.5
1	H	50-400	8+			245.9	38.0	225.7	-2.6	245.9	38.0	225.7	-2.6

ID: 97K0958B Strike: 0.0, Dip: 0.0 Long: 284.0, Lat: 41.4

Core Y: 0.0, Z': 0.0

C	DMT	Range	n	P	St	G_Dec	G_Inc	G_Long	G_Lat	S_Dec	S_Inc	S_Long	S_lat
0	N	0- 0	1			271.8	49.6	216.8	20.8	271.8	49.6	216.8	20.8
1	T	100-450	8+			282.7	39.2	203.3	23.7	282.7	39.2	203.3	23.7

Study: 97K0960A Record File: B
RFSP-5.PMG

1/3/83 ?

0:?? PM

Location; Long: 284.0 Lat: 41.4
General Attitude; Strike: 0.0 Dip: 0.0
Age: 12K
Local: BRF-1
Description: 960 CM

ID: 97K0960A Strike: 0.0, Dip: 0.0 Long: 284.0, Lat: 41.4

Core Y: 0.0, Z': 0.0

C	DMT	Range	n	P	St	G_Dec	G_Inc	G_Long	G_Lat	S_Dec	S_Inc	S_Long	S_lat
0	N	0- 0	1			232.2	38.2	235.6	-10.7	232.2	38.2	235.6	-10.7
1	H	50-600	1+			242.4	34.4	226.4	-6.6	242.4	34.4	226.4	-6.6

ID: 97K0960B Strike: 0.0, Dip: 0.0 Long: 284.0, Lat: 41.4

Core Y: 0.0, Z': 0.0

C	DMT	Range	n	P	St	G_Dec	G_Inc	G_Long	G_Lat	S_Dec	S_Inc	S_Long	S_lat
0	N	0- 0	1			259.8	53.8	226.6	15.3	259.8	53.8	226.6	15.3
1	T	100-300	5+			274.2	48.8	214.9	22.1	274.2	48.8	214.9	22.1

Record File: B

Study: 97K0962A
RFSP-6.PMG

1/3/83 ?

0:?? PM
Location; Long: 284.0 Lat: 41.4
General Attitude; Strike: 0.0 Dip: 0.0
Age: 12K
Local: BRF-1
Description: 962 CM

==========

ID: 97K0962A Strike: 0.0, Dip: 0.0 Long: 284.0, Lat: 41.4
Core Y: 0.0, Z': 0.0

C	DMT	Range	n	P	St	G_Dec	G_Inc	G_Long	G_Lat	S_Dec	S_Inc	S_Long	S_lat
0	N	0- 0	1			239.3	34.8	228.8	-8.3	239.3	34.8	228.8	-8.3
1	H	1-700	1+			242.9	32.1	225.1	-7.4	242.9	32.1	225.1	-7.4

ID: 97K0962B Strike: 0.0, Dip: 0.0 Long: 284.0, Lat: 41.4
Core Y: 0.0, Z': 0.0

C	DMT	Range	n	P	St	G_Dec	G_Inc	G_Long	G_Lat	S_Dec	S_Inc	S_Long	S_lat
0	N	0- 0	1			268.4	41.8	213.5	14.5	268.4	41.8	213.5	14.5
1	T	100-400	7+			276.6	37.7	206.1	18.6	276.6	37.7	206.1	18.6

Study: 97K0968A
RFSP-7.PMG

Record File: B

1/3/83 ?

0:?? PM
Location; Long: 284.0 Lat: 41.4
General Attitude; Strike: 0.0 Dip: 0.0
Age: 12K
Local: BRF-1
Description: 968 CM

==========

ID: 97K0968A Strike: 0.0, Dip: 0.0 Long: 284.0, Lat: 41.4
Core Y: 0.0, Z': 0.0

C	DMT	Range	n	P	St	G_Dec	G_Inc	G_Long	G_Lat	S_Dec	S_Inc	S_Long	S_lat
0	N	0- 0	1			248.3	28.0	219.5	-5.6	248.3	28.0	219.5	-5.6
1	H	100-999	9+			257.7	22.9	211.0	-1.1	257.7	22.9	211.0	-1.1

ID: 97K0968B Strike: 0.0, Dip: 0.0 Long: 284.0, Lat: 41.4
Core Y: 0.0, Z': 0.0

C	DMT	Range	n	P	St	G_Dec	G_Inc	G_Long	G_Lat	S_Dec	S_Inc	S_Long	S_lat
0	N	0- 0	1			241.6	43.6	231.4	-2.2	241.6	43.6	231.4	-2.2
1	T	100-350	6+			254.7	37.5	219.6	3.0	254.7	37.5	219.6	3.0

ID: 97K0970A Strike: 0.0, Dip: 0.0 Long: 284.0, Lat: 41.4
Core Y: 0.0, Z': 0.0

C	DMT	Range	n	P	St	G_Dec	G_Inc	G_Long	G_Lat	S_Dec	S_Inc	S_Long	S_lat
0	N	0- 0	1			251.2	28.9	217.9	-3.3	251.2	28.9	217.9	-3.3
1	H	1-600	8+			253.8	23.5	213.9	-3.7	253.8	23.5	213.9	-3.7

ID: 97K0970B Strike: 0.0, Dip: 0.0 Long: 284.0,
Lat: 41.4

C	DMT	Range	n	Core P	St	G_Dec	G_Inc	G_Long	G_Lat	S_Dec	S_Inc	S_Long	S_lat
				Y: 0.0,	Z': 0.0								
0	N	0- 0	1			253.2	38.4	221.0	2.4	253.2	38.4	221.0	2.4
1	T	100-400	7+			264.3	31.2	210.4	6.9	264.3	31.2	210.4	6.9

ID: 97K0972A Strike: 0.0, Dip: 0.0 Long: 284.0,
Lat: 41.4

C	DMT	Range	n	Core P	St	G_Dec	G_Inc	G_Long	G_Lat	S_Dec	S_Inc	S_Long	S_lat
				Y: 0.0,	Z': 0.0								
0	N	0- 0	1			246.2	36.9	224.9	-2.9	246.2	36.9	224.9	-2.9
1	H	100-600	7+			256.2	32.6	216.3	1.8	256.2	32.6	216.3	1.8

ID: 97K0972B Strike: 0.0, Dip: 0.0 Long: 284.0,
Lat: 41.4

C	DMT	Range	n	Core P	St	G_Dec	G_Inc	G_Long	G_Lat	S_Dec	S_Inc	S_Long	S_lat
				Y: 0.0,	Z': 0.0								
0	N	0- 0	1			255.1	31.2	216.3	0.4	255.1	31.2	216.3	0.4
1	T	100-400	7+			268.2	25.3	205.2	7.4	268.2	25.3	205.2	7.4

Record File: B

Study: 97K0975A
RFSP-8.PMG

1/3/83 ?

0:?? PM
Location; Long: 284.0 Lat: 41.4
General Attitude; Strike: 0.0 Dip: 0.0
Age: 12K
Local: BRF-1
Description: 975 CM

==========

ID: 97K0975A Strike: 0.0, Dip: 0.0 Long: 284.0, Lat: 41.4

Core Y: 0.0, Z': 0.0

C	DMT Range	n	P St	G_Dec	G_Inc	G_Long	G_Lat	S_Dec	S_Inc	S_Long	S_lat
0	N 0- 0	1		238.1	39.5	231.8	-6.6	238.1	39.5	231.8	-6.6
1	H100-800	8+		247.7	32.5	221.9	-4.0	247.7	32.5	221.9	-4.0

ID: 97K0975B Strike: 0.0, Dip: 0.0 Long: 284.0, Lat: 41.4

Core Y: 0.0, Z': 0.0

C	DMT Range	n	P St	G_Dec	G_Inc	G_Long	G_Lat	S_Dec	S_Inc	S_Long	S_lat
0	N 0- 0	1		250.7	29.9	218.7	-3.2	250.7	29.9	218.7	-3.2
1	T100-625	1+		258.2	26.0	212.0	0.4	258.2	26.0	212.0	0.4

Record File: B

Study: 97K0979A
RFSP-9.PMG

1/3/83 ?

0:?? PM

Location; Long: 284.0 Lat: 41.4
General Attitude; Strike: 0.0 Dip: 0.0
Age: 12K
Local: BRF-1
Description: 979 CM

==========

ID: 97K0979A Strike: 0.0, Dip: 0.0 Long: 284.0, Lat: 41.4

Core Y: 0.0, Z': 0.0

C	DMT	Range	n	P	St	G_Dec	G_Inc	G_Long	G_Lat	S_Dec	S_Inc	S_Long	S_lat
0	N	0- 0	1			239.7	37.7	229.8	-6.6	239.7	37.7	229.8	-6.6
1	H	1-999	1+			241.6	33.5	226.6	-7.5	241.6	33.5	226.6	-7.5

ID: 97K0979B Strike: 0.0, Dip: 0.0 Long: 284.0, Lat: 41.4

Core Y: 0.0, Z': 0.0

C	DMT	Range	n	P	St	G_Dec	G_Inc	G_Long	G_Lat	S_Dec	S_Inc	S_Long	S_lat
0	N	0- 0	1			236.1	38.0	232.6	-8.6	236.1	38.0	232.6	-8.6
1	T100	-525	1+			244.1	33.8	225.0	-5.8	244.1	33.8	225.0	-5.8

ID: 97K0981A Strike: 0.0, Dip: 0.0 Long: 284.0, Lat: 41.4

Core Y: 0.0, Z': 0.0

C	DMT	Range	n	P	St	G_Dec	G_Inc	G_Long	G_Lat	S_Dec	S_Inc	S_Long	S_lat
0	N	0- 0	1			238.6	28.9	226.9	-11.6	238.6	28.9	226.9	-11.6
1	H100	-800	8+			243.8	22.2	220.4	-11.1	243.8	22.2	220.4	-11.1

ID: 97K0981B Strike: 0.0, Dip: 0.0 Long: 284.0,
Lat: 41.4

Core Y: 0.0, Z': 0.0

C	DMT	Range	n	P	St	G_Dec	G_Inc	G_Long	G_Lat	S_Dec	S_Inc	S_Long	S_lat
0	N	0- 0	1			236.5	27.4	227.9	-13.6	236.5	27.4	227.9	-13.6
1	T	100-625	1+			239.6	22.1	223.4	-13.9	239.6	22.1	223.4	-13.9

ID: 97K0983A Strike: 0.0, Dip: 0.0 Long: 284.0,
Lat: 41.4

Core Y: 0.0, Z': 0.0

C	DMT	Range	n	P	St	G_Dec	G_Inc	G_Long	G_Lat	S_Dec	S_Inc	S_Long	S_lat
0	N	0- 0	1			214.3	12.2	242.1	-33.0	214.3	12.2	242.1	-33.0
1	H	1-999	1+			215.0	10.0	240.7	-33.6	215.0	10.0	240.7	-33.6

ID: 97K0983B Strike: 0.0, Dip: 0.0 Long: 284.0,
Lat: 41.4

Core Y: 0.0, Z': 0.0

C	DMT	Range	n	P	St	G_Dec	G_Inc	G_Long	G_Lat	S_Dec	S_Inc	S_Long	S_lat
0	N	0- 0	1			217.6	10.8	238.3	-31.9	217.6	10.8	238.3	-31.9
1	T	1-625	1+			217.6	7.8	237.3	-33.2	217.6	7.8	237.3	-33.2

Study: 97K0986A
RFSP-10.PMG

Record File: B

1/3/83 ?

0:?? PM

Location; Long: 284.0 Lat: 41.4
General Attitude; Strike: 0.0 Dip: 0.0
Age: 12K
Local: BRF-1
Description: 986 CM

ID: 97K0986A Strike: 0.0, Dip: 0.0 Long: 284.0, Lat: 41.4

Core Y: 0.0, Z': 0.0

C	DMT	Range	n	P	St	G_Dec	G_Inc	G_Long	G_Lat	S_Dec	S_Inc	S_Long	S_lat
0	N	0- 0	1			226.7	22.3	233.8	-21.8	226.7	22.3	233.8	-21.8
1	H	1-999	1+			228.1	18.6	231.3	-22.6	228.1	18.6	231.3	-22.6

ID: 97K0986B Strike: 0.0, Dip: 0.0 Long: 284.0, Lat: 41.4

Core Y: 0.0, Z': 0.0

C	DMT	Range	n	P	St	G_Dec	G_Inc	G_Long	G_Lat	S_Dec	S_Inc	S_Long	S_lat
0	N	0- 0	1			228.0	20.5	232.1	-21.8	228.0	20.5	232.1	-21.8
1	T	1-625	1+			230.6	15.8	228.2	-22.3	230.6	15.8	228.2	-22.3

ID: 97K0988A Strike: 0.0, Dip: 0.0 Long: 284.0, Lat: 41.4

Core Y: 0.0, Z': 0.0

C	DMT	Range	n	P	St	G_Dec	G_Inc	G_Long	G_Lat	S_Dec	S_Inc	S_Long	S_lat
0	N	0- 0	1			230.5	36.6	236.2	-12.5	230.5	36.6	236.2	-12.5
1	H	100-800	8+			241.6	26.6	223.7	-10.7	241.6	26.6	223.7	-10.7

ID: 97K0988B Strike: 0.0, Dip: 0.0 Long: 284.0, Lat: 41.4

Core Y: 0.0, Z': 0.0

C	DMT	Range	n	P	St	G_Dec	G_Inc	G_Long	G_Lat	S_Dec	S_Inc	S_Long	S_lat
0	N	0- 0	1			229.6	19.4	230.4	-21.4	229.6	19.4	230.4	-21.4
1	T	100-500	9+			234.7	13.8	224.2	-20.5	234.7	13.8	224.2	-20.5

Study: 97K0992A
rfsp-11.pmg

Record File: b

1/3/83 ?

0:?? PM

Location; Long: 284.0 Lat: 41.4
General Attitude; Strike: 0.0 Dip: 0.0
Age: 12K
Local: BRF-1
Description: 992 CM

==========

ID: 97K0992A Strike: 0.0, Dip: 0.0 Long: 284.0, Lat: 41.4

Core Y: 0.0, Z': 0.0

C	DMT	Range	n	P	St	G_Dec	G_Inc	G_Long	G_Lat	S_Dec	S_Inc	S_Long	S_lat
0	N	0- 0	1			243.7	44.0	230.2	-0.7	243.7	44.0	230.2	-0.7
1	H100-600		7+			256.7	24.5	212.4	-1.2	256.7	24.5	212.4	-1.2

ID: 97K0992B Strike: 0.0, Dip: 0.0 Long: 284.0, Lat: 41.4

Core Y: 0.0, Z': 0.0

C	DMT	Range	n	P	St	G_Dec	G_Inc	G_Long	G_Lat	S_Dec	S_Inc	S_Long	S_lat
0	N	0- 0	1			235.9	28.7	228.8	-13.4	235.9	28.7	228.8	-13.4
1	T100-450		8+			244.3	20.2	219.2	-11.6	244.3	20.2	219.2	-11.6

ID: 97K0994A Strike: 0.0, Dip: 0.0 Long: 284.0, Lat: 41.4

Core Y: 0.0, Z': 0.0

C	DMT	Range	n	P	St	G_Dec	G_Inc	G_Long	G_Lat	S_Dec	S_Inc	S_Long	S_lat
0	N	0- 0	1			232.0	40.1	236.5	-9.7	232.0	40.1	236.5	-9.7
1	H100-999		9+			240.7	24.5	223.6	-12.2	240.7	24.5	223.6	-12.2

ID: 97K0994B Strike: 0.0, Dip: 0.0 Long: 284.0, Lat: 41.4

Core Y: 0.0, Z': 0.0

C	DMT	Range	n	P	St	G_Dec	G_Inc	G_Long	G_Lat	S_Dec	S_Inc	S_Long	S_lat
0	N	0- 0	1			226.3	38.9	240.4	-13.5	226.3	38.9	240.4	-13.5
1	T	100-450	8+			234.4	27.2	229.4	-15.0	234.4	27.2	229.4	-15.0

ID: 97K0996A Strike: 0.0, Dip: 0.0 Long: 284.0, Lat: 41.4

Core Y: 0.0, Z': 0.0

C	DMT	Range	n	P	St	G_Dec	G_Inc	G_Long	G_Lat	S_Dec	S_Inc	S_Long	S_lat
0	N	0- 0	1			242.7	32.8	225.5	-7.2	242.7	32.8	225.5	-7.2
1	H	100-600	7+			259.2	31.6	213.9	3.4	259.2	31.6	213.9	3.4

ID: 97K0996B Strike: 0.0, Dip: 0.0 Long: 284.0, Lat: 41.4

Core Y: 0.0, Z': 0.0

C	DMT	Range	n	P	St	G_Dec	G_Inc	G_Long	G_Lat	S_Dec	S_Inc	S_Long	S_lat
0	N	0- 0	1			223.6	17.7	235.0	-25.6	223.6	17.7	235.0	-25.6
1	T	1-500	1+			226.0	13.9	231.5	-25.8	226.0	13.9	231.5	-25.8

ID: Strike: 0.0, Dip: 0.0 Long: 284.0, Lat: 41.4

Core Y: 0.0, Z': 0.0

C	DMT	Range	n	P	St	G_Dec	G_Inc	G_Long	G_Lat	S_Dec	S_Inc	S_Long	S_lat

APPENDIX C

Zijderveld diagrams from demagnetization of all samples

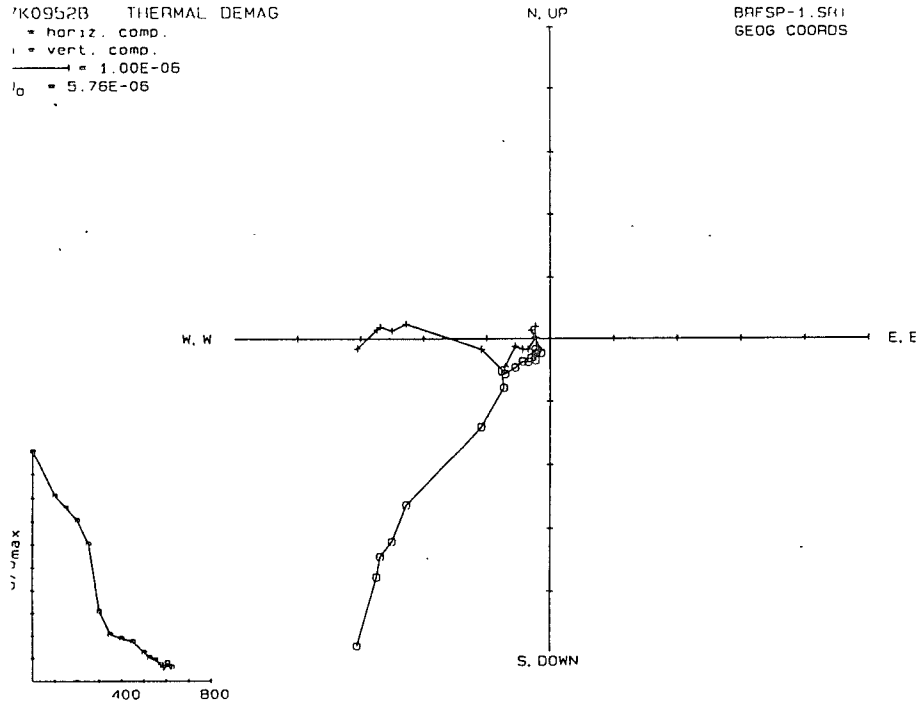
7K0952B THERMAL DEMAG
+ = horiz. comp.
o = vert. comp.
= 1.00E-06
J_o = 5.76E-06
BRFSP-1.SRT
GEOG COORDS
N, UP
W, W
E, E
S, DOWN
J/Jmax
400
800

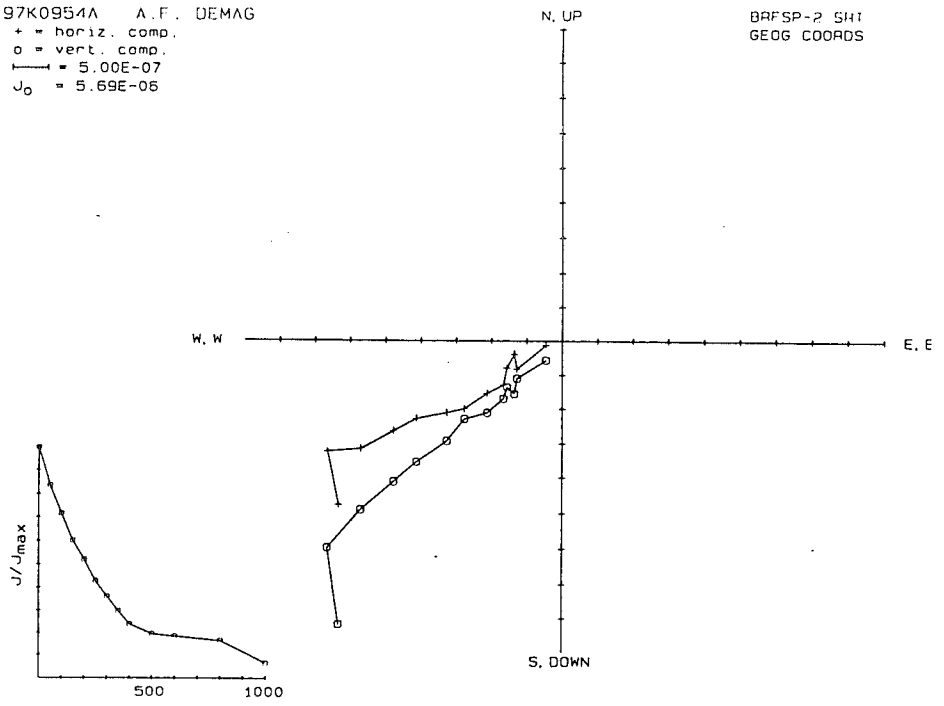
97K0954A A.F. DEMAG
+ = horiz. comp.
o = vert. comp.
= 5.00E-07
J_o = 5.69E-06
BRFSP-2.SRT
GEOG COORDS
N, UP
W, W
E, E
S, DOWN
J/Jmax
500
1000

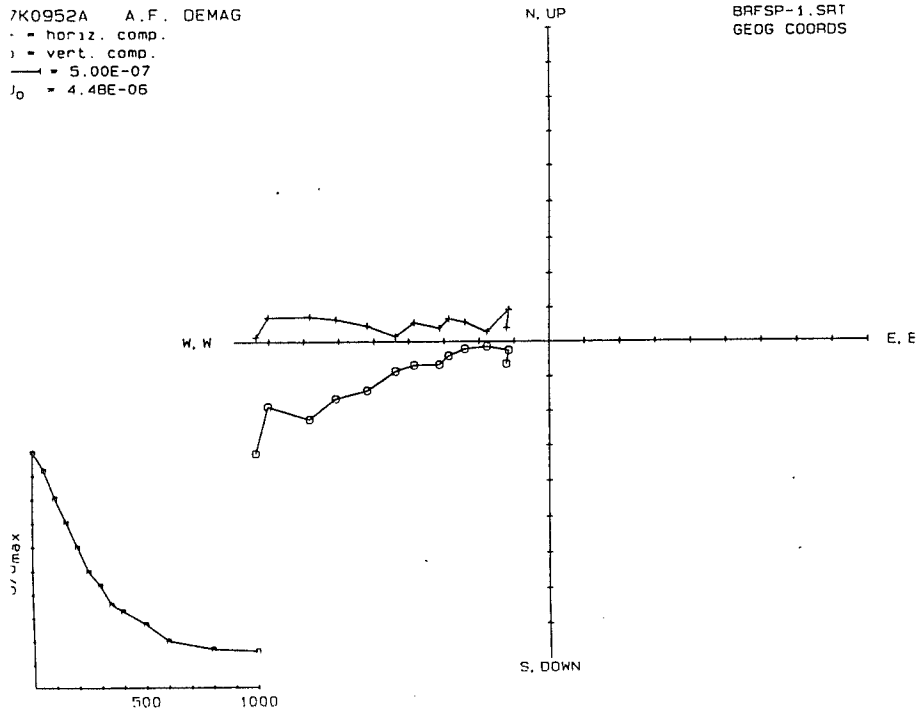
7K0952A A.F. DEMAG
= horiz. comp.
= vert. comp.
= 5.00E-07
J_o = 4.48E-06
BRFSP-1.SRT
GEOG COORDS
N, UP
W, W
E, E
S, DOWN
J/Jmax
500
1000

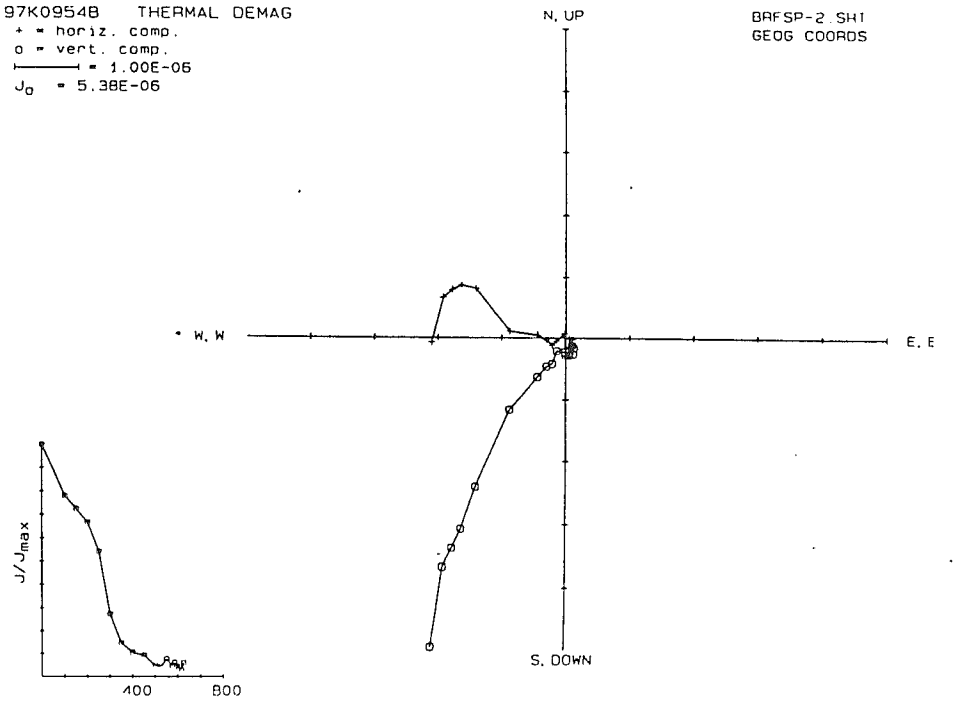
97K0954B THERMAL DEMAG
+ = horiz. comp.
o = vert. comp.
= 1.00E-06
J_o = 5.38E-06
BRFSP-2.SRT
GEOG COORDS
N, UP
W, W
E, E
S, DOWN
J/Jmax
400
800

97K0956A A.F. DEMAG
+ = horiz. comp.
o = vert. comp.
= 1.00E-06
J_o = 7.09E-06

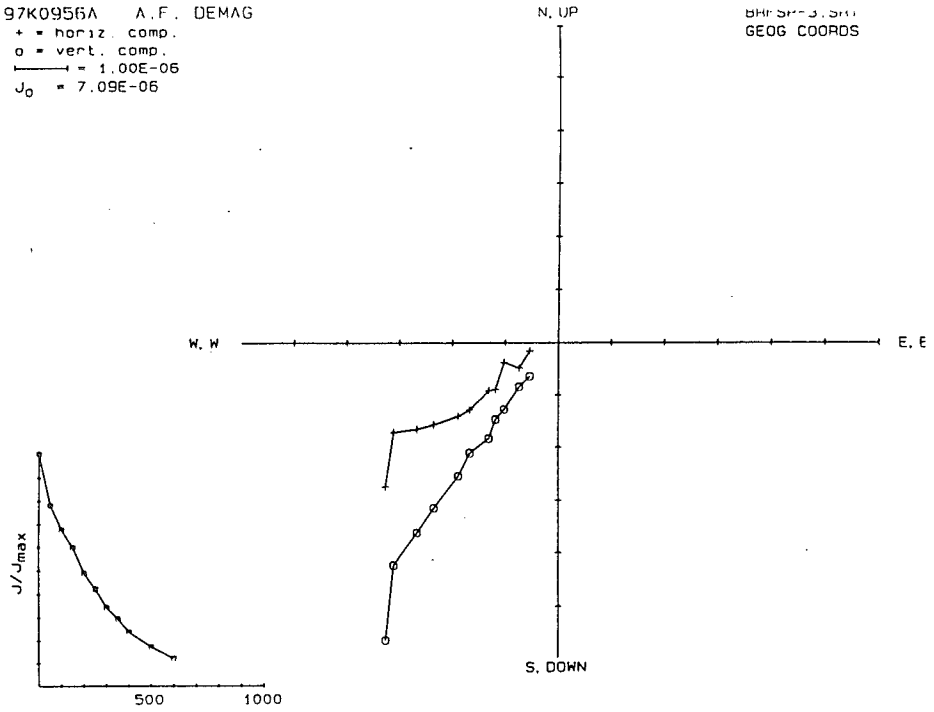

97K0958A A.F. DEMAG
+ = horiz. comp.
o = vert. comp.
= 1.00E-06
J_o = 6.65E-06

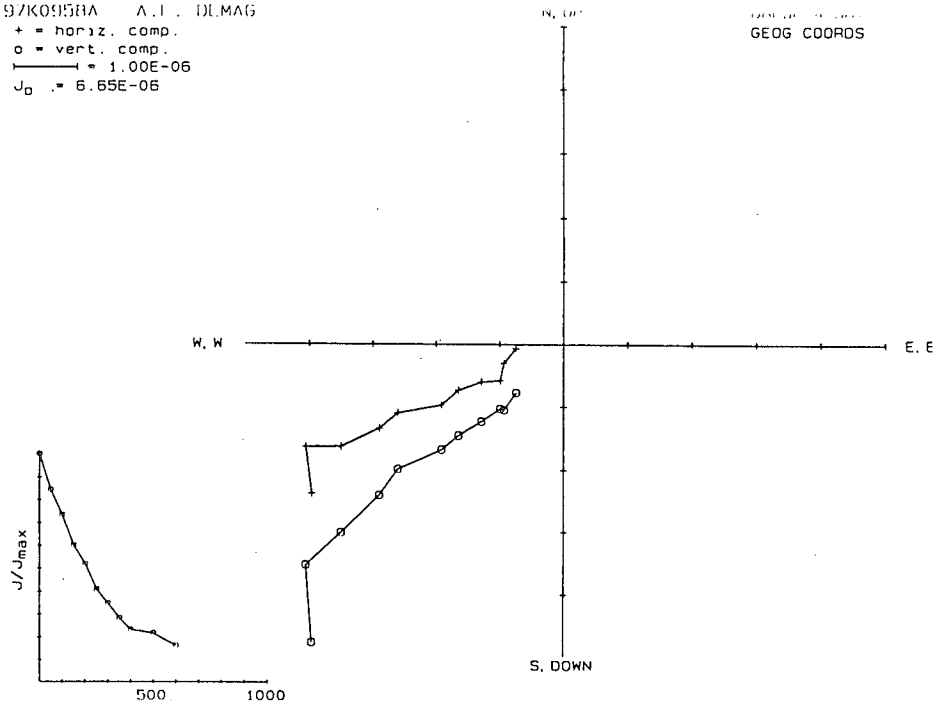

97K0956B THERMAL DEMAG
+ = horiz. comp.
o = vert. comp.
= 1.00E-06
J_o = 6.75E-06

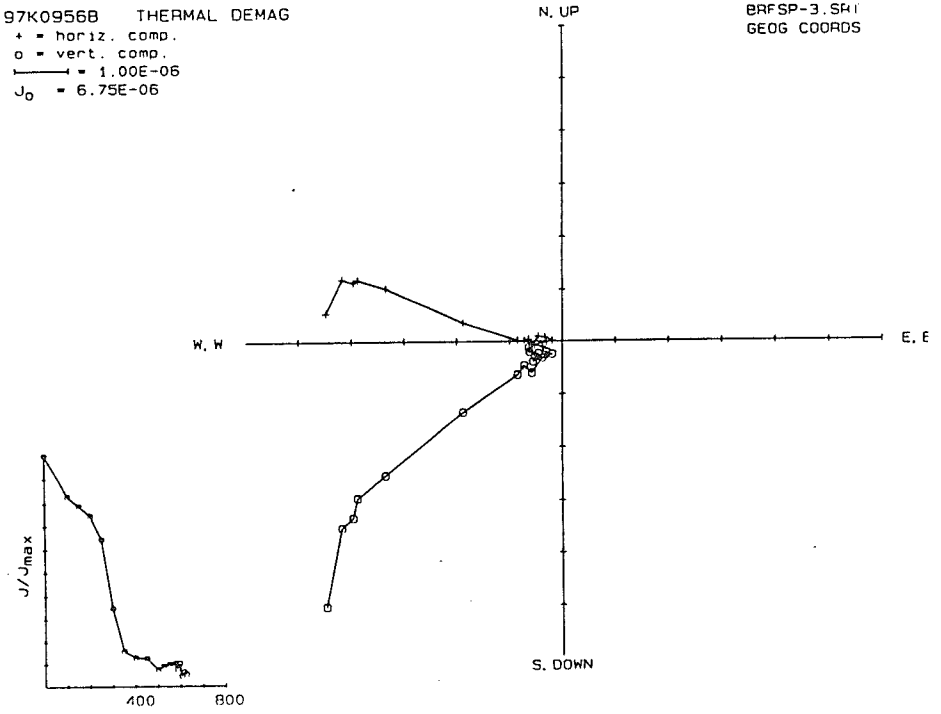

97K0958B THERMAL DEMAG
+ = horiz. comp.
o = vert. comp.
= 1.00E-06
J_o = 6.39E-06

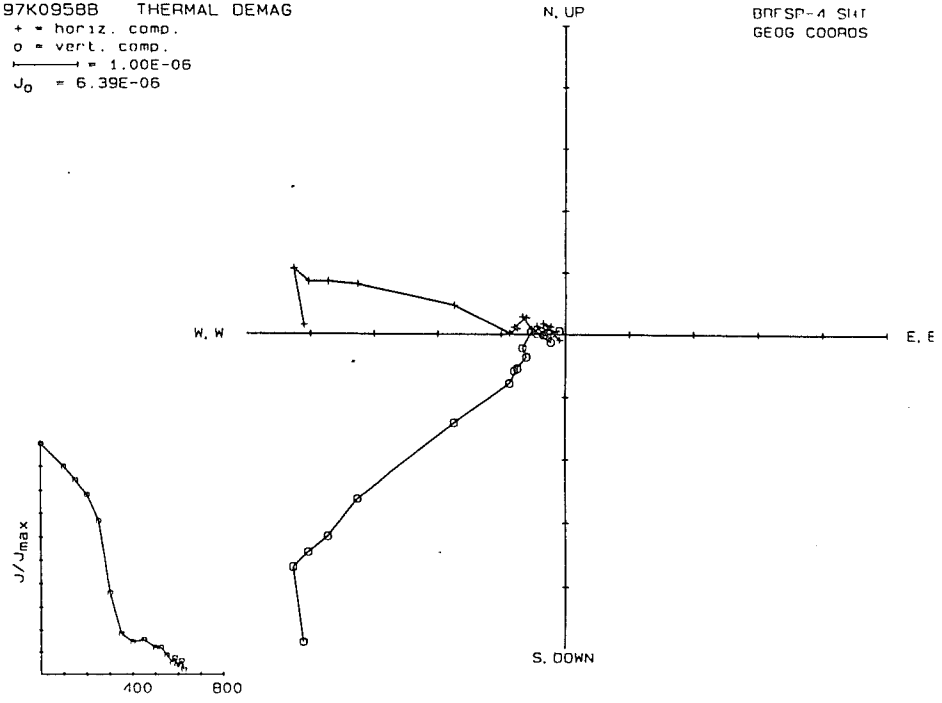

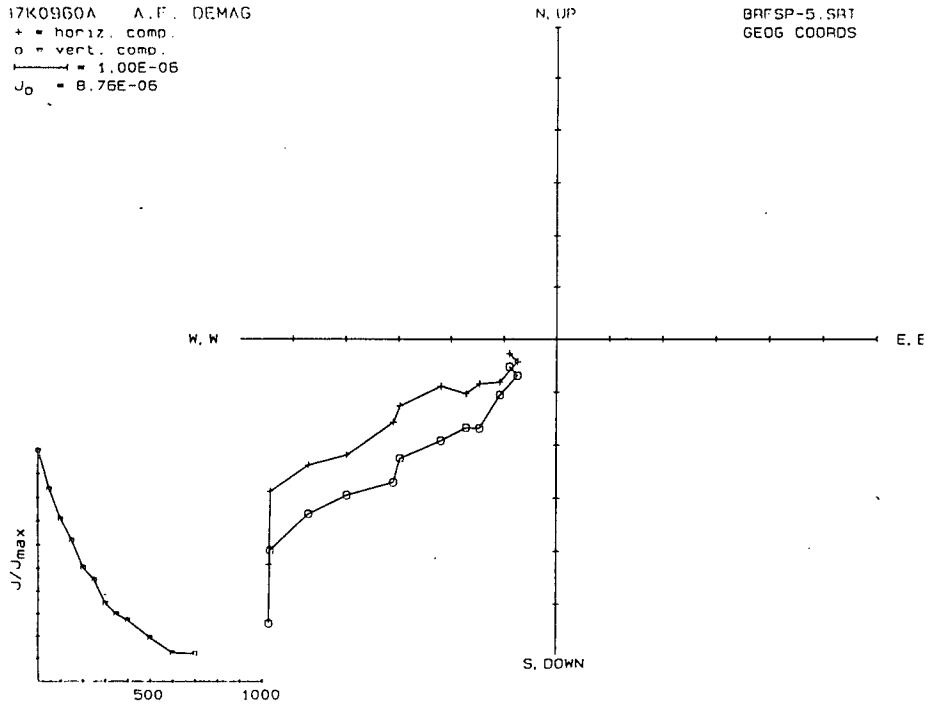
97K0960A A.F. DEMAG
+ = horiz. comp.
o = vert. comp.
= 1.00E-06
J_o = 8.76E-06
N, UP
BRFSP-5.SRT
GEOG COORDS
W, W
E, E
S, DOWN
J/Jmax
500
1000

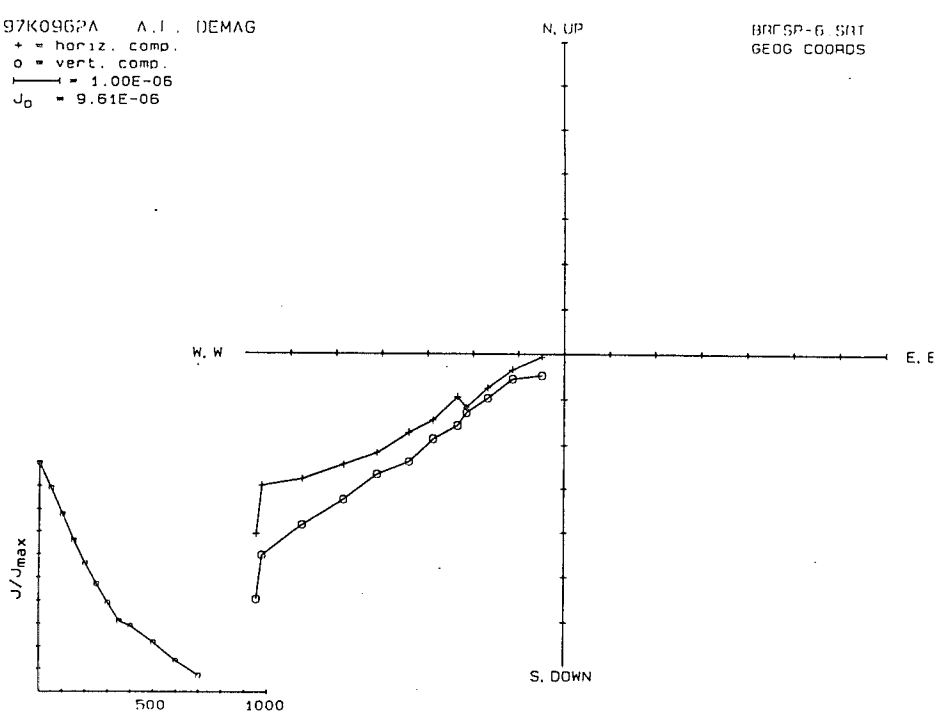
97K0962A A.F. DEMAG
+ = horiz. comp.
o = vert. comp.
= 1.00E-06
J_o = 9.61E-06
N, UP
BRFSP-6.SRT
GEOG COORDS
W, W
E, E
S, DOWN
J/Jmax
500
1000

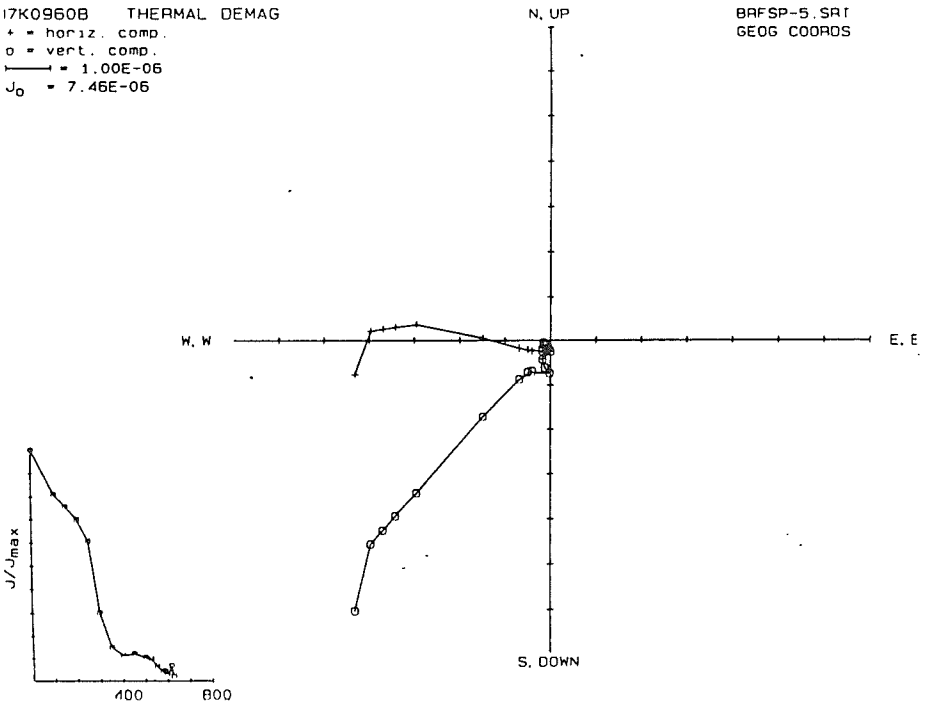
97K0960B THERMAL DEMAG
+ = horiz. comp.
o = vert. comp.
= 1.00E-06
J_o = 7.46E-06
N, UP
BRFSP-5.SRT
GEOG COORDS
W, W
E, E
S, DOWN
J/Jmax
400
800

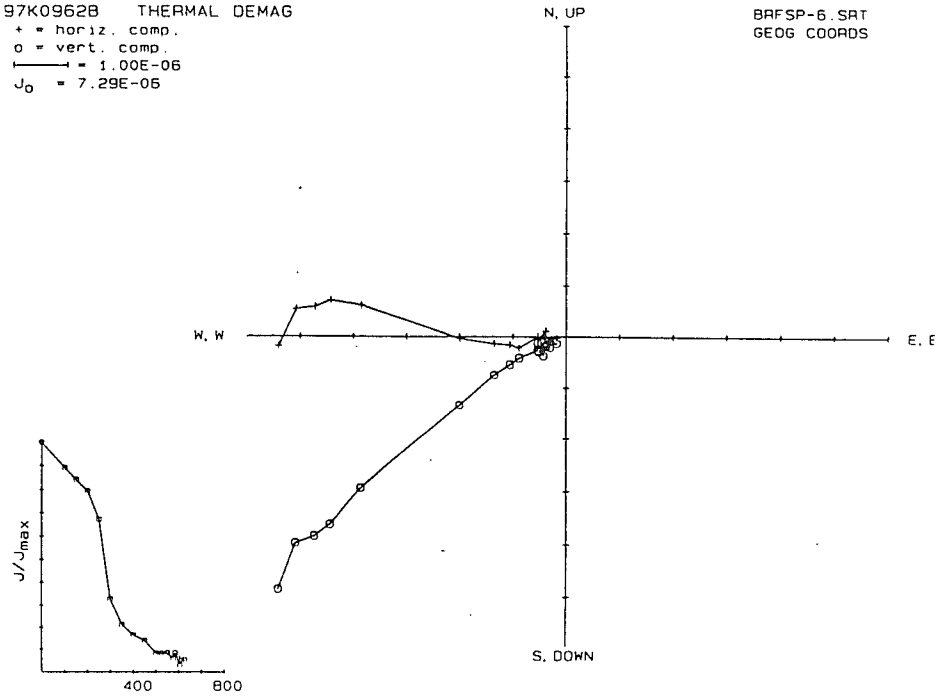
97K0962B THERMAL DEMAG
+ = horiz. comp.
o = vert. comp.
= 1.00E-06
J_o = 7.29E-06
N, UP
BRFSP-6.SRT
GEOG COORDS
W, W
E, E
S, DOWN
J/Jmax
400
800

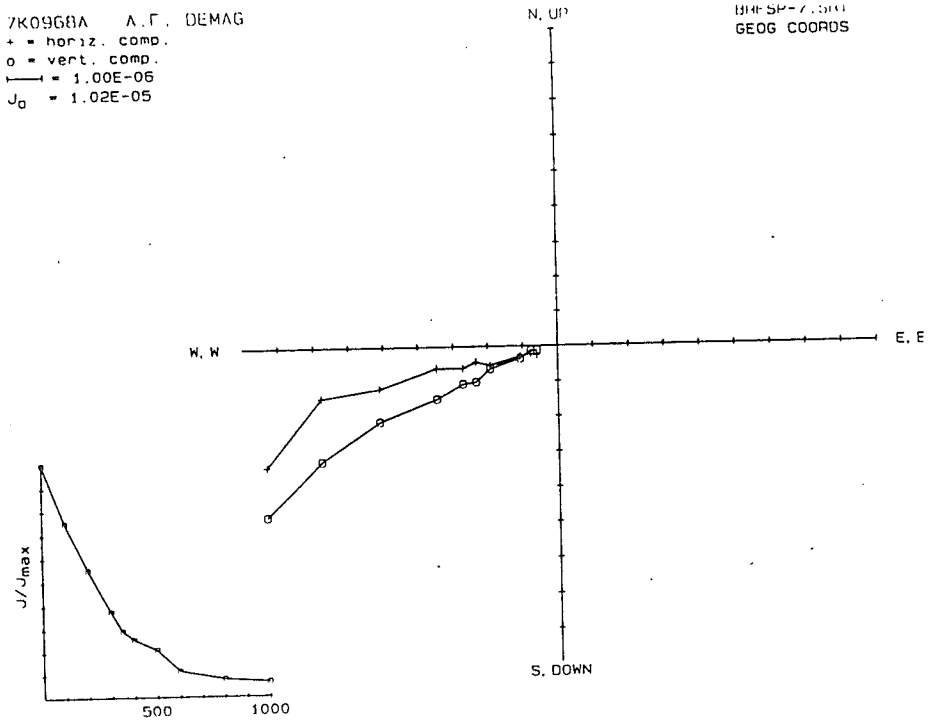
7K0968A A.F. DEMAG
+ = horiz. comp.
o = vert. comp.
= 1.00E-06
J_o = 1.02E-05
N, UP
BRFSP-7.SRT
GEOG COORDS
W, W
E, E
S, DOWN
J/Jmax
500
1000

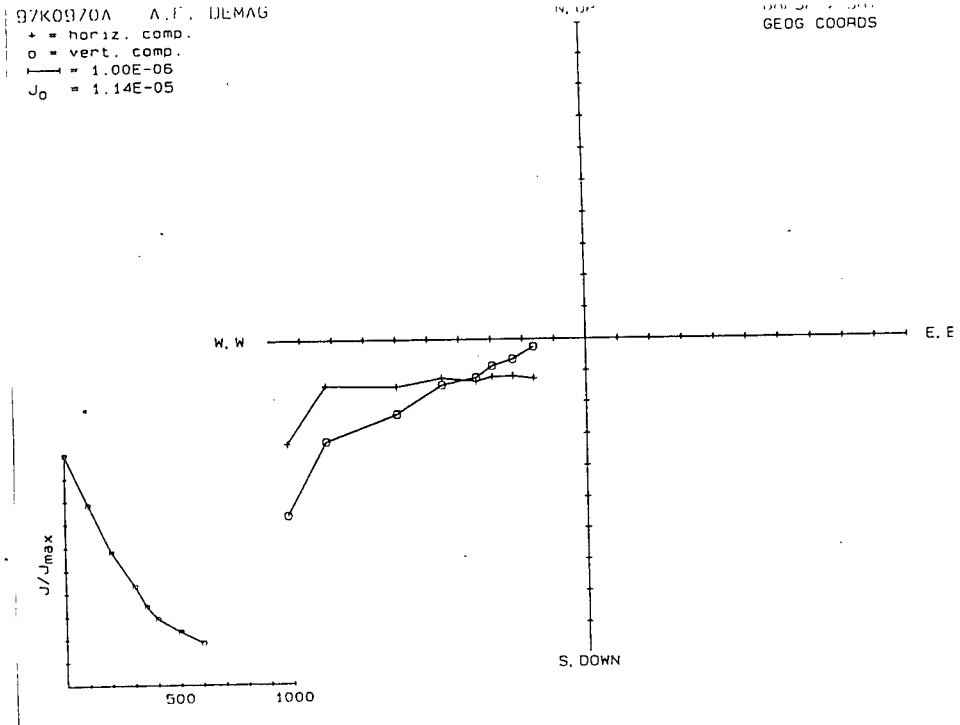
97K0970A A.F. DEMAG
+ = horiz. comp.
o = vert. comp.
= 1.00E-06
J_o = 1.14E-05
GEOG COORDS
W, W
E, E
S, DOWN
J/Jmax
500
1000

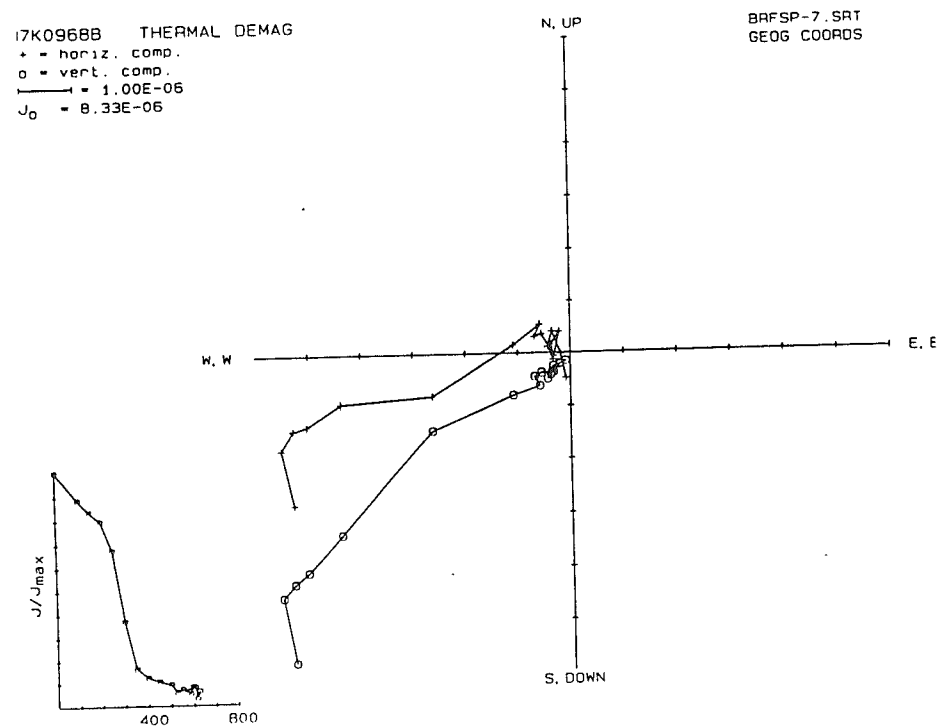
17K0968B THERMAL DEMAG
+ = horiz. comp.
o = vert. comp.
= 1.00E-06
J_o = 8.33E-06
N, UP
BRFSP-7.SRT
GEOG COORDS
W, W
E, E
S, DOWN
J/Jmax
400
800

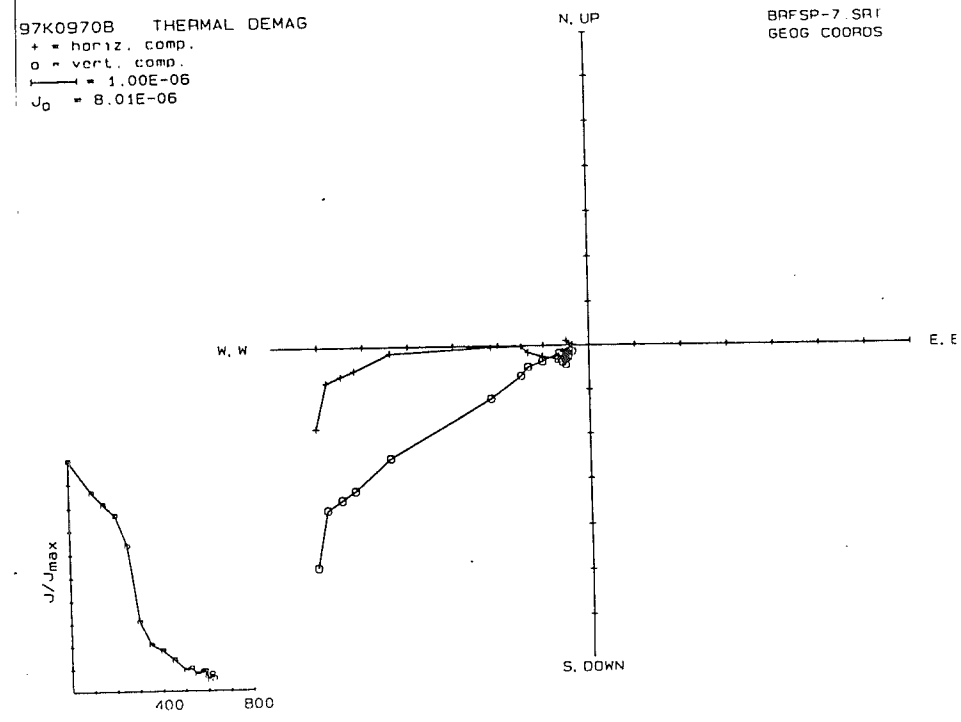
97K0970B THERMAL DEMAG
+ = horiz. comp.
o = vert. comp.
= 1.00E-06
J_o = 8.01E-06
N, UP
BRFSP-7.SRT
GEOG COORDS
W, W
E, E
S, DOWN
J/Jmax
400
800

K0972B THERMAL DEMAG
+ = horiz. comp.
o = vert. comp.
⟷ = 1.00E-06
J$_o$ = 7.34E-06

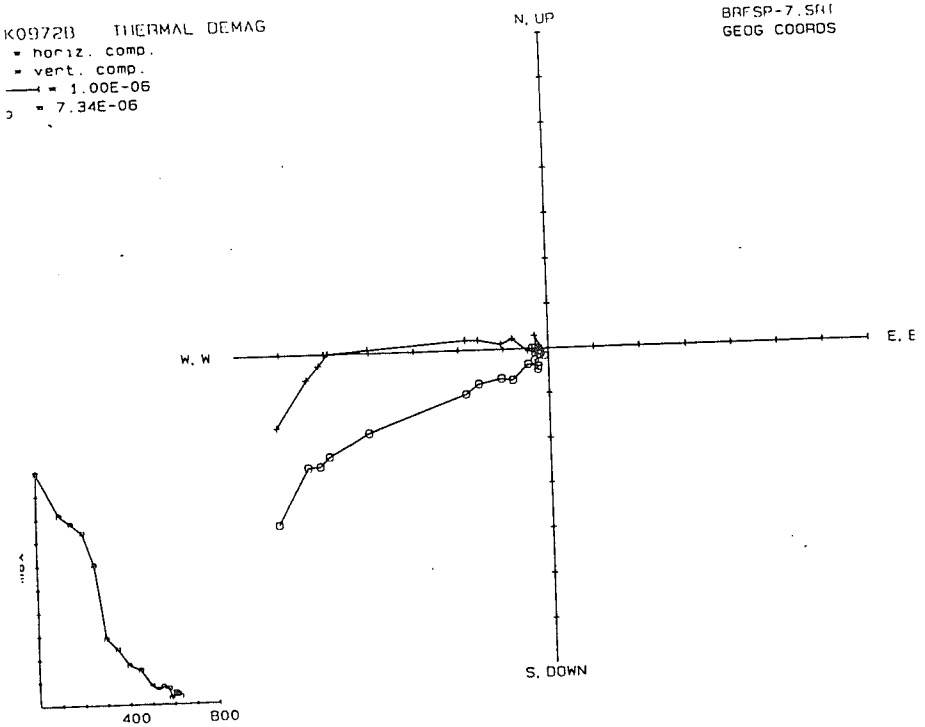

97K0975A A.F. DEMAG
+ = horiz. comp.
o = vert. comp.
⟷ = 1.00E-06
J$_o$ = 8.72E-06

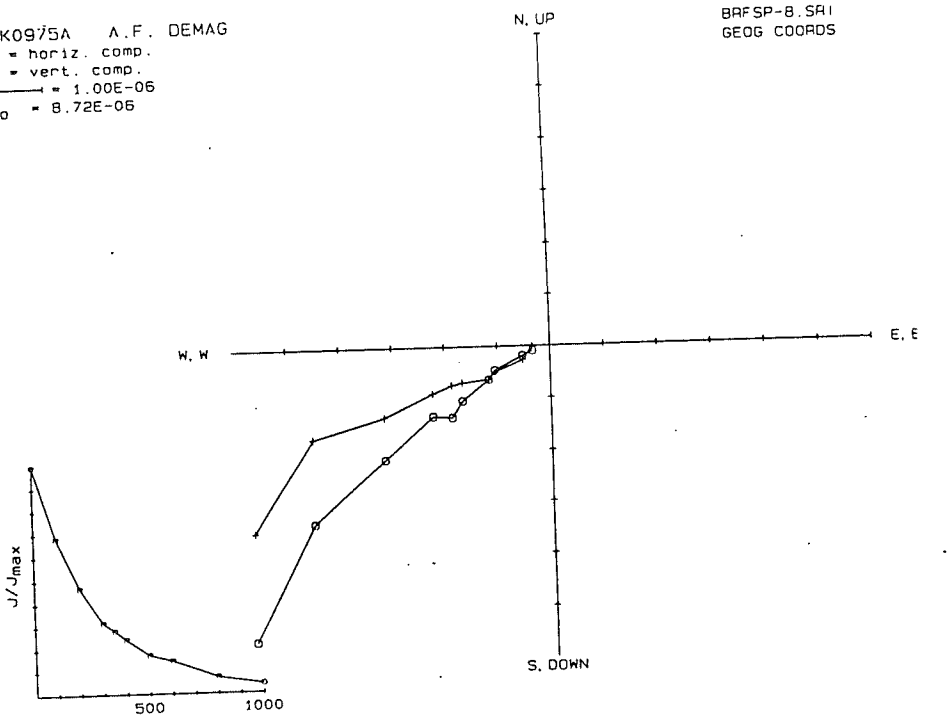

K0972A A.F. DEMAG
+ = horiz. comp.
o = vert. comp.
⟷ = 1.00E-06
o = 1.02E-05

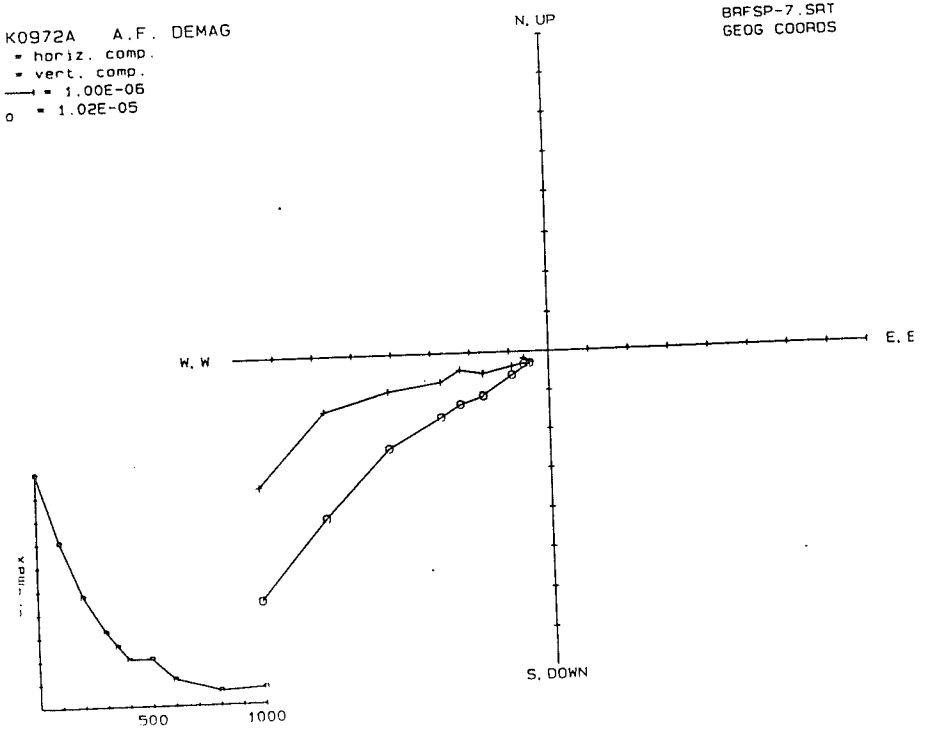

97K0975B THERMAL DEMAG
+ = horiz. comp.
o = vert. comp.
⟷ = 1.00E-06
J$_o$ = 7.65E-06

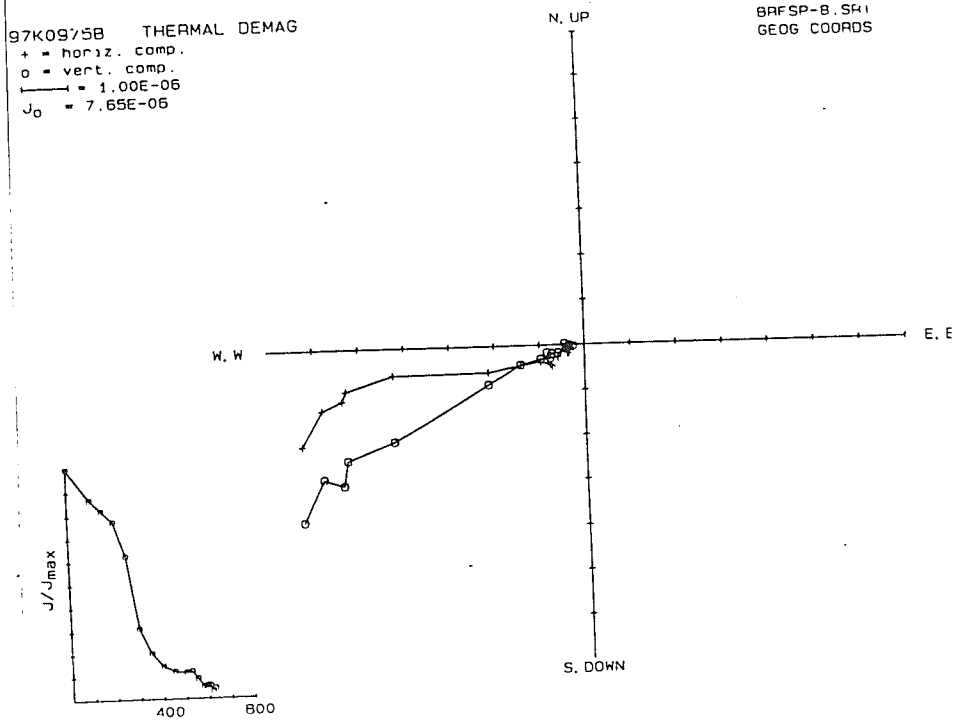

97K0979A A.F. DEMAG
+ = horiz. comp.
o = vert. comp.
1.00E-06
J_o = 8.40E-06

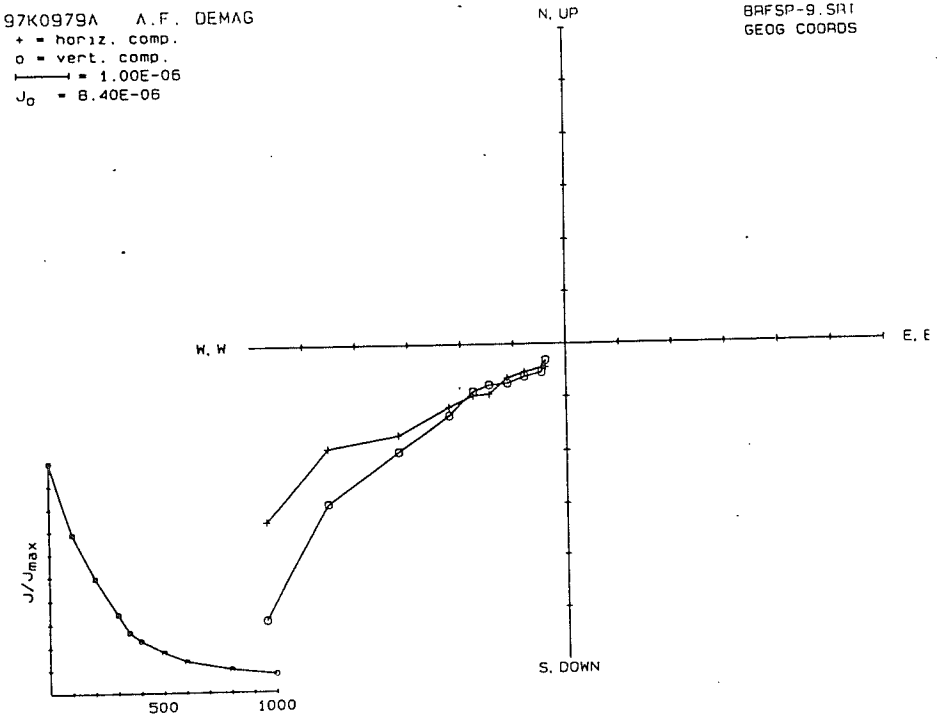

97K0981A A.F. DEMAG
+ = horiz. comp.
o = vert. comp.
1.00E-06
J_o = 8.82E-06

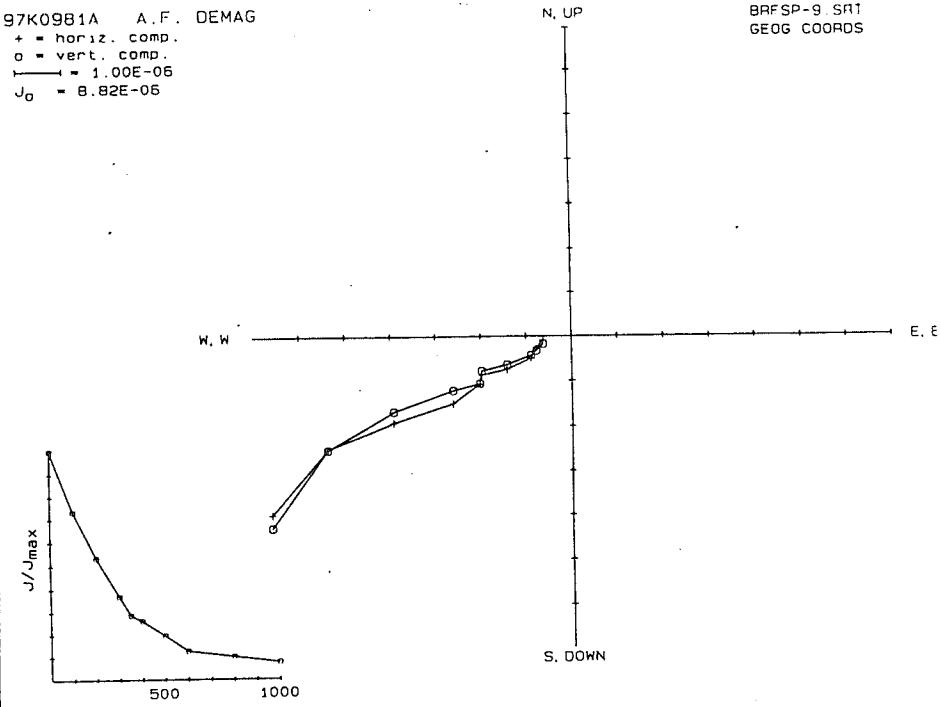

97K0979B THERMAL DEMAG
+ = horiz. comp.
o = vert. comp.
1.00E-06
J_o = 7.18E-06

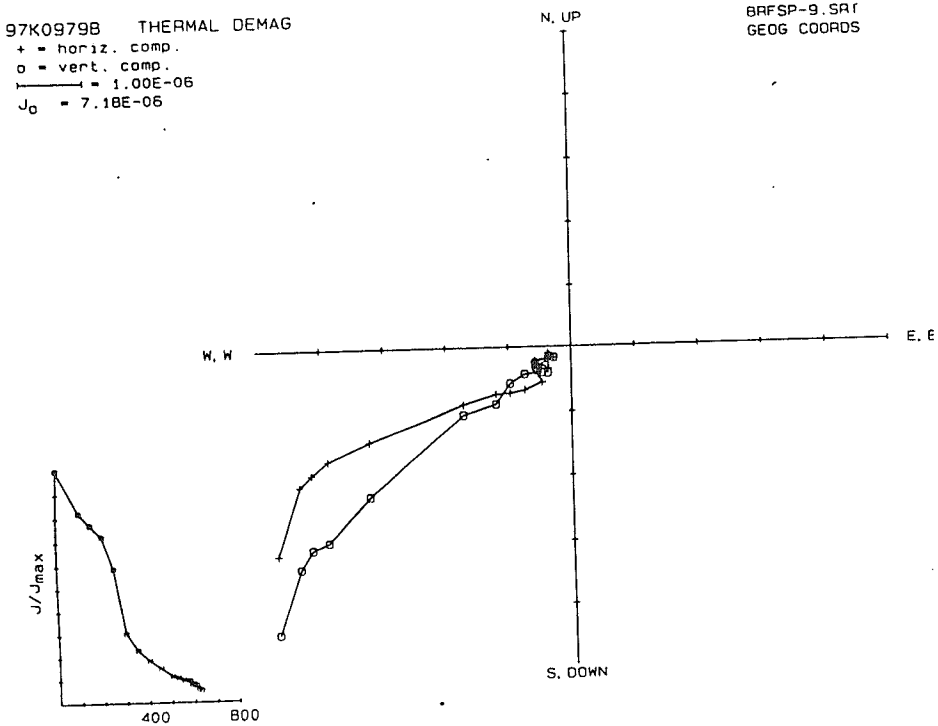

97K0981B THERMAL DEMAG
+ = horiz. comp.
o = vert. comp.
1.00E-06
J_o = 9.65E-06

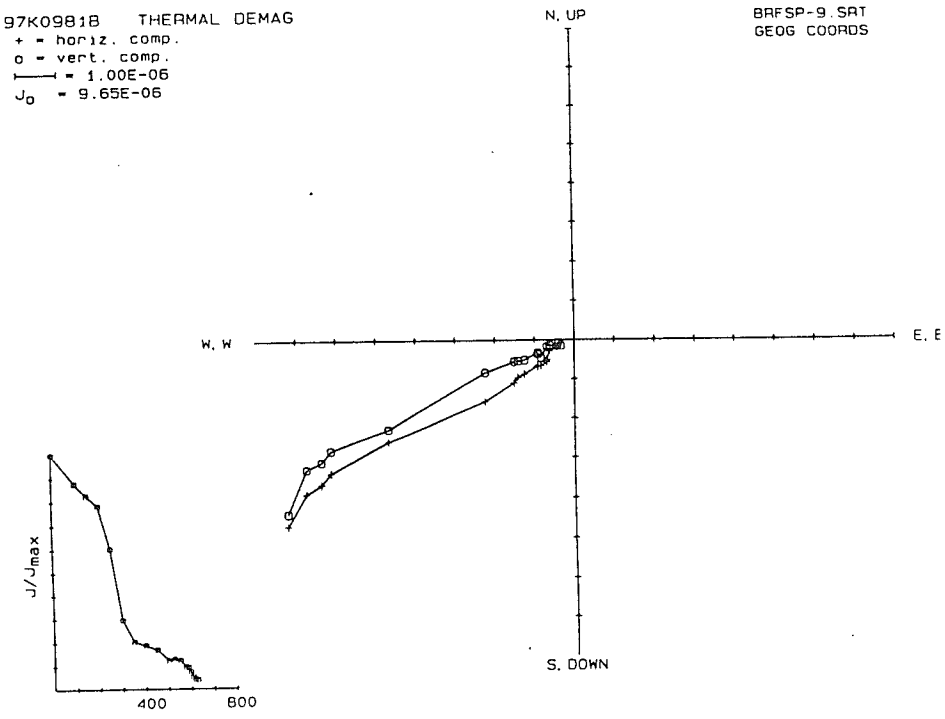

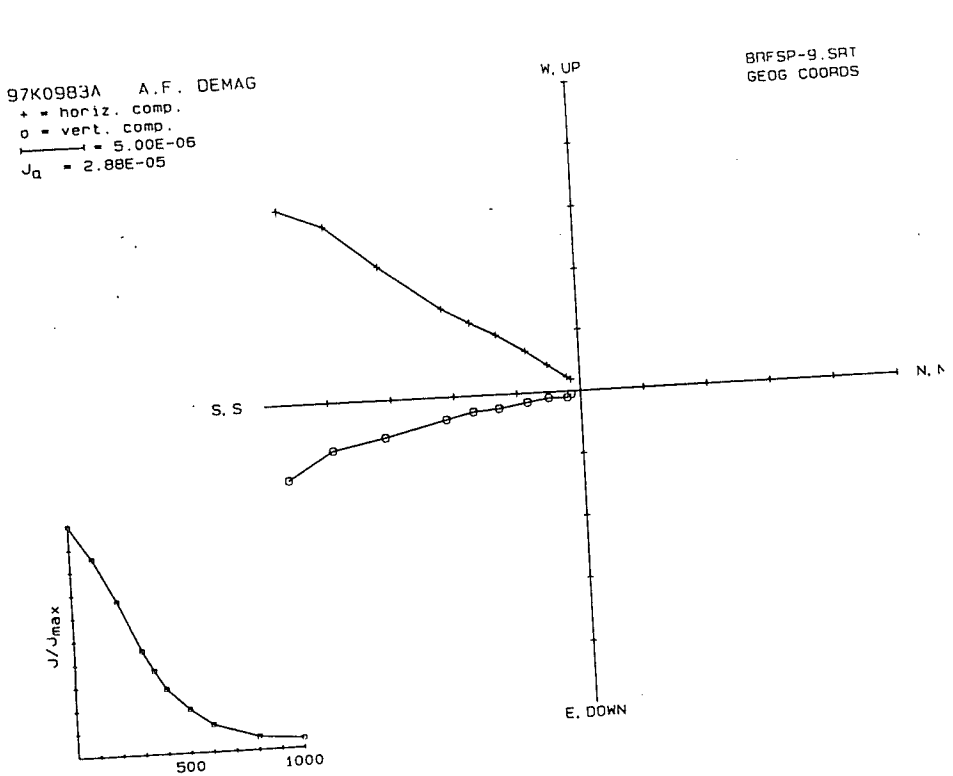
97K0983A A.F. DEMAG
+ = horiz. comp.
o = vert. comp.
= 5.00E-06
J_o = 2.88E-05
BRFSP-9.SRT
GEOG COORDS
W, UP
N, N
S, S
E, DOWN
J/Jmax
500
1000

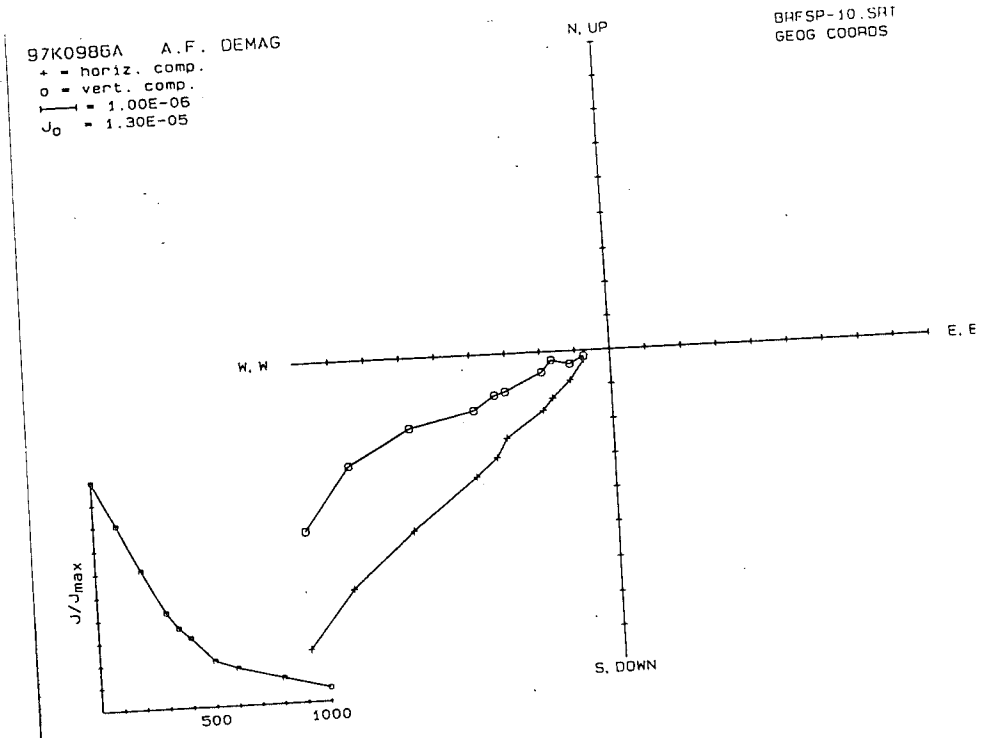
97K0986A A.F. DEMAG
+ = horiz. comp.
o = vert. comp.
= 1.00E-06
J_o = 1.30E-05
BRFSP-10.SRT
GEOG COORDS
N, UP
E, E
W, W
S, DOWN
J/Jmax
500
1000

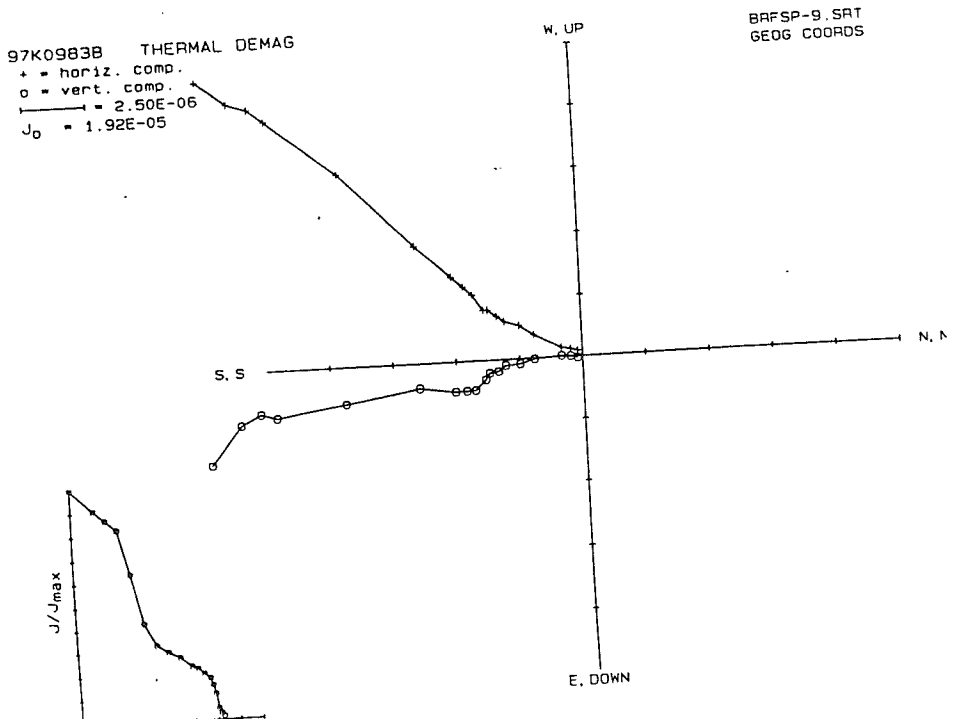
97K0983B THERMAL DEMAG
+ = horiz. comp.
o = vert. comp.
= 2.50E-06
J_o = 1.92E-05
BRFSP-9.SRT
GEOG COORDS
W, UP
N, N
S, S
E, DOWN
J/Jmax

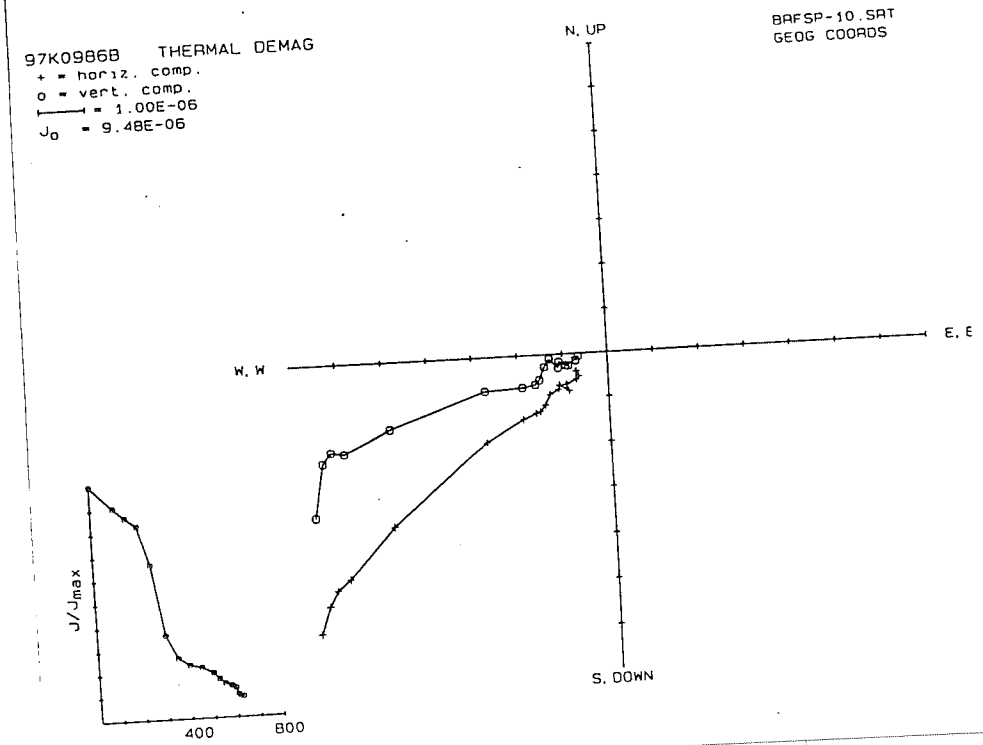
97K0986B THERMAL DEMAG
+ = horiz. comp.
o = vert. comp.
= 1.00E-06
J_o = 9.48E-06
BRFSP-10.SRT
GEOG COORDS
N, UP
E, E
W, W
S, DOWN
J/Jmax
400
800

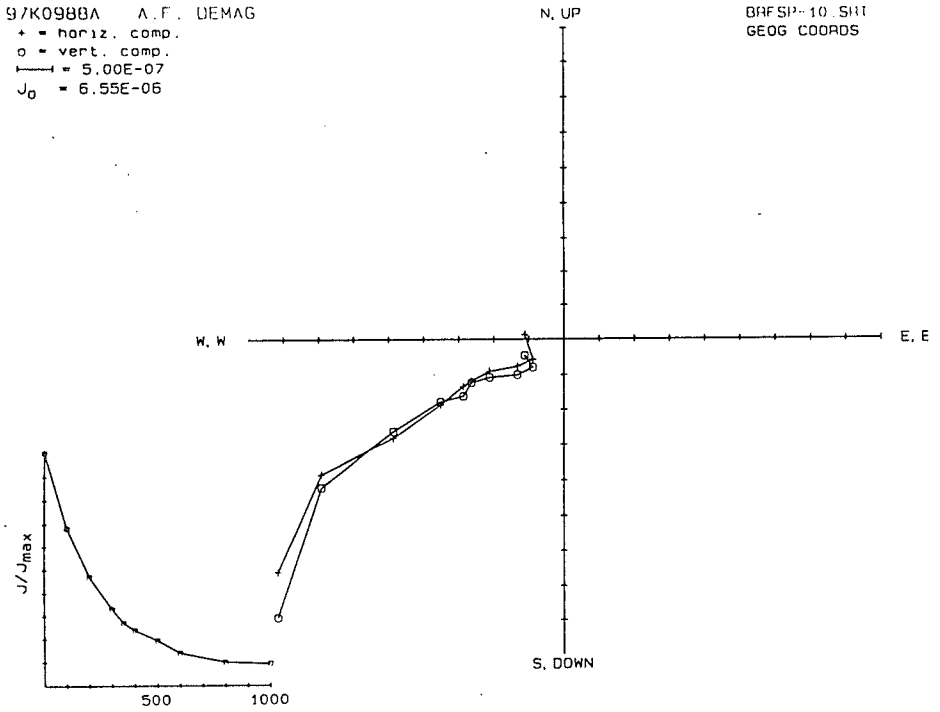
97K0988A A.F. DEMAG
+ = horiz. comp.
o = vert. comp.
= 5.00E-07
J_0 = 6.55E-06
N, UP
BAFSP-10.SRT
GEOG COORDS
W, W
E, E
S, DOWN
J/Jmax
500
1000

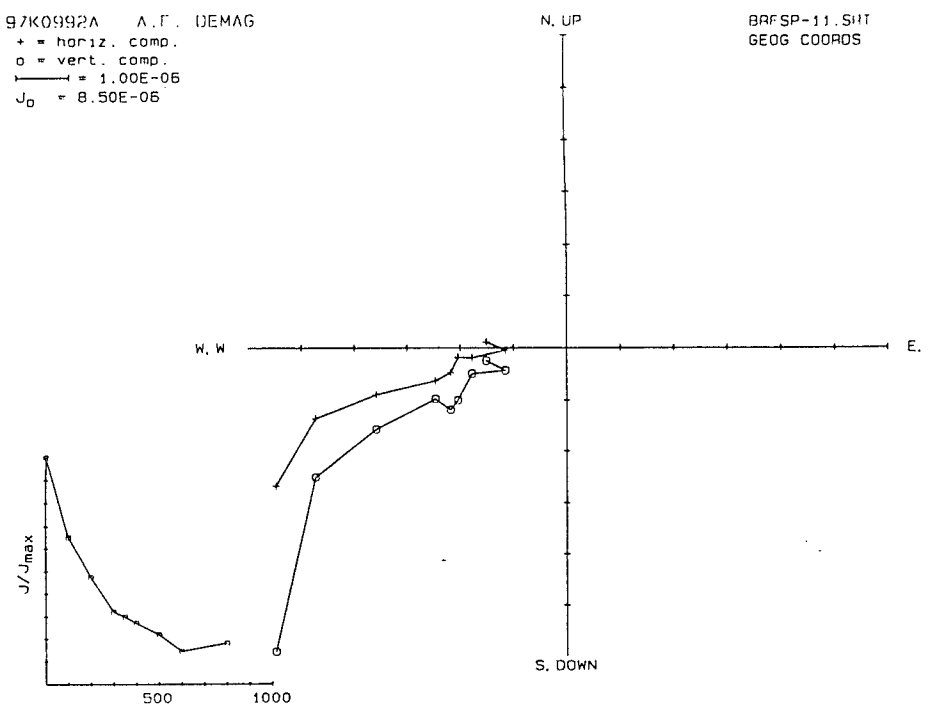
97K0992A A.F. DEMAG
+ = horiz. comp.
o = vert. comp.
= 1.00E-06
J_0 = 8.50E-06
N, UP
BAFSP-11.SRT
GEOG COORDS
W, W
E,
S, DOWN
J/Jmax
500
1000

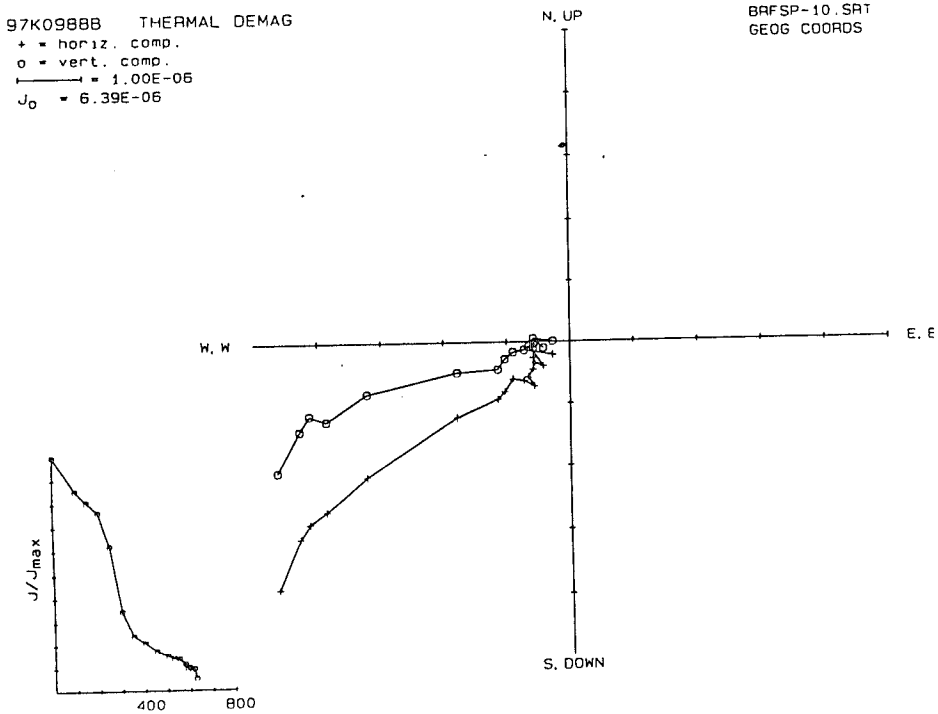
97K0988B THERMAL DEMAG
+ = horiz. comp.
o = vert. comp.
= 1.00E-06
J_0 = 6.39E-06
N, UP
BAFSP-10.SRT
GEOG COORDS
W, W
E, E
S, DOWN
J/Jmax
400
800

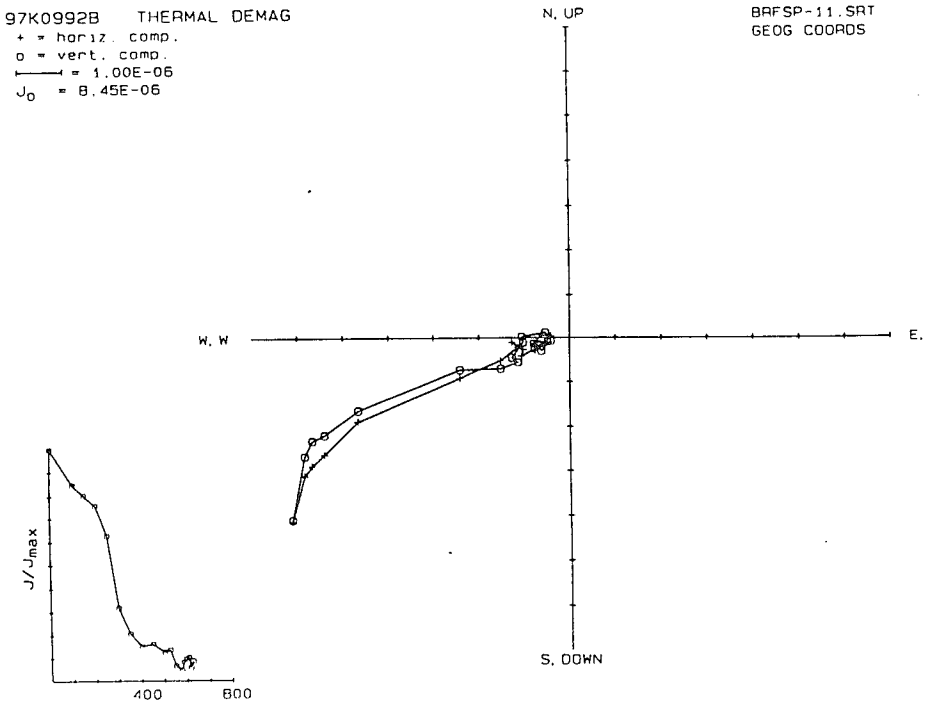
97K0992B THERMAL DEMAG
+ = horiz. comp.
o = vert. comp.
= 1.00E-06
J_0 = 8.45E-06
N, UP
BAFSP-11.SRT
GEOG COORDS
W, W
E,
S, DOWN
J/Jmax
400
800

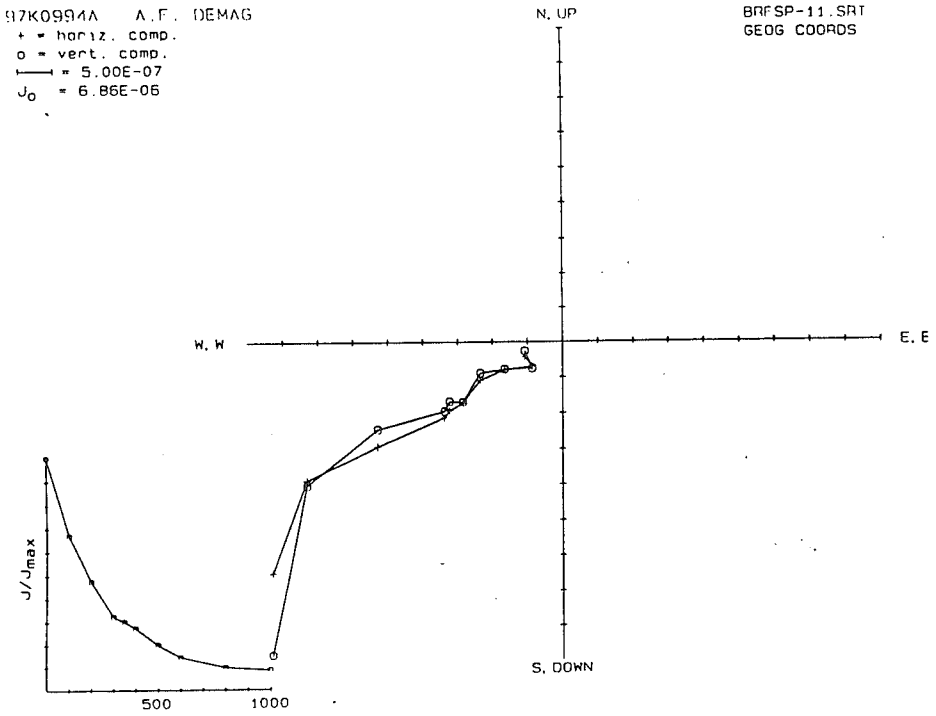
97K0994A A.F. DEMAG
+ = horiz. comp.
o = vert. comp.
= 5.00E-07
J_o = 6.86E-06
N, UP
BRFSP-11.SRT
GEOG COORDS
W, W
E, E
S, DOWN
J/Jmax
500
1000

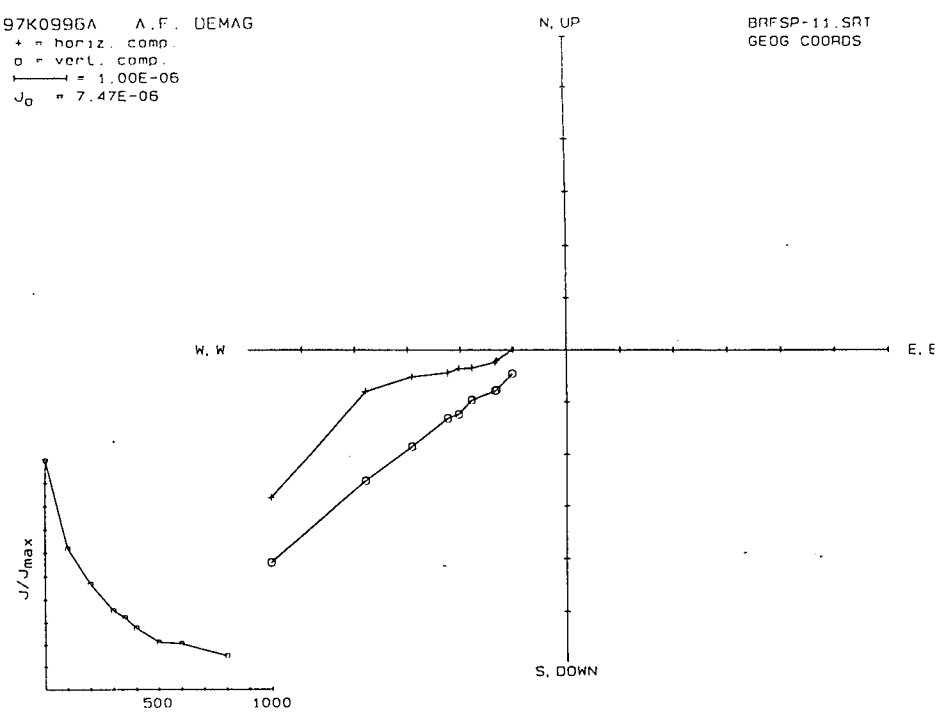
97K0996A A.F. DEMAG
+ = horiz. comp.
o = vert. comp.
= 1.00E-06
J_o = 7.47E-06
N, UP
BRFSP-11.SRT
GEOG COORDS
W, W
E, E
S, DOWN
J/Jmax
500
1000

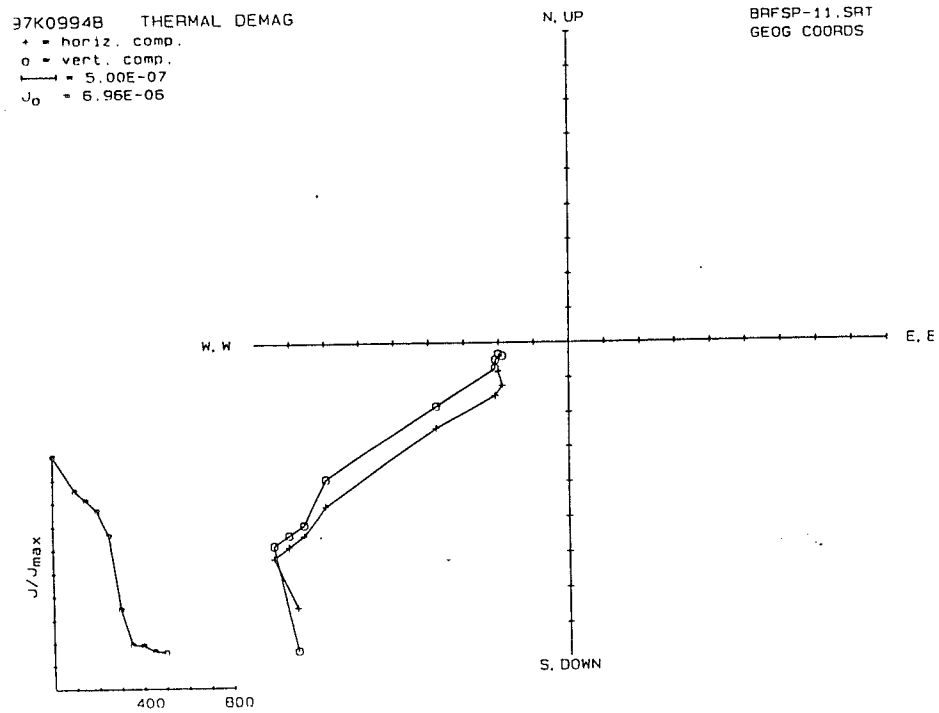
97K0994B THERMAL DEMAG
+ = horiz. comp.
o = vert. comp.
= 5.00E-07
J_o = 6.96E-06
N, UP
BRFSP-11.SRT
GEOG COORDS
W, W
E, E
S, DOWN
J/Jmax
400
800

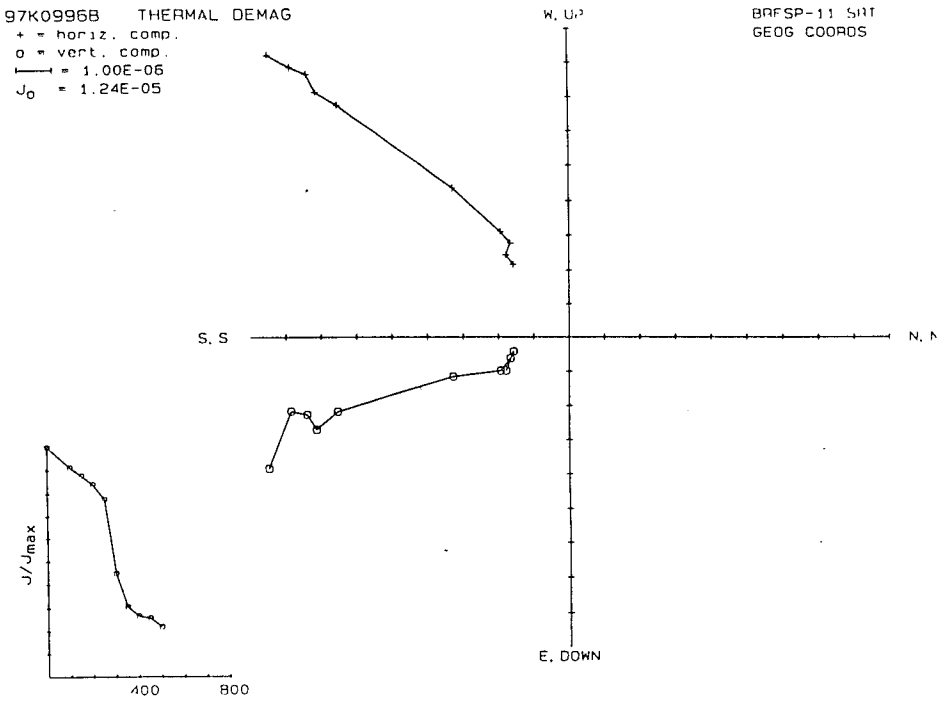
97K0996B THERMAL DEMAG
+ = horiz. comp.
o = vert. comp.
= 1.00E-06
J_o = 1.24E-05
BRFSP-11.SRT
GEOG COORDS
S, S
E, DOWN
J/Jmax
400
800

97K0902A A.F. DEMAG
+ = horiz. comp.
o = vert. comp.
= 1.00E-06
J_o = 6.34E-06

BRFSP-12.SRT
GEOG COORDS

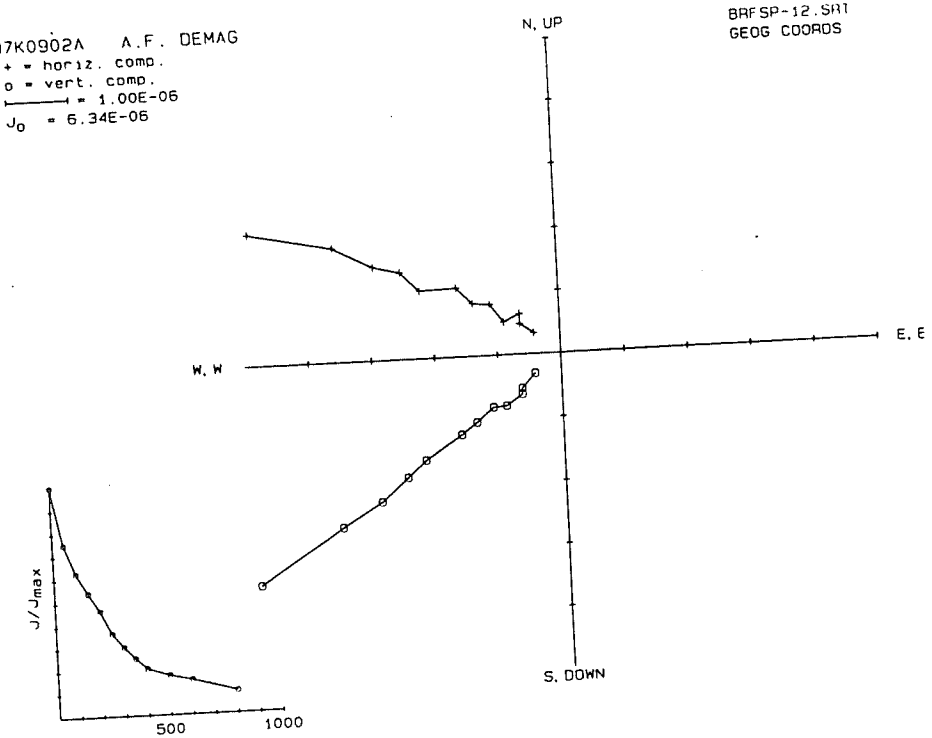

97K0905A A.F. DEMAG
+ = horiz. comp.
o = vert. comp.
= 1.00E-06
J_o = 9.15E-06

BRFSP-12.SRT
GEOG COORDS

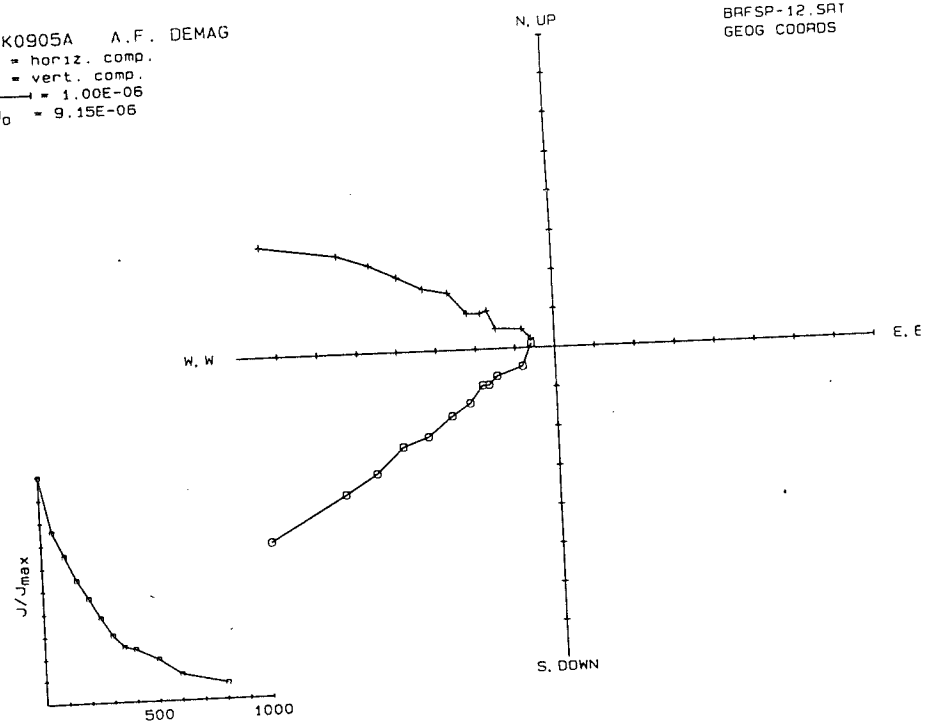

97K0904A A.F. DEMAG
+ = horiz. comp.
o = vert. comp.
= 1.00E-06
J_o = 6.54E-06

BRFSP-12.SRT
GEOG COORDS

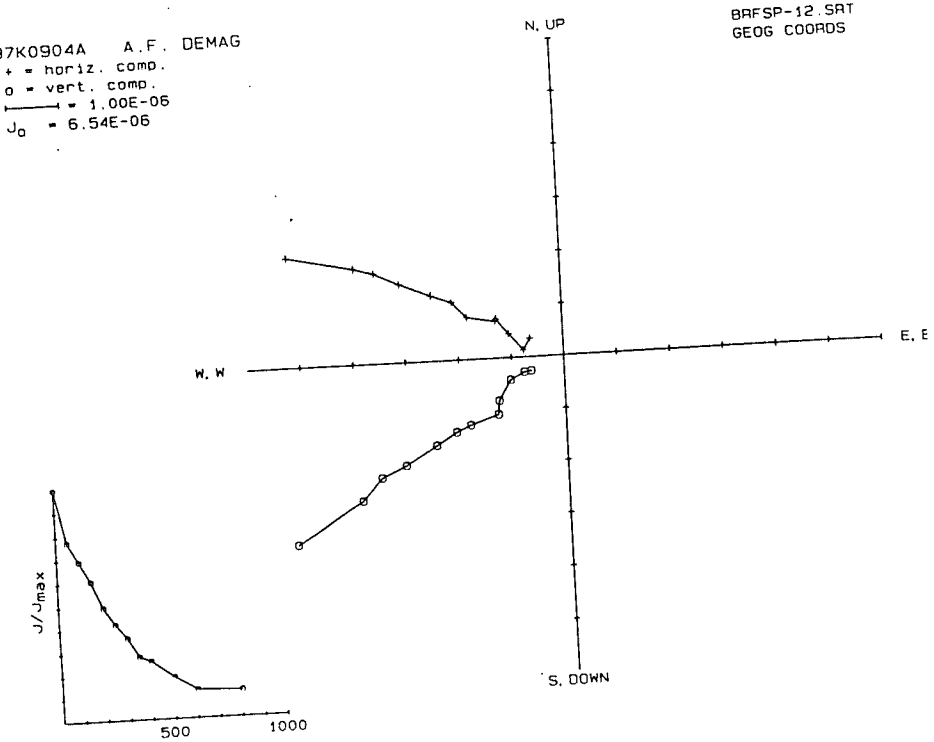

97K0907A A.F. DEMAG
+ = horiz. comp.
o = vert. comp.
= 1.00E-06
J_o = 7.99E-06

BRFSP-12.SRT
GEOG COORDS

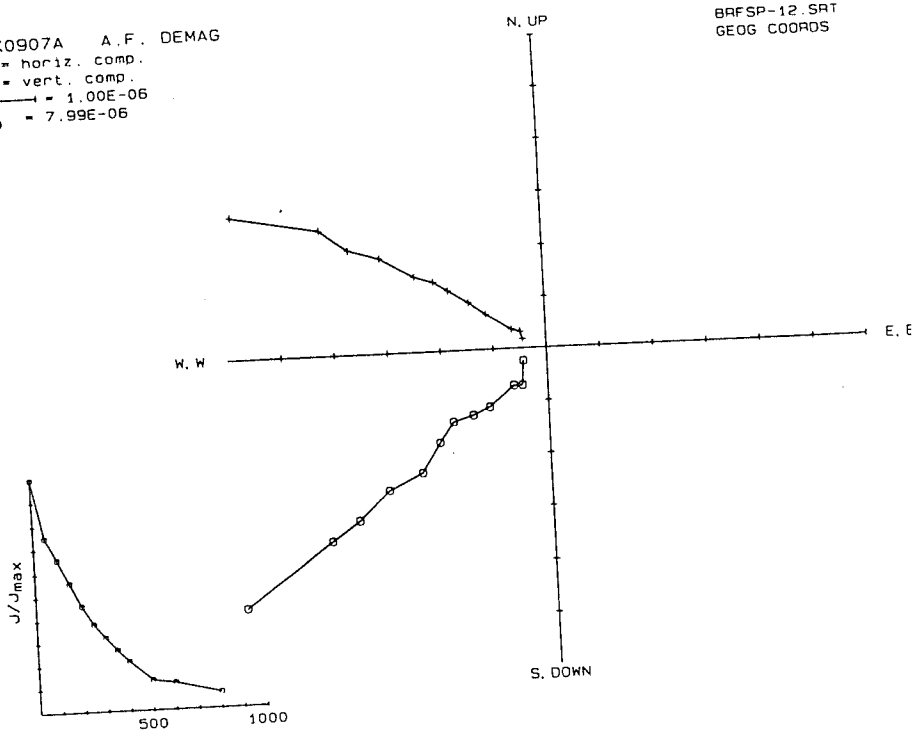

97K0912A A.F. DEMAG
+ = horiz. comp.
o = vert. comp.
= 1.00E-06
J_o = 6.84E-06

BRFSP-12.SRT
GEOG COORDS

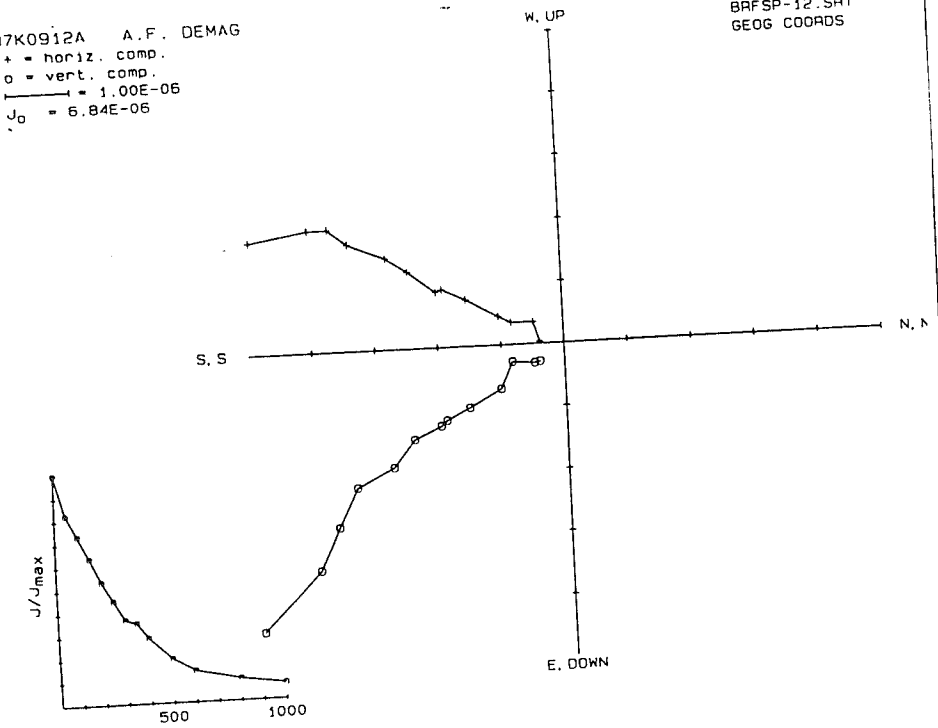

97K0916A A.F. DEMAG
+ = horiz. comp.
o = vert. comp.
= 5.00E-07
J_o = 6.00E-06

BRFSP-13.SRT
GEOG COORDS

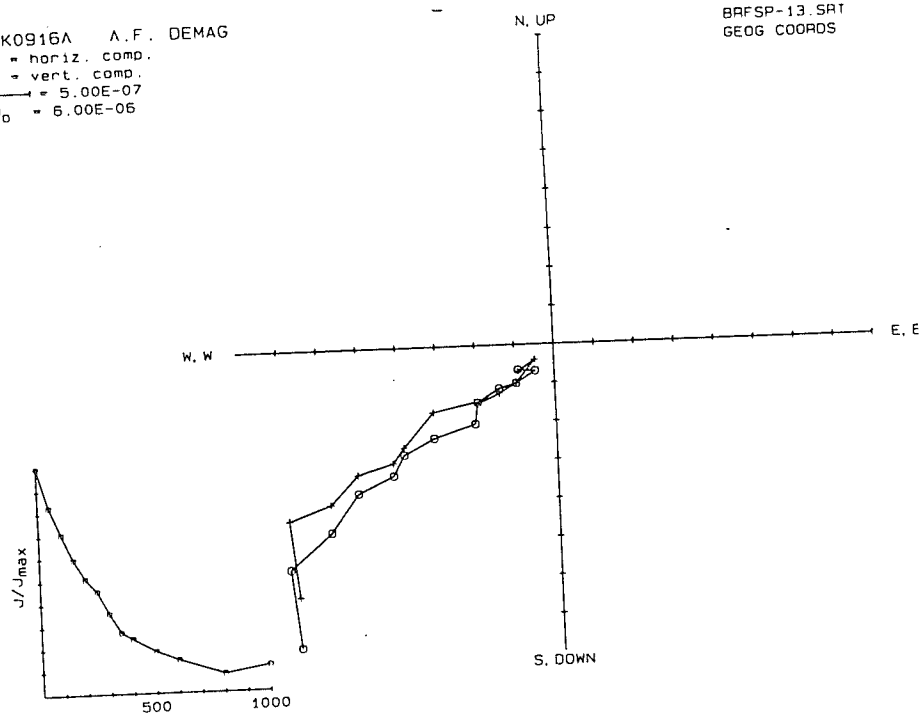

97K0914A A.F. DEMAG
+ = horiz. comp.
o = vert. comp.
= 1.00E-06
J_o = 6.91E-06

BRFSP-12.SRT
GEOG COORDS

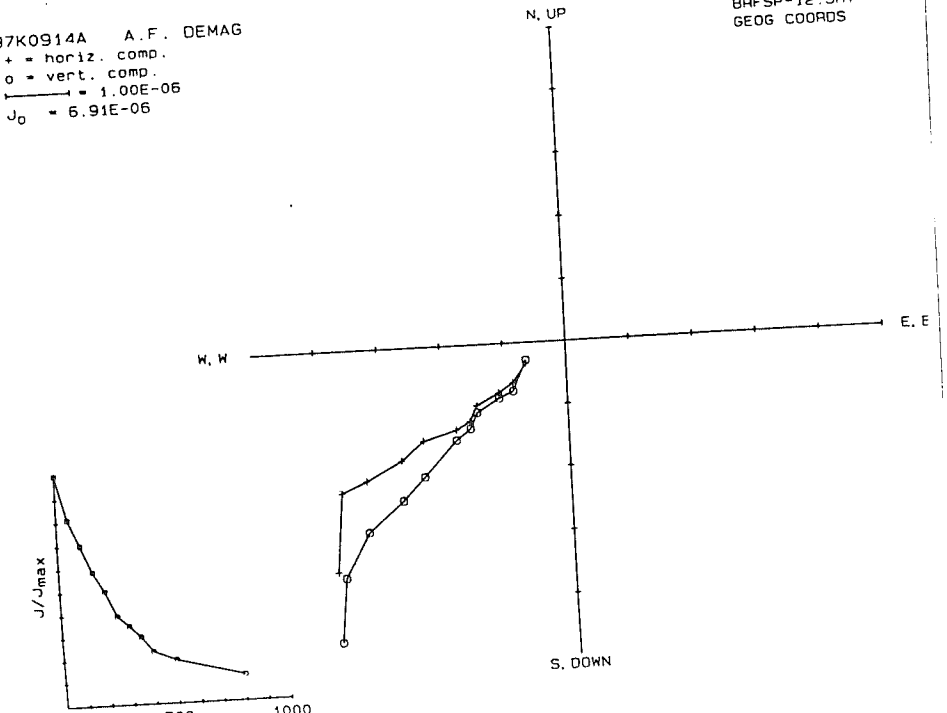

97K0921A A.F. DEMAG
+ = horiz. comp.
o = vert. comp.
= 1.00E-06
J_o = 9.28E-06

BRFSP-13.SRT
GEOG COORDS

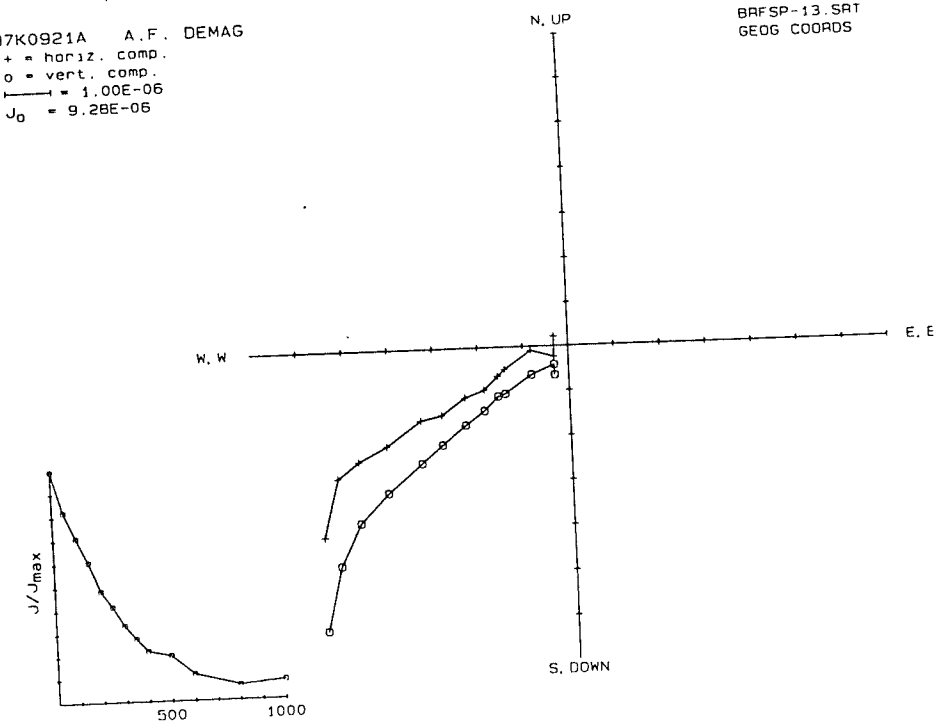

97K0923A A.F. DEMAG
+ = horiz. comp.
o = vert. comp.
|——| = 1.00E-06
J_o = 8.40E-06

BAFSP-13.SRT
GEOG COORDS

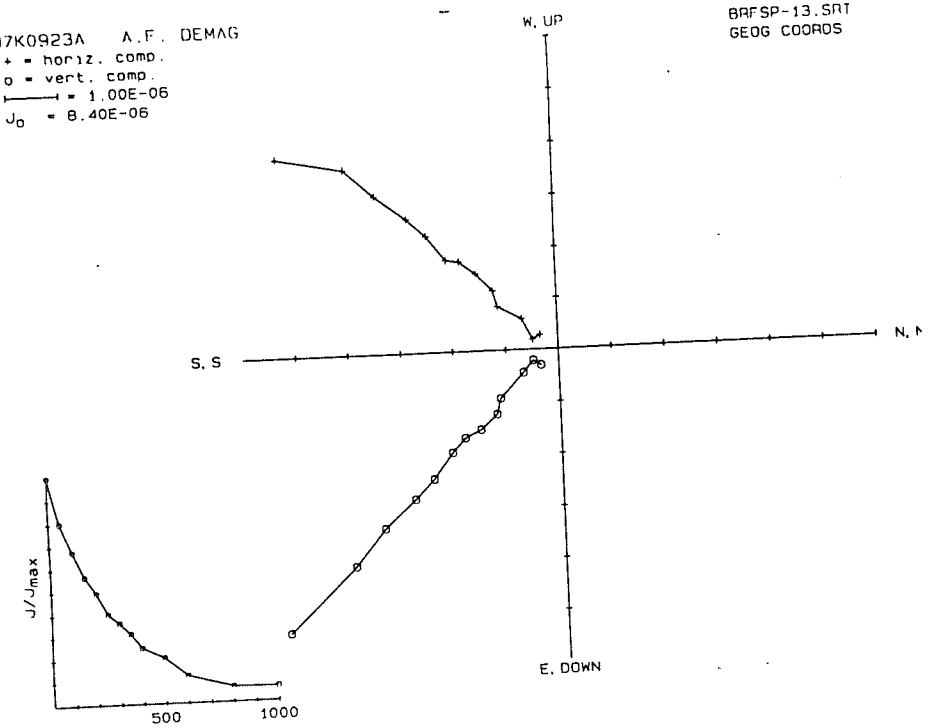

97K0931A A.F. DEMAG
+ = horiz. comp.
o = vert. comp.
|——| = 1.00E-06
J_o = 8.99E-06

BAFSP-13.SRT
GEOG COORDS

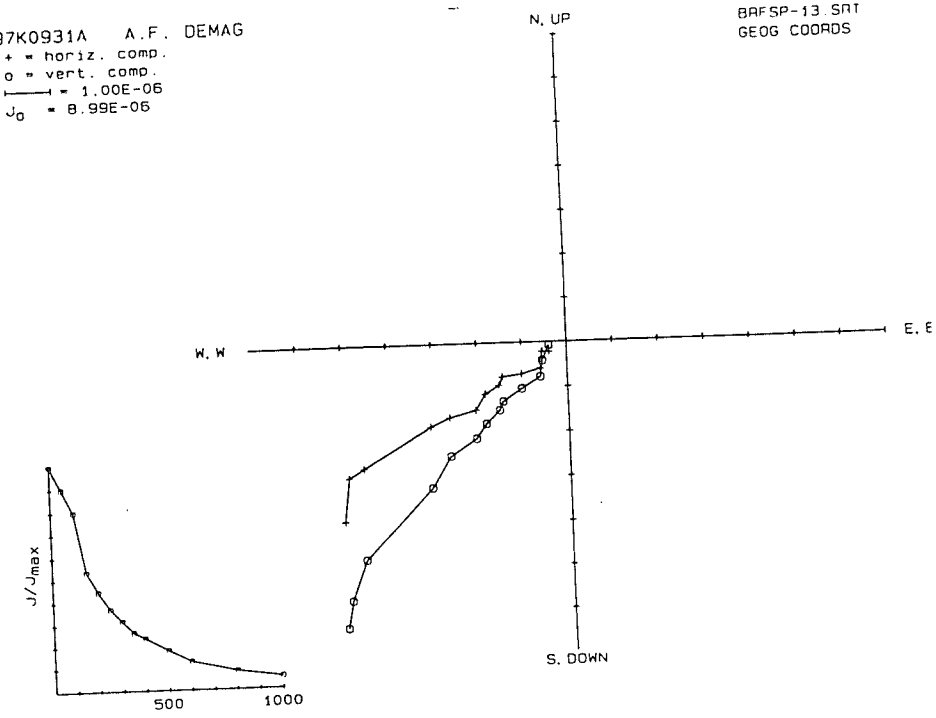

97K0924A A.F. DEMAG
+ = horiz. comp.
o = vert. comp.
|——| = 1.00E-06
J_o = 7.46E-06

BAFSP-13.SRT
GEOG COORDS

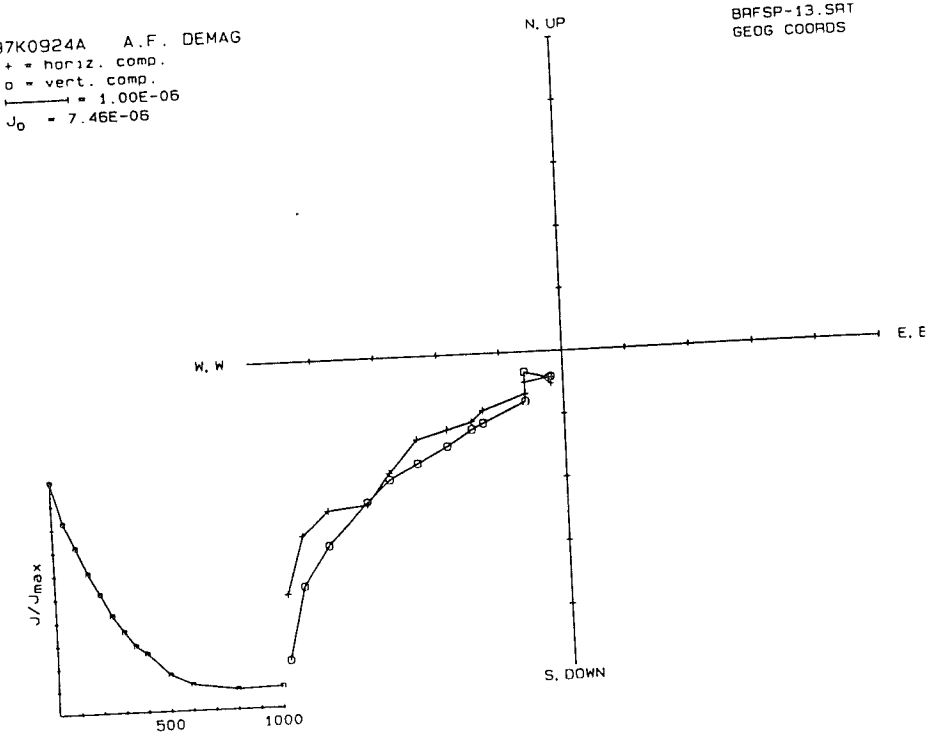

97K0852A A.F. DEMAG
+ = horiz. comp.
o = vert. comp.
|——| = 5.00E-07
J_o = 2.54E-06

BAFSP-17.SRT
GEOG COORDS

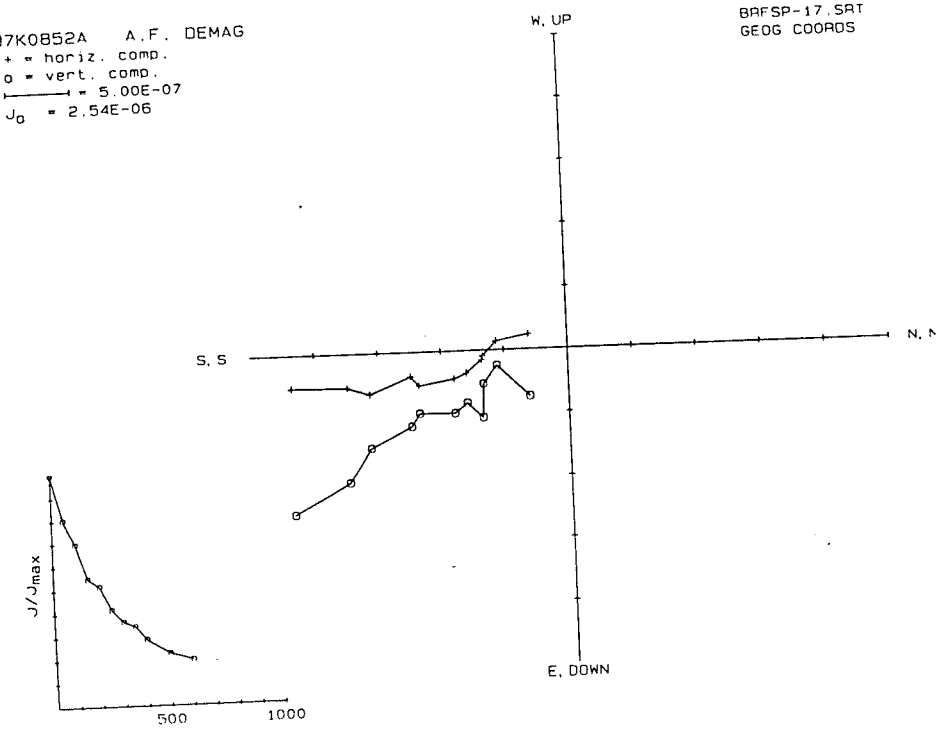

97K0854A A.F. DEMAG
+ = horiz. comp.
o = vert. comp.
= 5.00E-07
J_o = 2.60E-06

BRFSP-17.SRT
GEOG COORDS

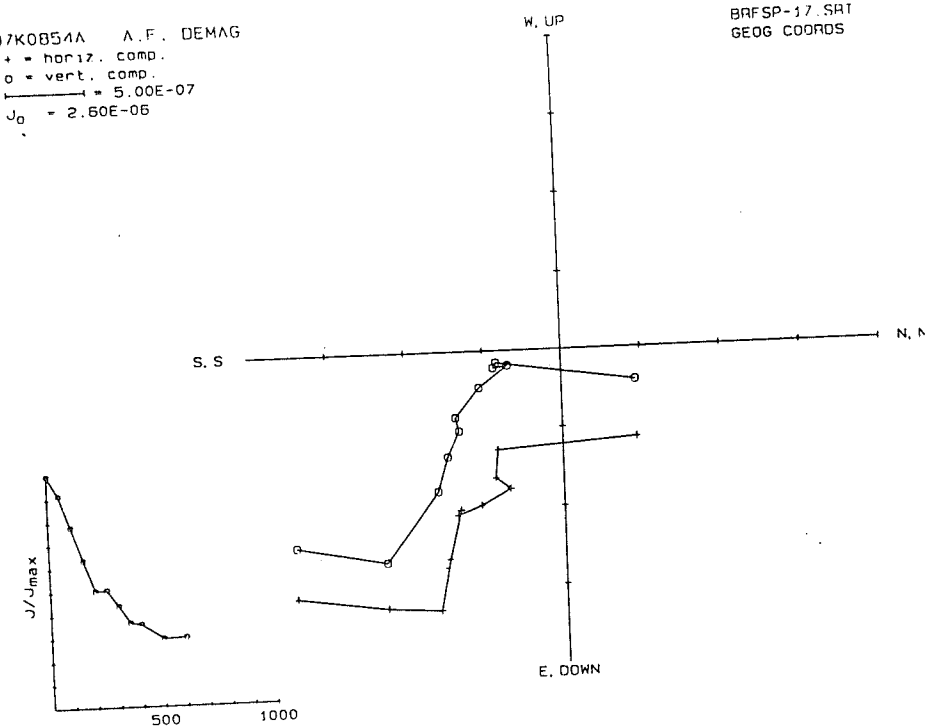

97K0856A A.F. DEMAG
+ = horiz. comp.
o = vert. comp.
= 5.00E-07
J_o = 2.54E-06

BRFSP-17.SRT
GEOG COORDS

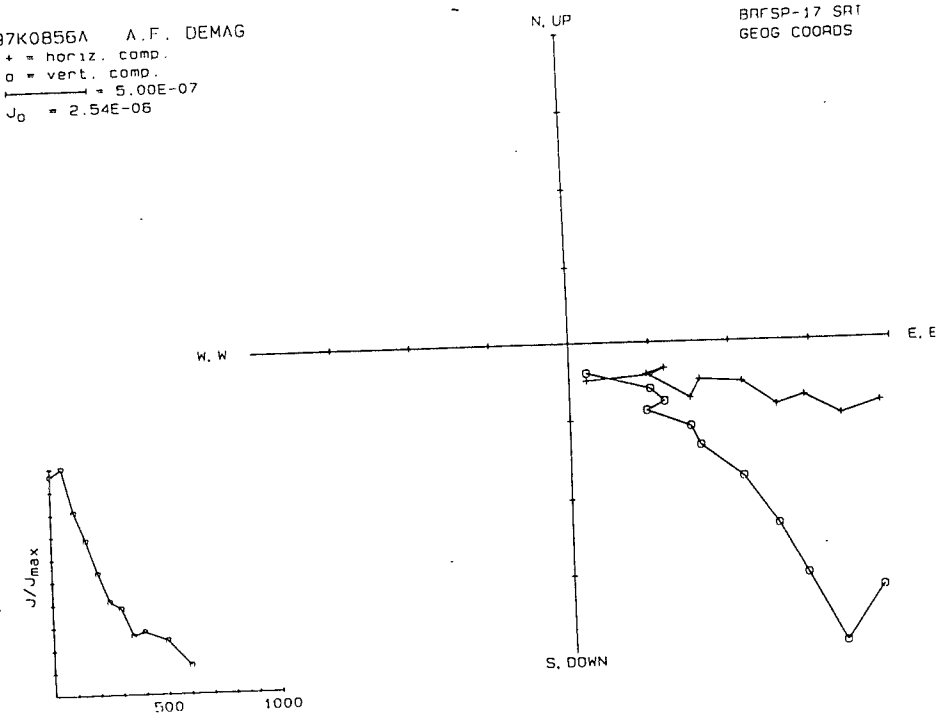

97K0854B A.F. DEMAG
+ = horiz. comp.
o = vert. comp.
= 5.00E-07
J_o = 3.01E-06

BRFSP-17.SRT
GEOG COORDS

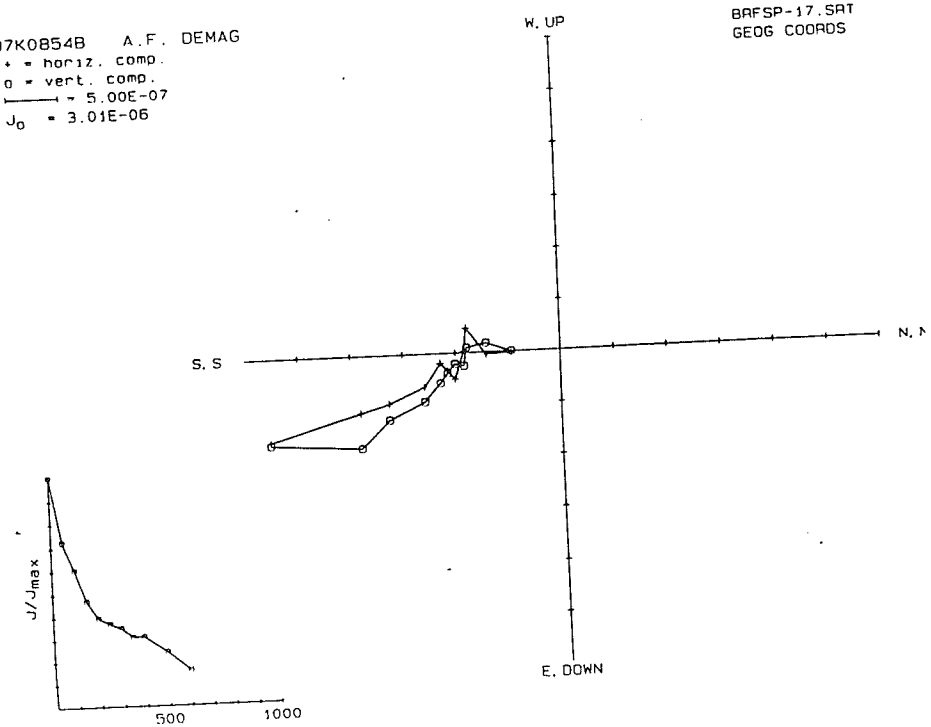

97K0856B A.F. DEMAG
+ = horiz. comp.
o = vert. comp.
= 5.00E-07
J_o = 2.96E-06

BRFSP-17.SRT
GEOG COORDS

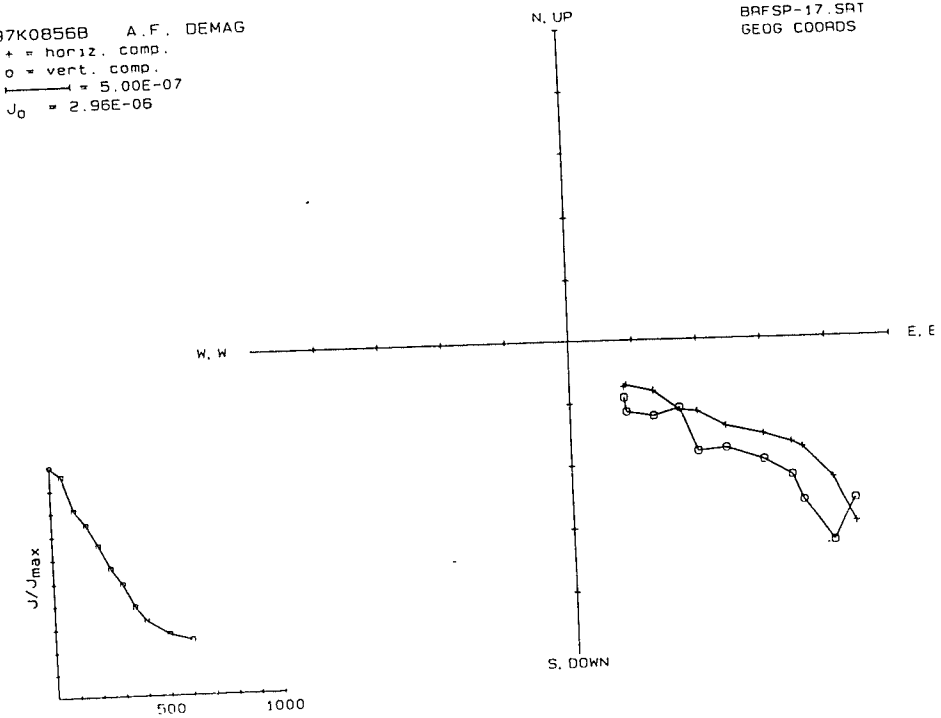

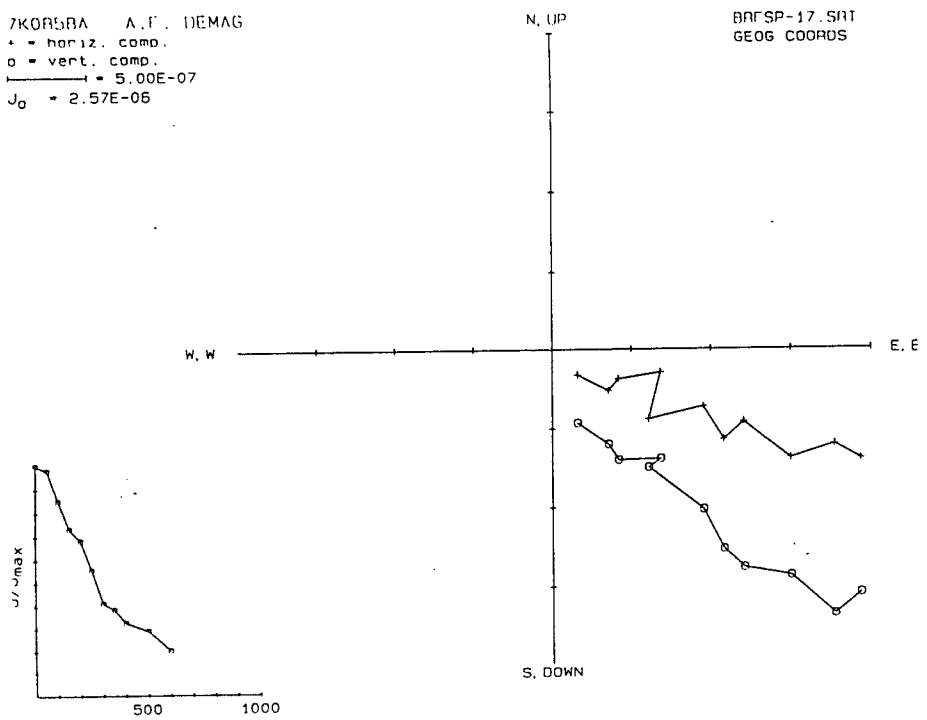
7K0858A A.F. DEMAG
+ = horiz. comp.
o = vert. comp.
= 5.00E-07
J_0 = 2.57E-06
N, UP
BRFSP-17.SRT
GEOG COORDS
W, W
E, E
S, DOWN
J/Jmax
500
1000

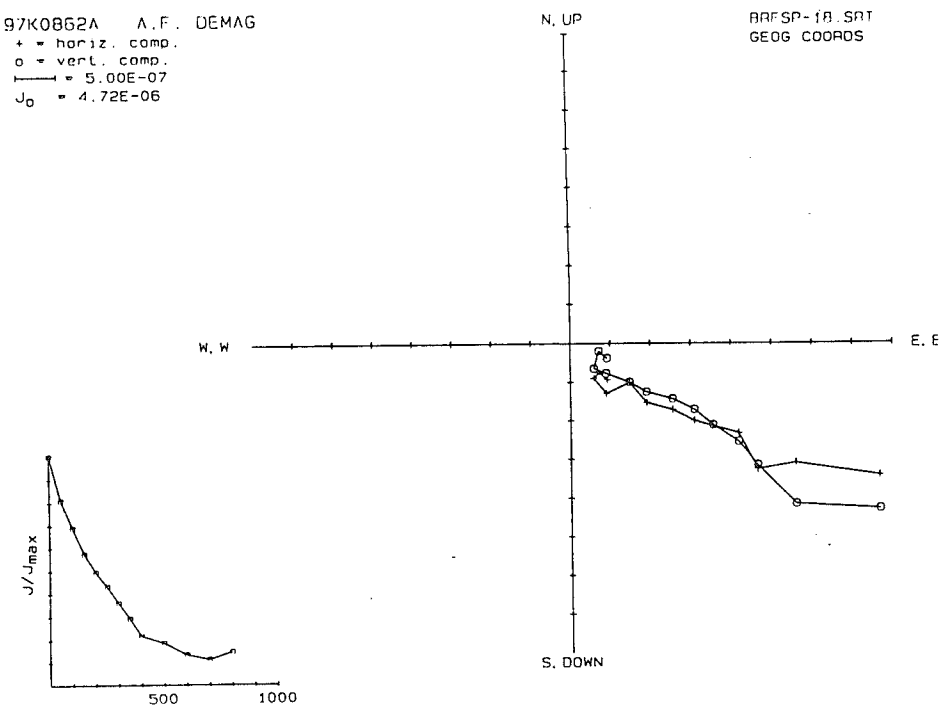
97K0862A A.F. DEMAG
+ = horiz. comp.
o = vert. comp.
= 5.00E-07
J_0 = 4.72E-06
N, UP
BRFSP-18.SRT
GEOG COORDS
W, W
E, E
S, DOWN
J/Jmax
500
1000

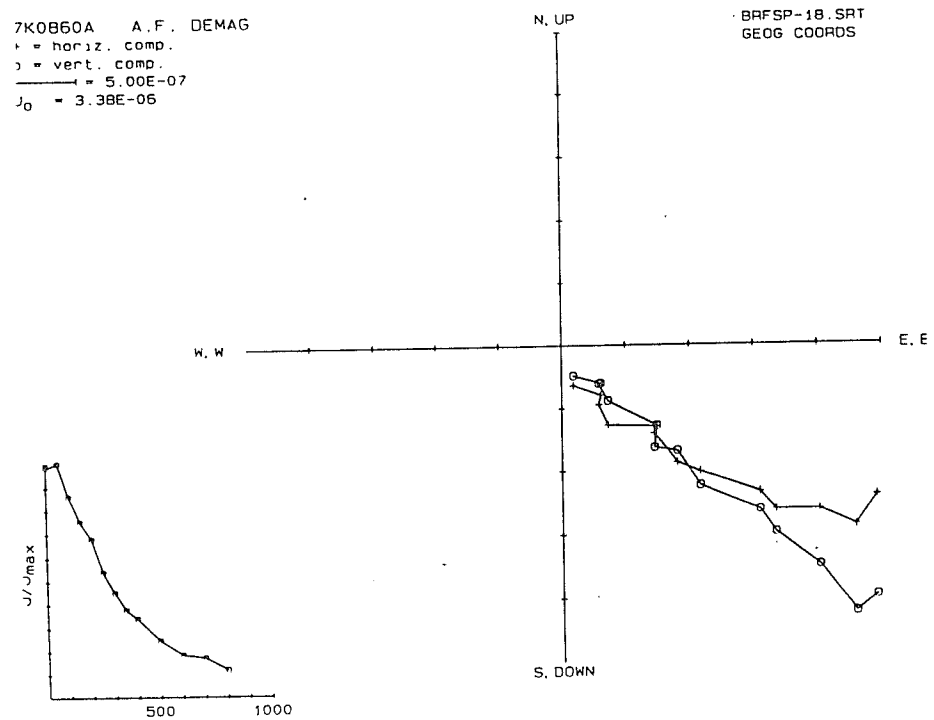
7K0860A A.F. DEMAG
+ = horiz. comp.
o = vert. comp.
= 5.00E-07
J_0 = 3.38E-06
N, UP
BRFSP-18.SRT
GEOG COORDS
W, W
E, E
S, DOWN
J/Jmax
500
1000

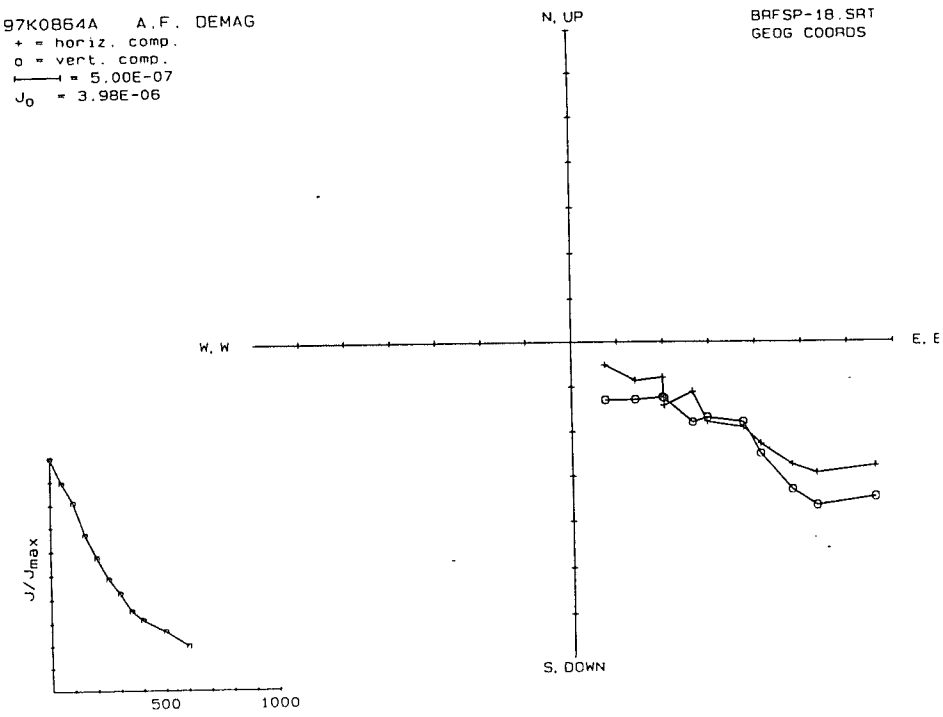
97K0864A A.F. DEMAG
+ = horiz. comp.
o = vert. comp.
= 5.00E-07
J_0 = 3.98E-06
N, UP
BRFSP-18.SRT
GEOG COORDS
W, W
E, E
S, DOWN
J/Jmax
500
1000

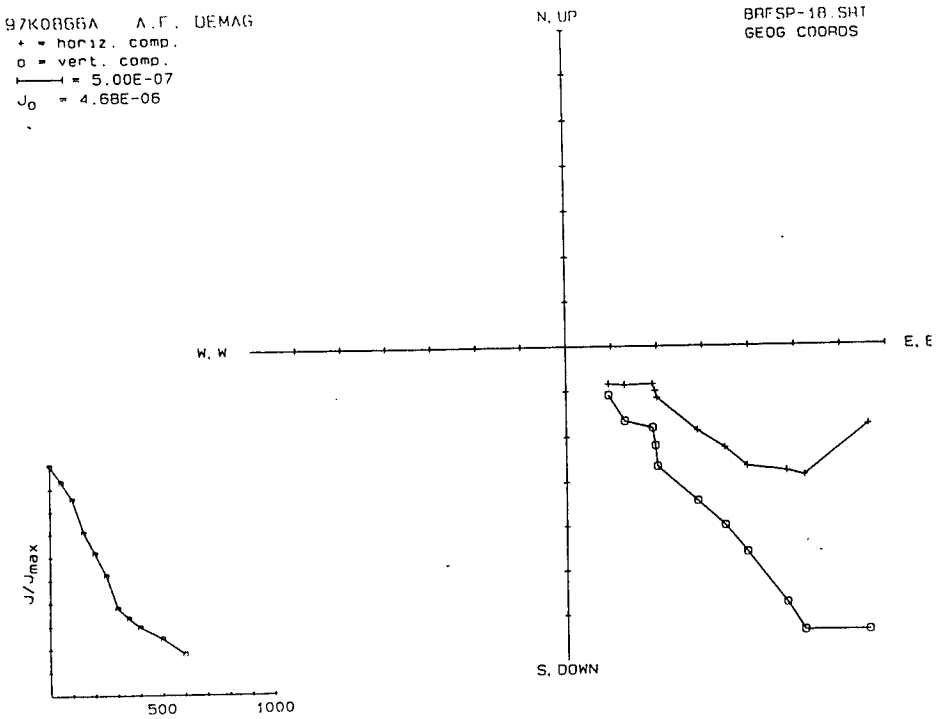
97K0866A A.F. DEMAG
+ = horiz. comp.
o = vert. comp.
= 5.00E-07
J_o = 4.68E-06
N, UP
BRFSP-18.SRT
GEOG COORDS
W, W
E, E
S, DOWN
J/Jmax
500
1000

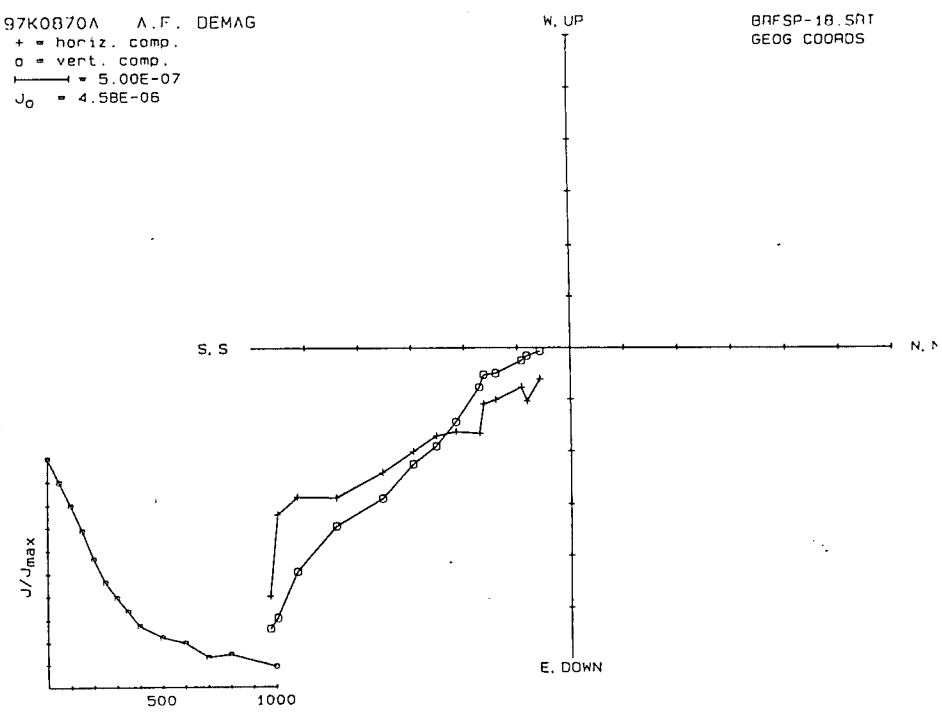
97K0870A A.F. DEMAG
+ = horiz. comp.
o = vert. comp.
= 5.00E-07
J_o = 4.58E-06
W, UP
BRFSP-18.SRT
GEOG COORDS
S, S
N, N
E, DOWN
J/Jmax
500
1000

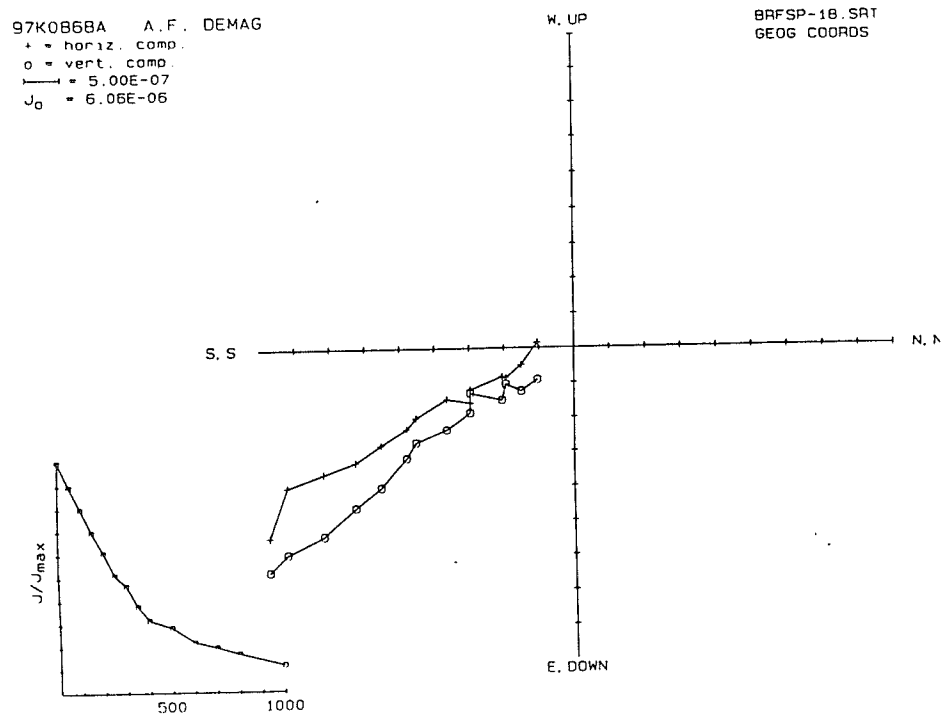
97K0868A A.F. DEMAG
+ = horiz. comp.
o = vert. comp.
= 5.00E-07
J_o = 6.06E-06
W, UP
BRFSP-18.SRT
GEOG COORDS
S, S
N, N
E, DOWN
J/Jmax
500
1000

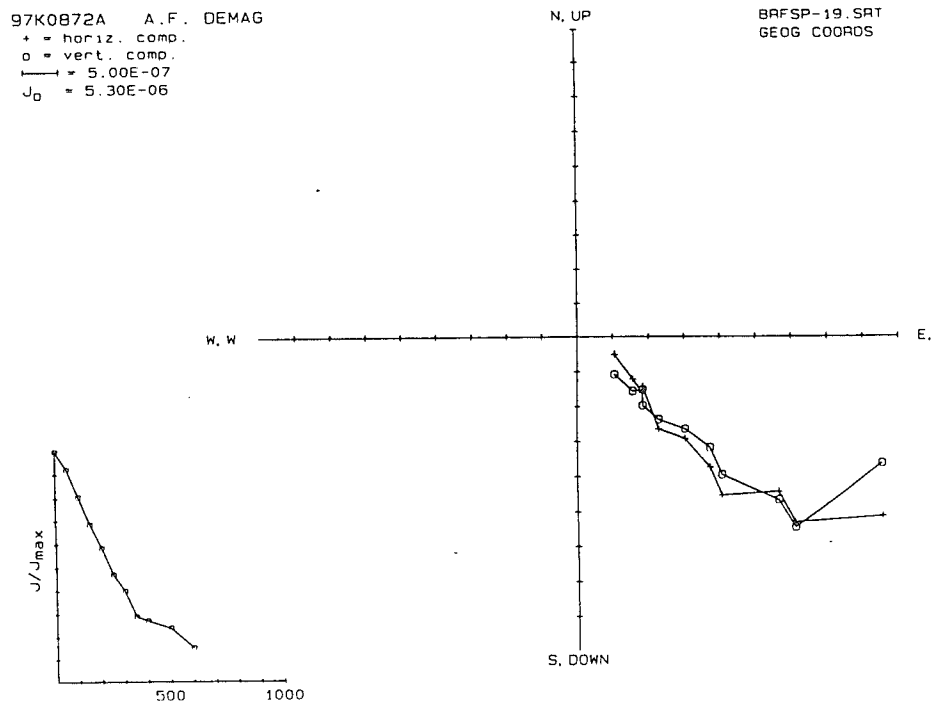
97K0872A A.F. DEMAG
+ = horiz. comp.
o = vert. comp.
= 5.00E-07
J_o = 5.30E-06
N, UP
BRFSP-19.SRT
GEOG COORDS
W, W
E, E
S, DOWN
J/Jmax
500
1000

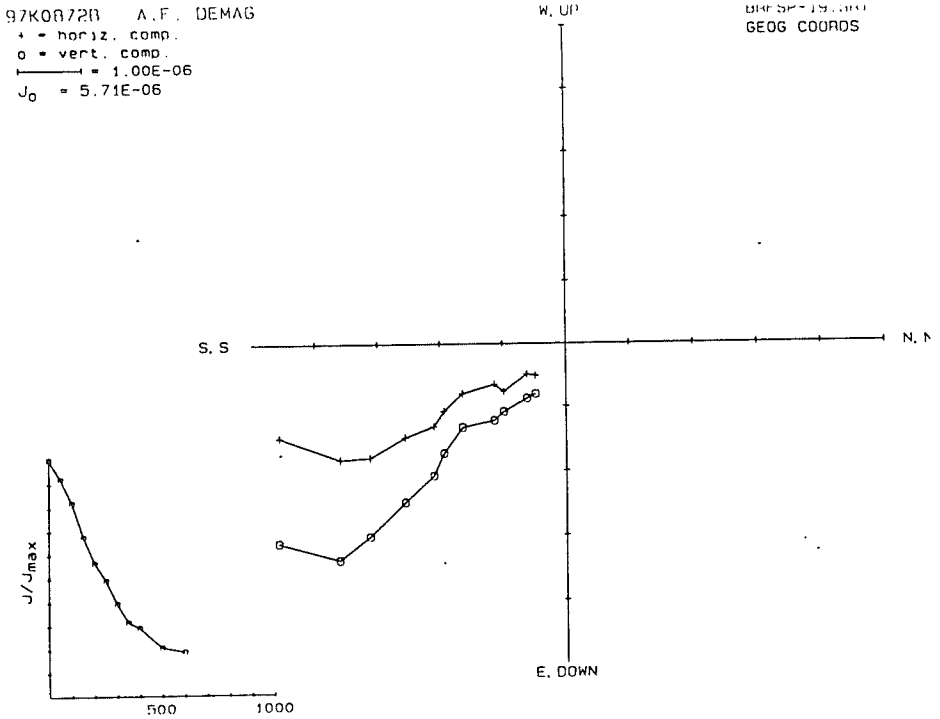
97K0872B A.F. DEMAG
+ = horiz. comp.
o = vert. comp.
= 1.00E-06
J_o = 5.71E-06
W, UP
BRFSP-19.SRT
GEOG COORDS
S, S
N, N
E, DOWN
J/Jmax
500
1000

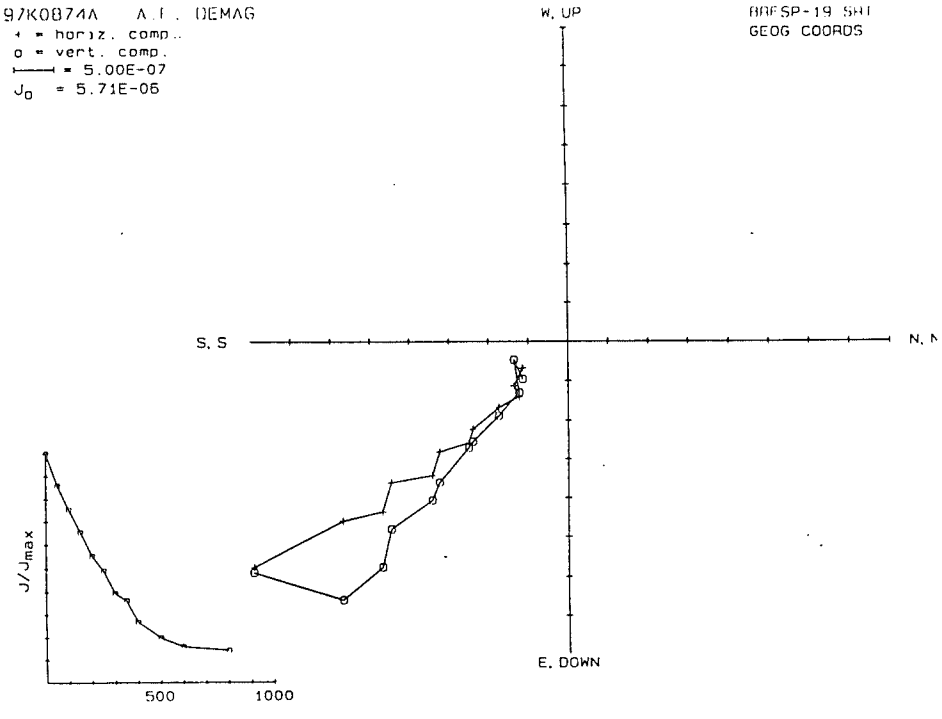
97K0874A A.F. DEMAG
+ = horiz. comp.
o = vert. comp.
= 5.00E-07
J_o = 5.71E-06
W, UP
BRFSP-19.SRT
GEOG COORDS
S, S
N, N
E, DOWN
J/Jmax
500
1000

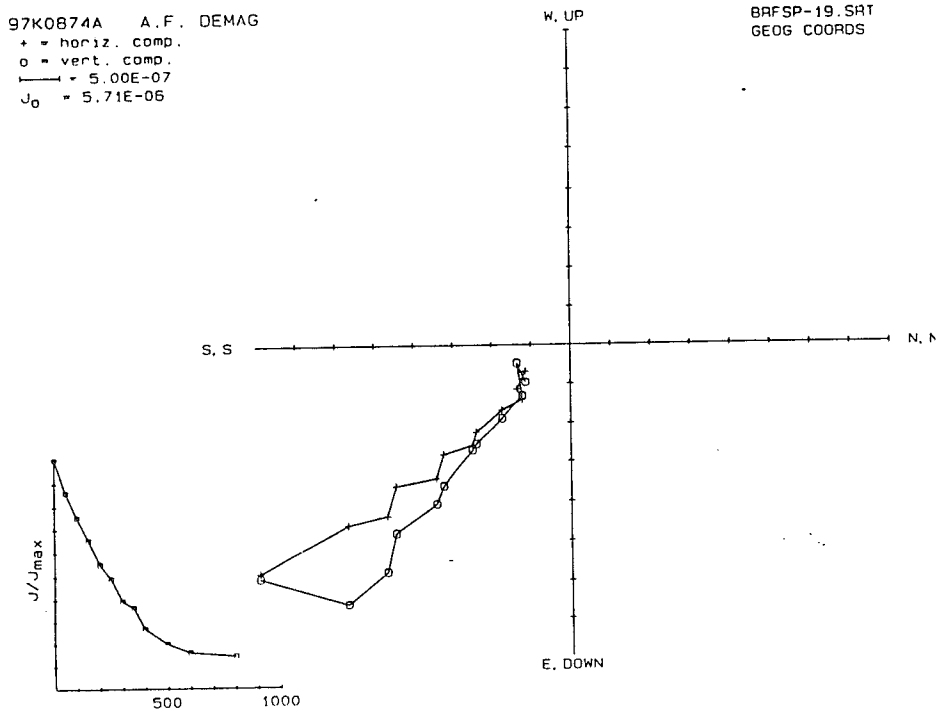
97K0874A A.F. DEMAG
+ = horiz. comp.
o = vert. comp.
= 5.00E-07
J_o = 5.71E-06
W, UP
BRFSP-19.SRT
GEOG COORDS
S, S
N, N
E, DOWN
J/Jmax
500
1000

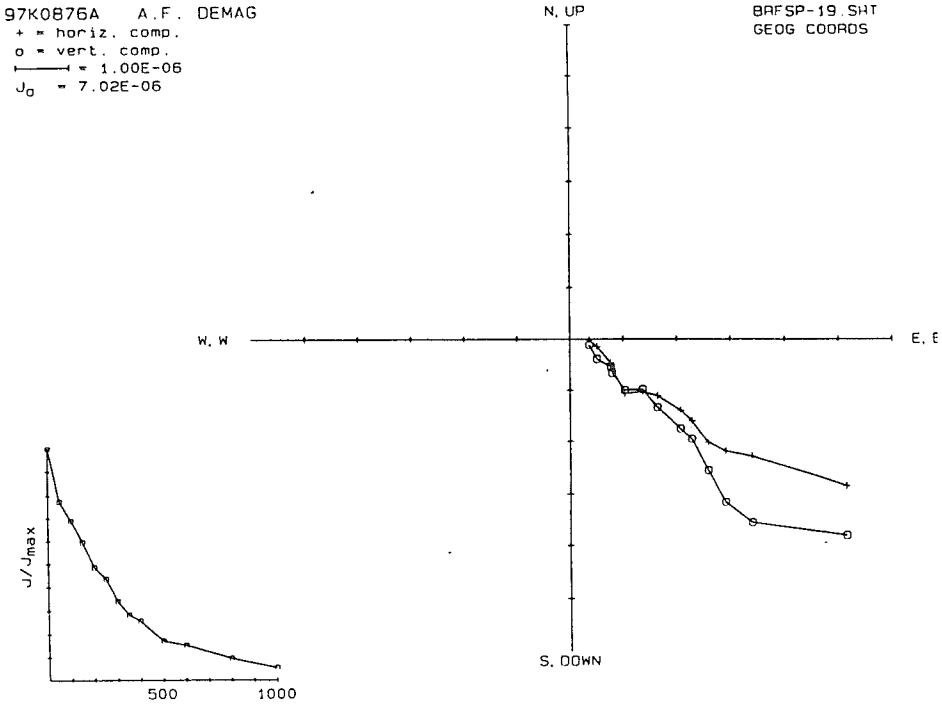
97K0876A A.F. DEMAG
+ = horiz. comp.
o = vert. comp.
= 1.00E-06
J_o = 7.02E-06
N, UP
BRFSP-19.SRT
GEOG COORDS
W, W
E, E
S, DOWN
J/Jmax
500
1000

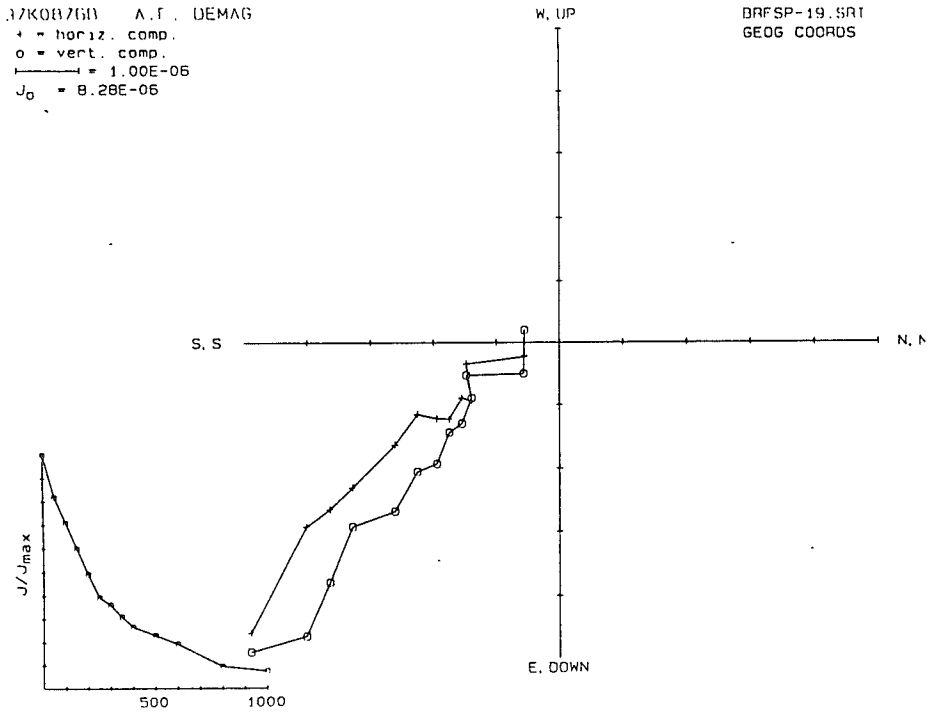
97K0876A A.F. DEMAG
+ = horiz. comp.
o = vert. comp.
= 1.00E-06
J_o = 8.28E-06
W, UP
BRFSP-19.SRT
GEOG COORDS
S, S
N, N
E, DOWN
J/Jmax
500
1000

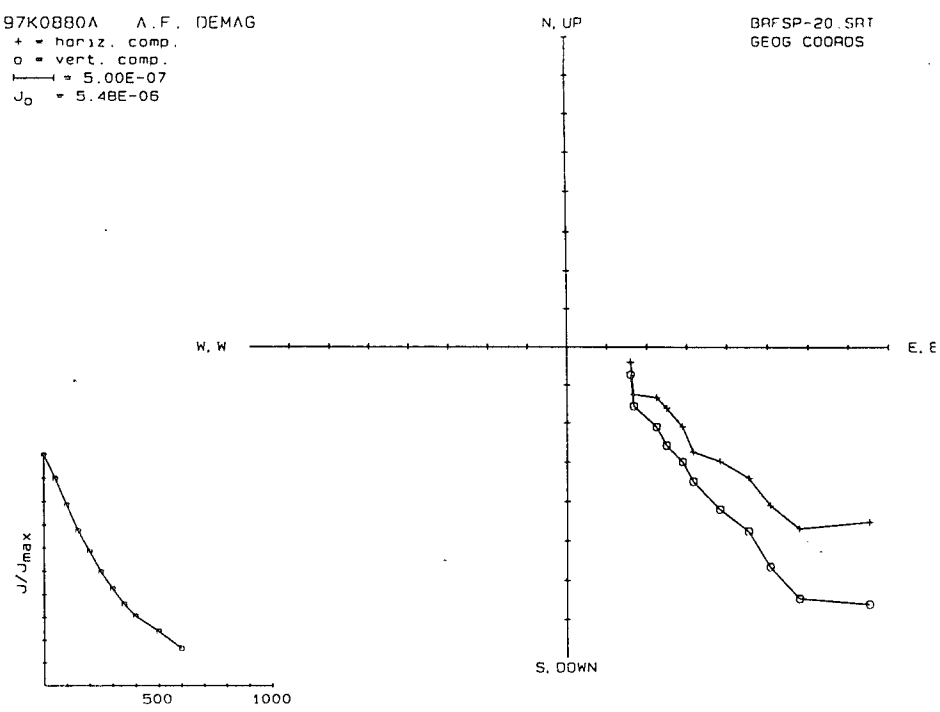
97K0880A A.F. DEMAG
+ = horiz. comp.
o = vert. comp.
= 5.00E-07
J_o = 5.48E-06
N, UP
BRFSP-20.SRT
GEOG COORDS
W, W
E, E
S, DOWN
J/Jmax
500
1000

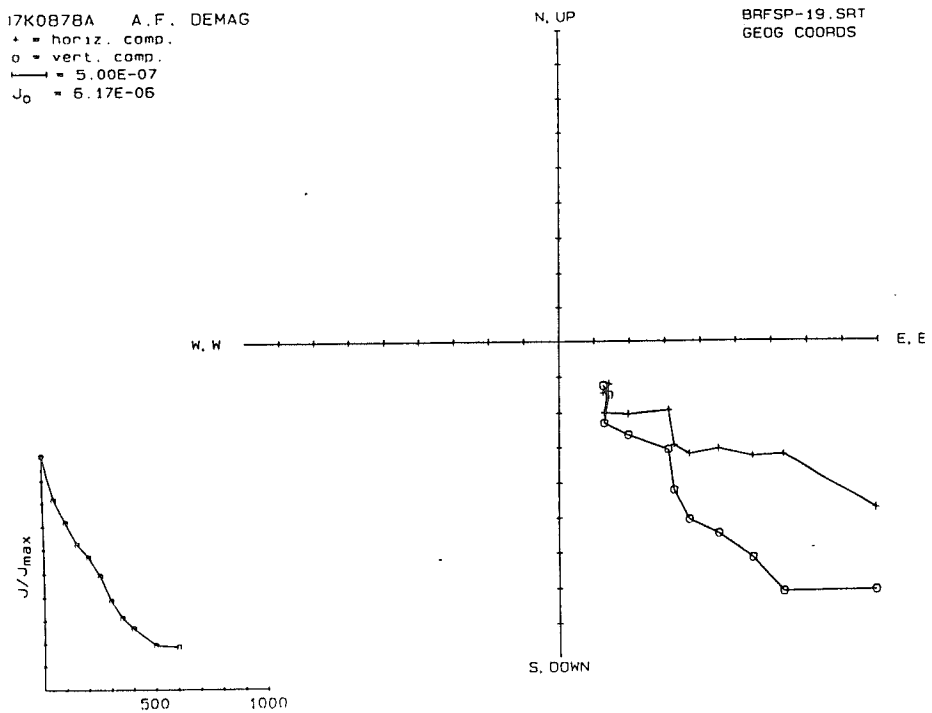
97K0878A A.F. DEMAG
+ = horiz. comp.
o = vert. comp.
= 5.00E-07
J_o = 6.17E-06
N, UP
BRFSP-19.SRT
GEOG COORDS
W, W
E, E
S, DOWN
J/Jmax
500
1000

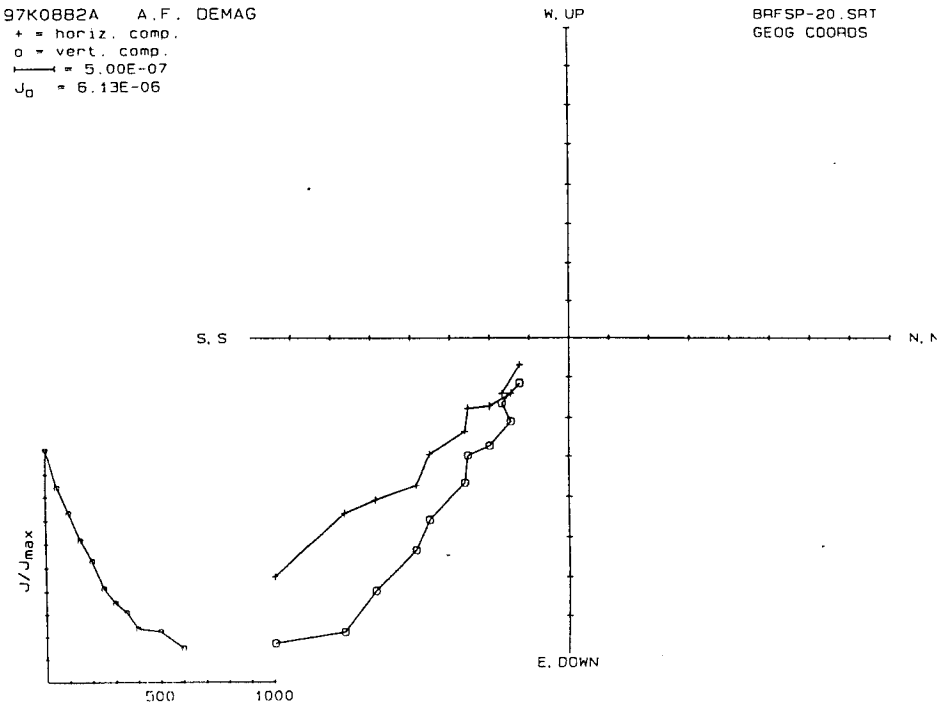
97K0882A A.F. DEMAG
+ = horiz. comp.
o = vert. comp.
= 5.00E-07
J_o = 6.13E-06
W, UP
BRFSP-20.SRT
GEOG COORDS
S, S
N, N
E, DOWN
J/Jmax
500
1000

97K0886A A.F. DEMAG
+ = horiz. comp.
o = vert. comp.
⊢——⊣ = 5.00E-07
J_o = 4.75E-06

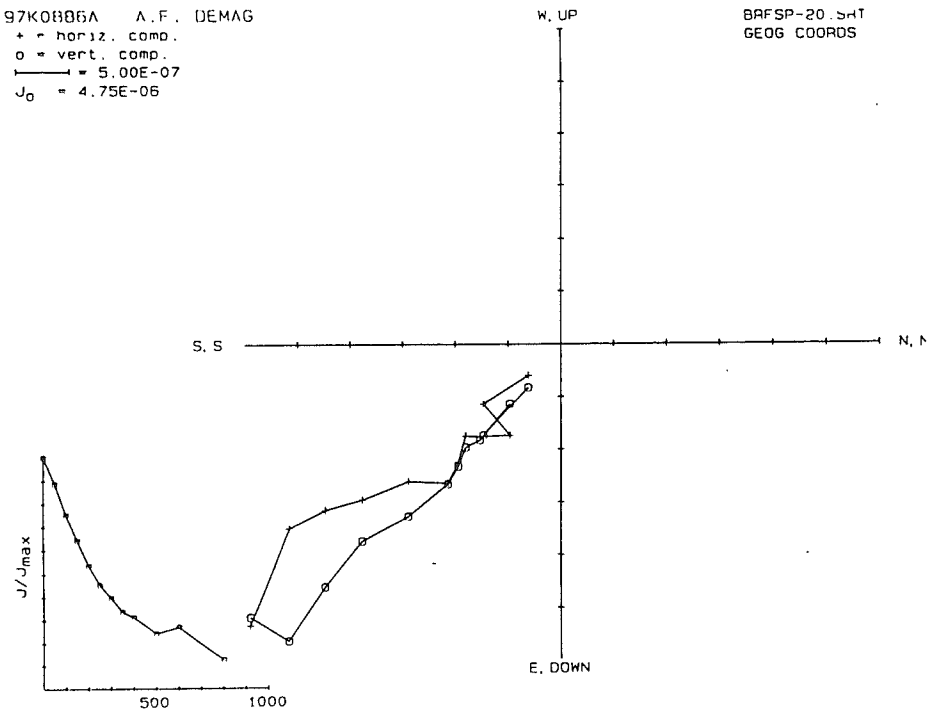

BAFSP-20.SHT
GEOG COORDS

97K0890A A.F. DEMAG
+ = horiz. comp.
o = vert. comp.
⊢——⊣ = 1.00E-06
J_o = 6.63E-06

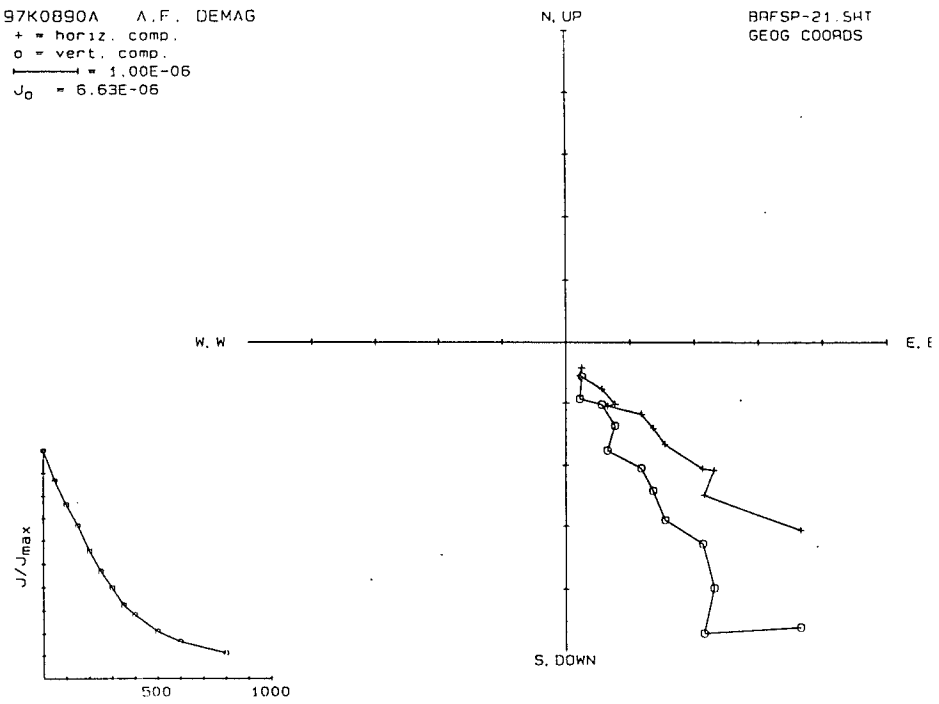

BAFSP-21.SHT
GEOG COORDS

97K0888B A.F. DEMAG
+ = horiz. comp.
o = vert. comp.
⊢——⊣ = 1.00E-06
J_o = 1.13E-05

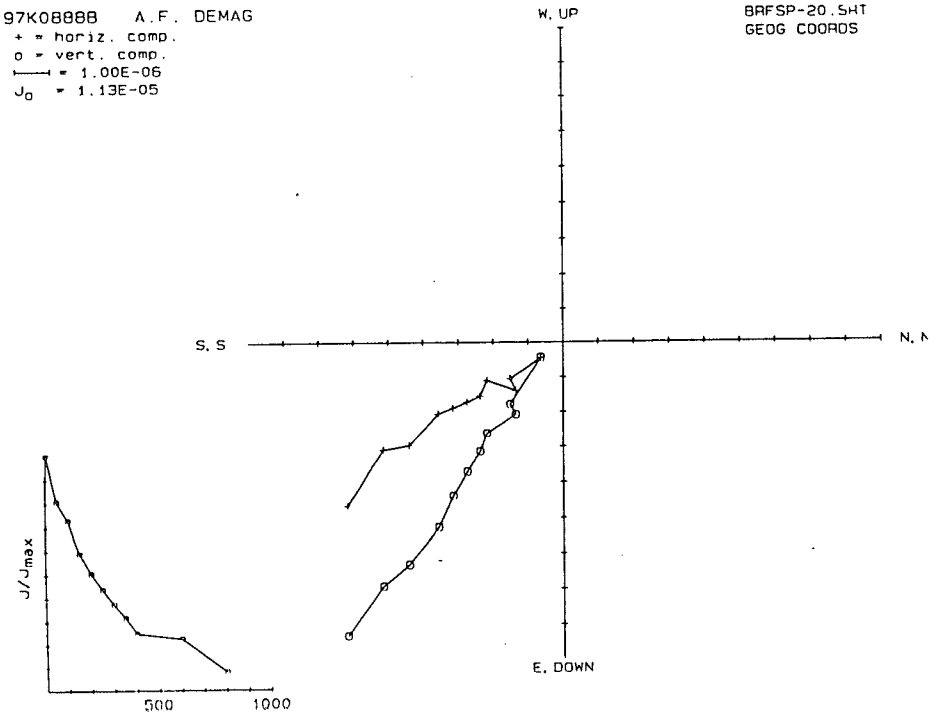

BAFSP-20.SHT
GEOG COORDS

97K0892A A.F. DEMAG
+ = horiz. comp.
o = vert. comp.
⊢——⊣ = 5.00E-07
J_o = 5.73E-06

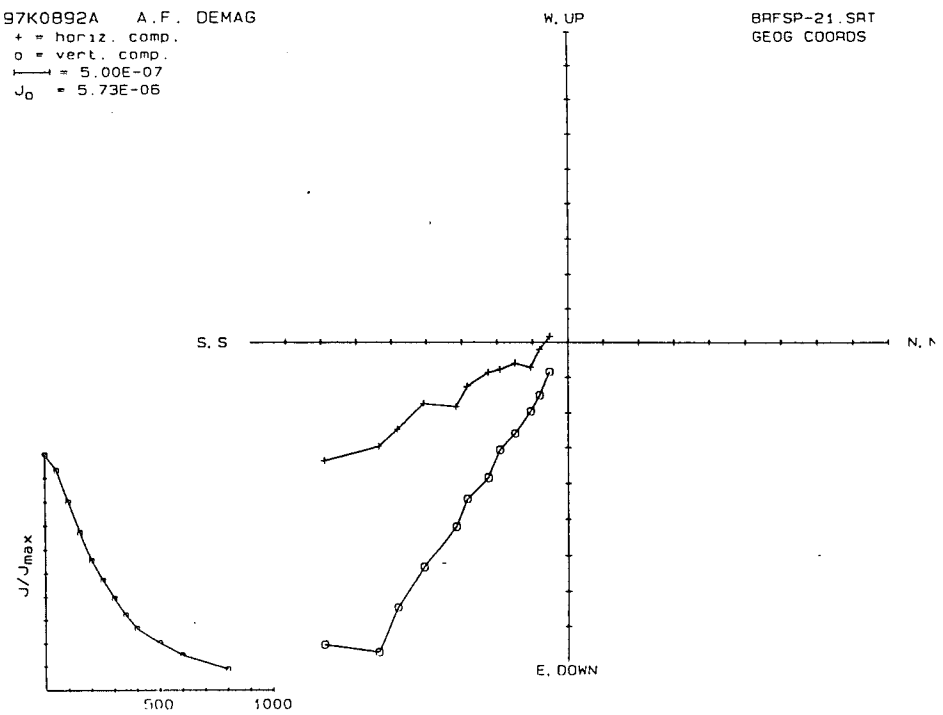

BAFSP-21.SHT
GEOG COORDS

97K0894A A.F. DEMAG
+ = horiz. comp.
o = vert. comp.
⊢⊣ = 5.00E-07
J_o = 6.50E-06

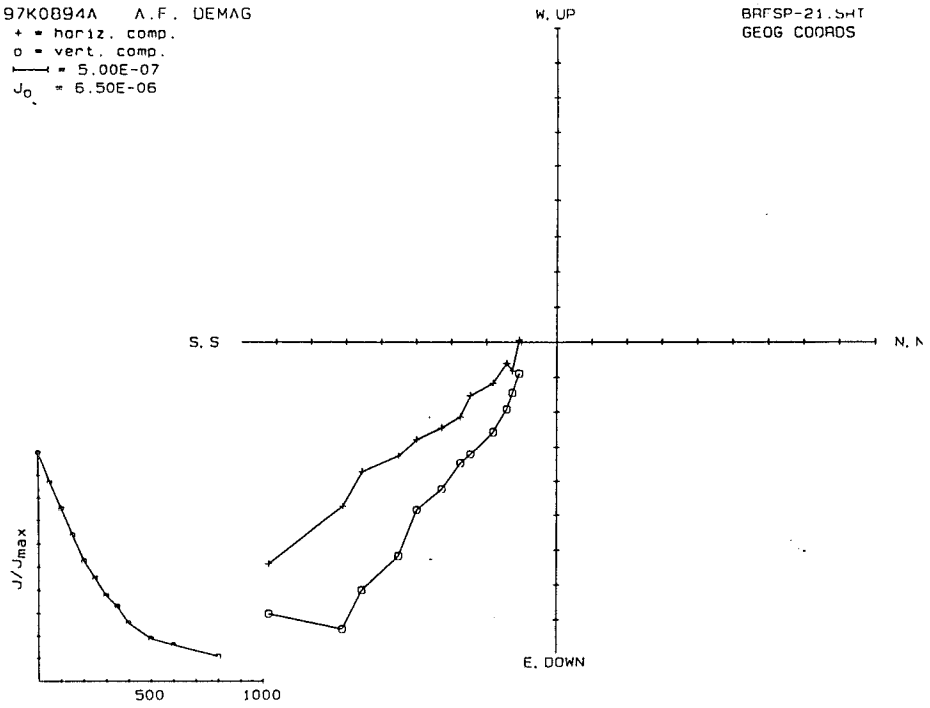

BRFSP-21.SHT
GEOG COORDS

97K0898A A.F. DEMAG
+ = horiz. comp.
o = vert. comp.
⊢⊣ = 1.00E-06
J_o = 9.77E-06

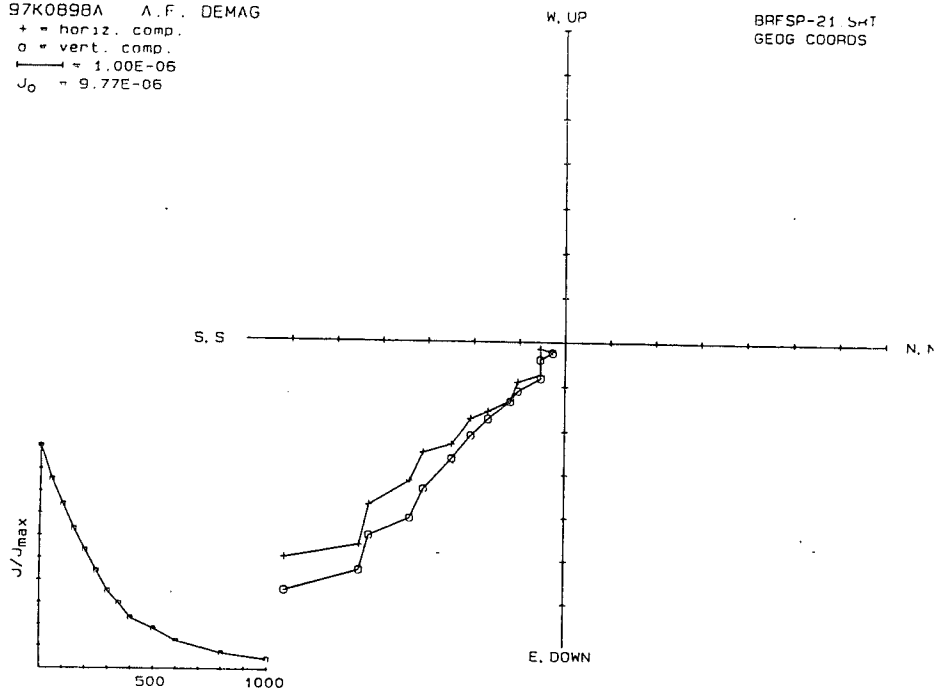

BRFSP-21.SHT
GEOG COORDS

97K0896A A.F. DEMAG
+ = horiz. comp.
o = vert. comp.
⊢⊣ = 5.00E-07
J_o = 6.80E-06

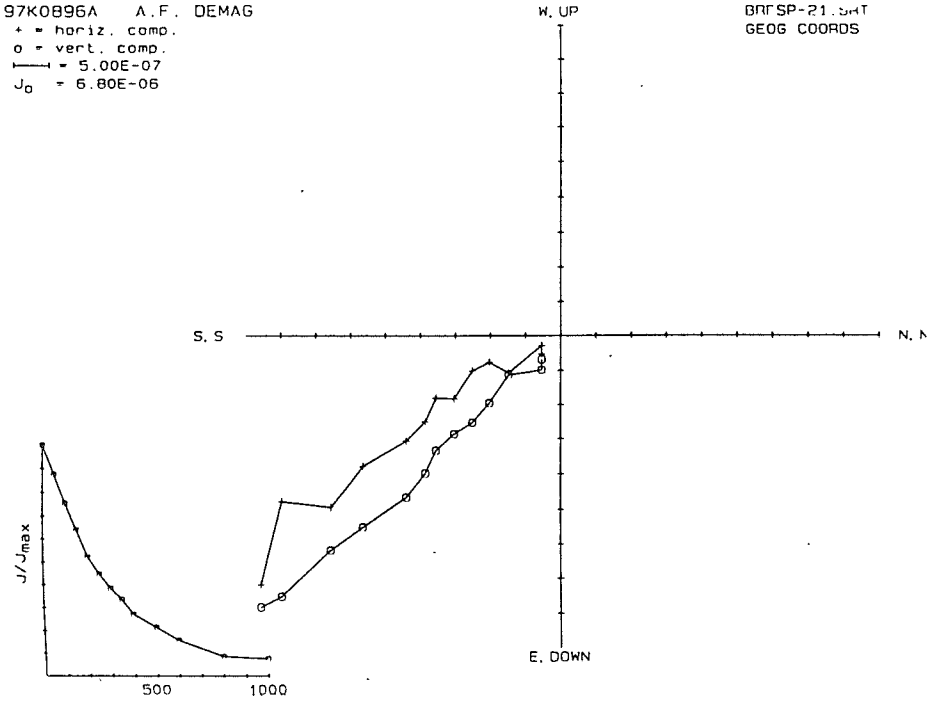

BRFSP-21.SHT
GEOG COORDS